

# Gauge Coupling Unification in Realistic Free-Fermionic String Models

Keith R. Dienes\* and Alon E. Faraggi†

*School of Natural Sciences, Institute for Advanced Study  
Olden Lane, Princeton, N.J. 08540 USA*

## Abstract

We discuss the unification of gauge couplings within the framework of a wide class of realistic free-fermionic string models which have appeared in the literature, including the flipped  $SU(5)$ ,  $SO(6) \times SO(4)$ , and various  $SU(3) \times SU(2) \times U(1)$  models. If the matter spectrum below the string scale is that of the Minimal Supersymmetric Standard Model (MSSM), then string unification is in disagreement with experiment. We therefore examine several effects that may modify the minimal string predictions. First, we develop a systematic procedure for evaluating the one-loop heavy string threshold corrections in free-fermionic string models, and we explicitly evaluate these corrections for each of the realistic models. We find that these string threshold corrections are small, and we provide general arguments explaining why such threshold corrections are suppressed in string theory. Thus heavy thresholds cannot resolve the disagreement with experiment. We also study the effect of non-standard hypercharge normalizations, light SUSY thresholds, and intermediate-scale gauge structure, and similarly conclude that these effects cannot resolve the disagreement with low-energy data. Finally, we examine the effects of additional color triplets and electroweak doublets beyond the MSSM. Although not required in ordinary grand unification scenarios, such states generically appear within the context of certain realistic free-fermionic string models. We show that if these states exist at the appropriate thresholds, then the gauge couplings will indeed unify at the string scale. Thus, within these string models, string unification can be in agreement with low-energy data.

---

\* E-mail address: dienes@sns.ias.edu

† E-mail address: faraggi@sns.ias.edu

# 1 Introduction

LEP precision data provides remarkable confirmation of the Standard Model of particle physics. However, many fundamental problems are not addressed in the context of the Standard Model, leading to the expectation that a more fundamental theory must exist in which the Standard Model appears as an effective low-energy limit. While many possible extensions of the Standard Model are highly constrained or ruled out by experiment, supersymmetric theories are in agreement with all available data. Furthermore, the top-quark mass range required in supersymmetric scenarios of electroweak symmetry breaking [1] is in agreement with that suggested by CDF/D0 direct observation [2] and LEP precision data [3]. In recent years it has also been suggested that the success of gauge coupling unification in the Minimal Supersymmetric Standard Model (MSSM) [4] provides evidence for the validity of supersymmetric grand unified theories (SUSY GUT's).

While SUSY GUT's provide a useful parametrization of the sparticle spectrum at low energies and of the boundary conditions at the GUT scale, they are incomplete theories. First, they do not explain the origin of the Standard Model spectrum. Second, in order to evade proton-lifetime constraints, some *ad hoc* global symmetries must be imposed, and a doublet-triplet splitting mechanism is required. Finally, despite the fact that the unification scale is just one or two orders of magnitude below the Planck scale, a consistent treatment of quantum gravity is lacking.

Remarkably, superstring theories [5], the only available candidates for a consistent theory of quantum gravity, accommodate  $N = 1$  supersymmetric theories as their low-energy effective theories. Even more remarkably, heterotic string theories [6] provide a general framework in which the origin of the observed particle spectrum and interactions may be understood [7] and the doublet-triplet splitting problem may be resolved [8].

Among the string models constructed to date, the most phenomenologically realistic have been formulated within the so-called “free-fermionic” construction [9, 10, 11]. Indeed, within this construction, many three-generation models can be obtained. While this may be an accident, it is more likely to be a reflection of some fundamental properties of string compactification. The free-fermionic construction is formulated at a highly symmetric point in the compactification space at which spacetime symmetries are maximally enhanced. It turns out that the realistic free-fermionic models admit a  $Z_2 \times Z_2$  orbifold structure with standard embedding which is realized in this construction through the so-called “NAHE set” [12] of fermionic boundary-condition basis vectors. Such  $Z_2 \times Z_2$  orbifolds possess a structure which can naturally accommodate three generations due to the existence of exactly three twisted sectors. These result from the action of the  $Z_2 \times Z_2$  twist on a six-dimensional compactified space. In general, the  $Z_2 \times Z_2$  orbifold does not produce a number of fixed points that can be reduced to three generations. However, precisely at the free-fermionic point in the toroidal compactification space, the number of fixed points is such that a reduction

to three generations can be achieved. Indeed, the number of fixed points from each twisted sector is reduced to one. Thus, each twisted sector produces one of the chiral generations of the Standard Model.

The realistic free-fermionic models achieve remarkable success in trying to explain the different features of the Standard Model spectrum. In addition to naturally producing three generations with Standard Model gauge group, they also provide a plausible explanation for the heavy top-quark mass and the fermion mass hierarchy. Indeed, the realistic standard-like models suggest that only the top quark mass term is obtained at the cubic level of the superpotential, while the lighter fermion mass terms are obtained from non-renormalizable terms which are naturally suppressed relative to the leading cubic-level mass term. In fact, in this way a successful prediction of the mass of the top quark was obtained in Ref. [13], three years prior to its experimental observation. Furthermore, an analysis of non-renormalizable terms up to eighth order then reveals how the fermion masses and mixing angles may also be generated [14].

The realistic free-fermionic models are therefore very appealing from a theoretical point of view, and may successfully explain the different features of the Standard Model. However, string theory in general, and the free-fermionic models in particular, predict that the string unification scale is related to the Planck scale, and should be numerically of the order of  $\mathcal{O}(5 \cdot 10^{17})$  GeV. Thus, a factor of approximately twenty separates the string unification scale from the usual MSSM unification scale extrapolated from low-energy data. This discrepancy is one of major problems confronting string model-building.

One possible solution is to construct string GUT models in which the GUT symmetry is broken in the effective low-energy field theory [15, 16]. However, no realistic models of this sort have yet been constructed. Moreover, in this scenario, the problems with proton-lifetime constraints reemerge. Indeed, this problem is more severe in string GUT's due to the possible appearance of baryon- and lepton-number-violating dimension-four operators [8] and the anticipated difficulty in implementing the GUT doublet-triplet splitting mechanism in string models.

Another solution is provided if additional thresholds exist in the desert between the electroweak scale and the string unification scale. In fact, the availability of such additional thresholds in realistic free-fermionic models has been demonstrated in Ref. [17]. In this respect, imposing the restriction that the spectrum below the string scale is just that of the MSSM is *ad hoc*, and may be too restrictive. The successful unification of gauge couplings within the MSSM would then indicate that the MSSM is only an approximation to the complete theory between the weak scale and the Planck scale.

A third suggestion, due to Ibáñez [18], is that in string models the normalization of the weak hypercharge is, in general, different from that in grand-unified theories, and may just have the right value to allow string unification, even if the spectrum below the string scale is that of the MSSM. It is found that if  $k_1$  is in the range  $1.2 \leq k_1 \leq 1.4$ , then unification at the string scale can be consistent with low-energy

data. However, whether such values of  $k_1$  can be achieved within consistent string models remains an open question. Moreover, we will argue that in string models we must have  $k_1 \geq 5/3$ .

A final possibility is that the contributions arising from the infinite towers of heavy string states can modify the above string tree-level predictions. Within this scenario, one would hope that these heavy string states can give rise to additional heavy string threshold corrections which shift the unification point down to  $\mathcal{O}(10^{16})$  GeV.

In this paper, we systematically re-examine the problem of gauge coupling unification within the context of a wide variety of realistic free-fermionic models which have appeared in the literature. There are various reasons why this is an important undertaking. For example, while many of the possible effects that we consider have been discussed previously, each was treated in an abstract setting and in isolation. However, within the tight constraints of a given realistic string model, the mechanisms giving rise to three generations and the MSSM gauge group may ultimately prove inconsistent with, for example, large threshold corrections or extra non-MSSM matter. Moreover, the increased complexity of the known realistic string models may substantially alter previous expectations based on simplified or idealized scenarios. It is therefore important to rigorously calculate all of these effects simultaneously, within the context of a wide variety of actual realistic string models, in order to determine which path to successful gauge coupling unification (if any) such models actually take.

Our analysis proceeds in several steps. First, we study the role of threshold corrections due to the infinite tower of heavy string states. In this we follow the definition of threshold corrections as given by Kaplunovsky [19], and explicitly calculate these corrections for a wide range of realistic free-fermionic models including the flipped  $SU(5)$  “revamped” model [20], several  $SU(3) \times SU(2) \times U(1)$  models [21, 13, 22, 23], an  $SO(6) \times SO(4)$  model [24], and even models with non-supersymmetric spacetime spectra. Our evaluation of these threshold corrections is done in two stages. First, we analytically evaluate the traces over the entire Fock space corresponding to a given string model, with various relevant combinations of gauge charge operators inserted into the trace. Then, for each combination of gauge charge insertions, these results are expanded level-by-level, and the contributions from the states at each string energy level are integrated over the modular-group fundamental domain. In this manner, we can obtain results to any desired accuracy. Moreover, as we shall see, various non-trivial consistency checks can be performed.

Our results show that threshold corrections due to the massive string states are small in free-fermionic string models. This result is *a priori* surprising, given the infinite numbers of heavy string states which potentially contribute to the string threshold corrections, but we are able to provide a general argument which explains why the threshold corrections from the massive string states are naturally suppressed in string theory. Our argument also explains why threshold corrections can grow large

only for large values of the string moduli.

Given these results, we then proceed to systematically examine the other effects which might potentially alleviate the discrepancy between the GUT and string scales. As discussed above, these include the effects of stringy non-standard  $U(1)$  hypercharge normalizations, light SUSY thresholds, intermediate gauge structure, and additional matter beyond that predicted by the MSSM. We find that the effects of hypercharge normalizations, light SUSY thresholds, and intermediate gauge structure are not sufficient to remove the discrepancy. By contrast, we surprisingly find that only the presence of additional matter in these models (in particular, certain color triplets and electroweak doublets with special hypercharge assignments) has a profound effect on the running of the gauge couplings, and precisely this matter appears naturally in a variety of the realistic string models. Indeed, within these models, we show the gauge couplings can indeed unify at the string scale when all of the above effects are taken into account. Thus, for such models, the disagreement between the GUT scale and the string scale can be naturally resolved.

It is remarkable that string theory, which predicts an unexpectedly high unification scale  $M_{\text{string}}$ , in many cases compensates by simultaneously also predicting precisely the extra exotic particles needed to reconcile this higher scale with low-energy data. Moreover, our analysis shows that while some string models naturally contain the extra matter needed to resolve this disagreement, other models do not and can actually be ruled out on this basis. Thus, the appearance of such extra matter becomes a low-energy prediction of these models which may be accessible to present-day experiments.

We stress that this is the first time that such an exhaustive examination of all possible effects has been performed within the context of actual realistic string models, and within the constraints that these models impose. Hence, one of the main results of our analysis is the new observation that only the appearance of extra exotic matter in particular representations can possibly resolve the experimental discrepancies. Indeed, because we have been able to rule out all other possible within these models, the appearance of such extra exotic matter becomes a *prediction* of successful string-scale unification. It is of course an old idea that the presence of extra matter can resolve the discrepancy between the GUT and string unification scales. What is highly non-trivial, however, is that this now appears to be the *only* way in which realistic string models can solve the problem.

This paper is organized as follows. In Sect. 2 we review the general features of the realistic free-fermionic models, and in Sect. 3 we discuss how heavy string threshold corrections may be evaluated within the context of such models. In Sect. 4 we then explicitly calculate the threshold corrections within the flipped  $SU(5)$ ,  $SO(6) \times SO(4)$ , and  $SU(3) \times SU(2) \times U(1)$  string models, and in Sect. 5 we test whether these models are in agreement with low-energy data by systematically analyzing these results along with the effects due to light SUSY thresholds, intermediate gauge and matter thresholds, as well as two-loop and Yukawa-coupling effects. It is here that

we find, contrary to naive expectations based on comparing  $M_{\text{GUT}}$  and  $M_{\text{string}}$ , that certain string models may be in full agreement with low-energy data and grand unification. Sect. 6 then contains a general argument based on the modular properties of the threshold corrections which explains why they must be small in the free-fermionic models, and Sect. 7 contains our conclusions. Finally, an Appendix contains an explicit listing of all of the string models that we will be considering in this paper. A short summary of some of the main results of this paper can also be found in Ref. [25].

## 2 Realistic free-fermionic models

In the free-fermionic formulation of the heterotic string [6], all of the worldsheet degrees of freedom needed to cancel the conformal anomaly are represented in terms of internal free fermions propagating on the string worldsheet. In four dimensions, this requires 44 real left-moving (Majorana-Weyl) fermions and 20 real right-moving Majorana-Weyl fermions (or equivalently, half as many complex fermions, or any such consistent combinations of real and complex fermions). Under parallel transport around a non-contractible loop on the toroidal string worldsheet, these fermionic fields can generally accrue a phase, and each set of specified phases for all worldsheet fermions around all such non-contractible loops is called the “spin structure” of the model. Such spin structures are usually given in the form of boundary-condition “vectors”, with each element of the vector specifying the phase of a corresponding worldsheet fermion. The possible spin structures which can be used in the construction of string models are constrained by various string consistency requirements (*e.g.*, the existence of a proper worldsheet supercurrent, proper spacetime spin-statistics assignments, physically sensible projections, and modular invariance). A model is therefore constructed by choosing a set of boundary condition vectors which satisfy these constraints. In general, these basis vectors  $\mathbf{b}_k$  must span a finite additive group  $\Xi = \sum_k n_k \mathbf{b}_k$  where  $n_k = 0, \dots, N_{z_k} - 1$ . The physical massless states in the Hilbert space of a given sector  $\alpha \in \Xi$  are then obtained by acting on the vacuum state of that sector with the worldsheet bosonic and fermionic mode operators, and by subsequently applying the generalized GSO projections. The  $U(1)$  charges  $\mathbf{Q}(f)$  with respect to the unbroken Cartan generators of the four-dimensional gauge group are in one-to-one correspondence with the  $U(1)$  currents  $f^*f$  for each complex worldsheet fermion  $f$ , and are given by:

$$\mathbf{Q}(f) = \frac{1}{2} \alpha(f) + F(f) . \quad (2.1)$$

Here  $\alpha(f)$  is the boundary condition of the worldsheet fermion  $f$  in the sector  $\alpha$ ;  $\alpha(f) = 0$  for Neveu-Schwarz boundary conditions, and  $\alpha(f) = 1$  for Ramond. Likewise,  $F_\alpha(f)$  is a fermion-number operator counting +1 for each mode of  $f$  (and  $-1$  for each mode of  $f^*$ , if  $f$  is complex). For periodic complex fermions [*i.e.*, for  $\alpha(f) = 1$ ],

the vacuum is a spinor with two degenerate vacuum states  $|+\rangle$  and  $|-\rangle$ . These states are respectively annihilated by the zero modes  $f_0$  and  $f_0^*$  which obey the Clifford algebra, and have fermion numbers  $F(f) = 0, -1$  respectively.

In the realistic free-fermion models that we will be considering, the worldsheet fermions are as follows:

- a complex right-moving fermion, denoted  $\psi^\mu$ , formed from the two real fermionic superpartners of the coordinate boson  $X^\mu$ ;
- six real right-moving fermions denoted  $\chi^{1,\dots,6}$ , often paired to form three complex right-moving fermions denoted  $\chi^{12}$ ,  $\chi^{34}$ , and  $\chi^{56}$ ;
- 12 real right-moving fermions, denoted  $y^{1,\dots,6}$  and  $\omega^{1,\dots,6}$ ;
- 12 corresponding real left-moving fermions, denoted  $\bar{y}^{1,\dots,6}$  and  $\bar{\omega}^{1,\dots,6}$ ; and
- 16 remaining complex left-moving fermions, denoted  $\bar{\psi}^{1,\dots,5}$ ,  $\bar{\eta}^{1,\dots,3}$ , and  $\bar{\phi}^{1,\dots,8}$ .

The realistic models in the free-fermionic formulation are then generated by specifying a special basis of boundary-condition vectors [20, 26, 24, 21, 13, 22, 27] for these worldsheet fermions. This basis is constructed in two stages. The first stage consists of introducing the so-called NAHE set [22], which is a set of five boundary condition basis vectors denoted  $\{\mathbf{1}, S, \mathbf{b}_1, \mathbf{b}_2, \mathbf{b}_3\}$ . With ‘0’ indicating Neveu-Schwarz boundary conditions and ‘1’ indicating Ramond boundary conditions, these vectors are as follows:

	$\psi^\mu$	$\chi^{12}$	$\chi^{34}$	$\chi^{56}$	$\bar{\psi}^{1,\dots,5}$	$\bar{\eta}^1$	$\bar{\eta}^2$	$\bar{\eta}^3$	$\bar{\phi}^{1,\dots,8}$
$\mathbf{1}$	1	1	1	1	1, ..., 1	1	1	1	1, ..., 1
$S$	1	1	1	1	0, ..., 0	0	0	0	0, ..., 0
$\mathbf{b}_1$	1	1	0	0	1, ..., 1	1	0	0	0, ..., 0
$\mathbf{b}_2$	1	0	1	0	1, ..., 1	0	1	0	0, ..., 0
$\mathbf{b}_3$	1	0	0	1	1, ..., 1	0	0	1	0, ..., 0

	$y^{3,\dots,6}$	$\bar{y}^{3,\dots,6}$	$y^{1,2}, \omega^{5,6}$	$\bar{y}^{1,2}, \bar{\omega}^{5,6}$	$\omega^{1,\dots,4}$	$\bar{\omega}^{1,\dots,4}$
$\mathbf{1}$	1, ..., 1	1, ..., 1	1, ..., 1	1, ..., 1	1, ..., 1	1, ..., 1
$S$	0, ..., 0	0, ..., 0	0, ..., 0	0, ..., 0	0, ..., 0	0, ..., 0
$\mathbf{b}_1$	1, ..., 1	1, ..., 1	0, ..., 0	0, ..., 0	0, ..., 0	0, ..., 0
$\mathbf{b}_2$	0, ..., 0	0, ..., 0	1, ..., 1	1, ..., 1	0, ..., 0	0, ..., 0
$\mathbf{b}_3$	0, ..., 0	0, ..., 0	0, ..., 0	0, ..., 0	1, ..., 1	1, ..., 1

(2.2)

As can be seen, the vector  $\mathbf{1}$  has periodic boundary conditions for all the worldsheet fermions. The vector  $S$  generates the spacetime supersymmetry, and the sectors  $\mathbf{b}_1$ ,  $\mathbf{b}_2$ , and  $\mathbf{b}_3$  correspond to the three twisted sectors of a  $Z_2 \times Z_2$  orbifold. Corresponding

to this set of boundary-condition vectors is the following choice of phases which define how the generalized GSO projections are to be performed in each sector of the theory:

$$C \begin{bmatrix} \mathbf{b}_i \\ \mathbf{b}_j \end{bmatrix} = C \begin{bmatrix} \mathbf{b}_i \\ S \end{bmatrix} = C \begin{bmatrix} \mathbf{1} \\ \mathbf{1} \end{bmatrix} = -1. \quad (2.3)$$

The remaining projection phases can be determined from those above through the self-consistency constraints. The precise rules governing the choices of such vectors and phases, as well as the procedures for generating the corresponding spacetime particle spectrum, are given in Refs. [9, 10]. The mapping between the notation used here [10] and the notation used in Ref. [9] is given in the Appendix.

After imposing the NAHE set, the resulting model has gauge group  $SO(10) \times SO(6)^3 \times E_8$  and  $N = 1$  spacetime supersymmetry. The vector  $S$  is the supersymmetry generator and the superpartners of the states from any given sector  $\alpha$  are obtained from the sector  $S + \alpha$ . The spacetime vector bosons that generate the gauge group arise from the Neveu-Schwarz sector and from the sector  $I \equiv \mathbf{1} + \mathbf{b}_1 + \mathbf{b}_2 + \mathbf{b}_3$ . The Neveu-Schwarz sector produces the generators of  $SO(10) \times SO(6)^3 \times SO(16)$ . The sector  $\mathbf{1} + \mathbf{b}_1 + \mathbf{b}_2 + \mathbf{b}_3$  produces the spinorial **128** of  $SO(16)$  and completes the hidden gauge group to  $E_8$ . The vectors  $\mathbf{b}_1$ ,  $\mathbf{b}_2$ , and  $\mathbf{b}_3$  correspond to the three twisted sectors in the corresponding orbifold formulation and produce 48 spinorial **16**'s of  $SO(10)$ , sixteen from each of the sectors  $\mathbf{b}_1$ ,  $\mathbf{b}_2$ , and  $\mathbf{b}_3$ .

As can be seen from (2.2), the NAHE set divides the 44 left-moving and 20 right-moving real internal fermions in the following way: the complex fermions  $\bar{\psi}^{1,\dots,5}$  produce the observable  $SO(10)$  symmetry; the complex fermions  $\bar{\phi}^{1,\dots,8}$  produce the hidden  $E_8$  gauge group; and the fermions  $\{\bar{\eta}^1, \bar{y}^{3,\dots,6}\}$ ,  $\{\bar{\eta}^2, \bar{y}^{1,2}, \bar{\omega}^{5,6}\}$ , and  $\{\bar{\eta}^3, \bar{\omega}^{1,\dots,4}\}$  give rise to the three horizontal  $SO(6)$  symmetries. The left-moving fermions  $\{y, \omega\}$  are divided as well, in groups  $\{y^{3,\dots,6}\}$ ,  $\{y^{1,2}, \omega^{5,6}\}$ , and  $\{\omega^{1,\dots,4}\}$ . The left-moving fermions  $\chi^{12}, \chi^{34}, \chi^{56}$  carry the supersymmetry charges. Each sector  $\mathbf{b}_1$ ,  $\mathbf{b}_2$ , and  $\mathbf{b}_3$  imposes periodic boundary conditions for the fermions ( $\psi^\mu | \bar{\psi}^{1,\dots,5}$ ) and for  $(\chi_{12}, \{y^{3,\dots,6} | \bar{y}^{3,\dots,6}\}, \bar{\eta}^1)$ ,  $(\chi_{34}, \{y^{1,2}, \omega^{5,6} | \bar{y}^{1,2} \bar{\omega}^{5,6}\}, \bar{\eta}^2)$ , or  $(\chi_{56}, \{\omega^{1,\dots,4} | \bar{\omega}^{1,\dots,4}\}, \bar{\eta}^3)$  respectively. This division of the internal fermions is a reflection of the equivalent underlying  $Z_2 \times Z_2$  orbifold compactification [12]. The set of internal fermions  $\{y, \omega | \bar{y}, \bar{\omega}\}^{1,\dots,6}$  corresponds to the left/right symmetric conformal field theory of the heterotic string, or equivalently to the six-dimensional compactified manifold in a bosonic formulation. This set of left/right symmetric internal fermions plays a fundamental role in the determination of the low-energy properties of the realistic free-fermionic models.

The second stage in the construction of the realistic models consists of adding three additional basis vectors to the above NAHE set. These three additional basis vectors, which are often called  $\{\alpha, \beta, \gamma\}$ , correspond to ‘‘Wilson lines’’ in the orbifold construction. The allowed fermion boundary conditions in these additional basis vectors are of course also constrained by the string consistency constraints, and must preserve modular invariance and worldsheet supersymmetry. The choice of these ad-



ditional basis vectors  $\{\alpha, \beta, \gamma\}$  nevertheless distinguishes between different models and determine their low-energy properties. For example, three additional vectors are needed to reduce the number of massless generations to three, one from each sector  $\mathbf{b}_1$ ,  $\mathbf{b}_2$ , and  $\mathbf{b}_3$ , and the choice of their boundary conditions for the internal fermions  $\{y, \omega | \bar{y}, \bar{\omega}\}^{1, \dots, 6}$  also determines the Higgs doublet-triplet splitting and the Yukawa couplings. These low-energy phenomenological requirements therefore impose strong constraints [22] on the possible assignment of boundary conditions to the set of internal world-sheet fermions  $\{y, \omega | \bar{y}, \bar{\omega}\}^{1, \dots, 6}$ .

One then finds a variety of possibilities, with the  $SO(10)$  gauge symmetry broken to one of its subgroups, either  $SU(5) \times U(1)$ ,  $SO(6) \times SO(4)$  or  $SU(3) \times SU(2) \times U(1)_{B-L} \times U(1)_{T_{3R}}$ . These breakings are achieved by the assignment of the following boundary conditions to the fermion set  $\bar{\psi}_{1/2}^{1 \dots 5}$ . To achieve a breaking to  $SU(5) \times U(1)$ , we need to assign boundary conditions 1/2 to all of these fermions simultaneously. By contrast, to achieve a breaking to  $SO(6) \times SO(4)$ , we assign boundary condition 1 to only the first three fermions, while assigning boundary condition 0 to the remaining two. Finally, to break the  $SO(10)$  symmetry to  $SU(3) \times SU(2) \times U(1)_C \times U(1)_L$ , we impose *both* of these breakings via two separate basis vectors.\* The complete listings of boundary conditions and GSO phases for each of the models we will be considering in this paper can be found in the Appendix.

Note that all of these realistic free-fermionic models have three  $U(1)$  symmetries, denoted by  $U(1)_{r_j}$  ( $j = 1, 2, 3$ ); these are respectively generated by the left-moving world-sheet currents  $\bar{\eta}_{1/2}^1 \bar{\eta}_{1/2}^{1*}$ ,  $\bar{\eta}_{1/2}^2 \bar{\eta}_{1/2}^{2*}$ , and  $\bar{\eta}_{1/2}^3 \bar{\eta}_{1/2}^{3*}$ . These three  $U(1)$  symmetries arise due to the  $Z_2 \times Z_2$  twist with standard embedding. Additional horizontal  $U(1)$  symmetries, denoted by  $U(1)_{r_j}$  ( $j = 4, 5, \dots$ ), arise by pairing two real fermions from the sets  $\{\bar{y}^{3, \dots, 6}\}$ ,  $\{\bar{y}^{1, 2}, \bar{\omega}^{5, 6}\}$ , and  $\{\bar{\omega}^{1, \dots, 4}\}$ . The final observable gauge group depends on the number of such pairings. Indeed, the rank of the entire gauge group can vary between  $r = 16$  to  $r = 22$ . To every one of the horizontal gauged right-moving  $U(1)$  symmetries corresponds a horizontal left-moving global  $U(1)$  symmetry. Finally, the realistic free-fermionic models also contain Ising-model operators that are obtained by pairing a right-moving real fermion with a left-moving real fermion [28].

The hidden sector in the free-fermionic standard-like models is determined by the boundary condition of the internal left-moving fermions  $\bar{\phi}^{1, \dots, 8}$ . In the NAHE set, the contribution to the hidden  $E_8$  gauge group comes from the Neveu-Schwarz sector and from the sector  $I \equiv \mathbf{1} + \mathbf{b}_1 + \mathbf{b}_2 + \mathbf{b}_3$ , which produces the adjoint and spinorial representations of  $SO(16)$  respectively. The final hidden gauge group is determined by the assignment of boundary conditions for the worldsheet fermions  $\bar{\phi}^{1, \dots, 8}$  from the vectors  $\{\alpha, \beta, \gamma\}$ , and by the choices of generalized GSO projection phases.

The realistic free-fermionic models contain three chiral generations from the sectors  $\mathbf{b}_1$ ,  $\mathbf{b}_2$ , and  $\mathbf{b}_3$ . At the level of the NAHE set alone, there are 48 generations, 16 from each of these sectors. However, the vector  $\gamma$  reduces the number of gener-

---

\*Recall that  $U(1)_C = \frac{3}{2}U(1)_{B-L}$  and that  $U(1)_L = 2U(1)_{T_{3R}}$ .

ations by a factor of two by fixing the charge under  $U(1)_{R_j}$  for each of the sectors  $\mathbf{b}_1$ ,  $\mathbf{b}_2$ , and  $\mathbf{b}_3$  to be either  $+1/2$  or  $-1/2$ . A further reduction to three generations is then obtained by carefully choosing the  $\{\alpha, \beta, \gamma\}$ -boundary conditions for the real fermions  $\{y, \omega|\bar{y}, \bar{\omega}\}^{1, \dots, 6}$ . Each one of the vectors  $\{\alpha, \beta, \gamma\}$  reduces by a factor of two the number of degenerate vacua that arise from the real fermions  $\{y, \omega|\bar{y}, \bar{\omega}\}^{1, \dots, 6}$  in each of the sectors  $\mathbf{b}_1$ ,  $\mathbf{b}_2$ , and  $\mathbf{b}_3$ . After the GSO projections from the vectors  $\{\alpha, \beta, \gamma\}$ , each sector  $\mathbf{b}_1$ ,  $\mathbf{b}_2$ , and  $\mathbf{b}_3$  produces one chiral generation. Thus, the assignment of boundary conditions for the set  $\{y, \omega|\bar{y}, \bar{\omega}\}^{1, \dots, 6}$  from the vectors  $\{\alpha, \beta, \gamma\}$  is constrained by requiring three light generations. Further constraints on the assignment of boundary conditions for the set  $\{y, \omega|\bar{y}, \bar{\omega}\}^{1, \dots, 6}$  from the vectors  $\{\alpha, \beta, \gamma\}$  are imposed by requiring other phenomenological criteria, such as the presence of Higgs doublets in the massless spectrum, the projection of colored Higgs triplets, the existence of a phenomenologically realistic supersymmetric vacuum, and the existence of non-vanishing Yukawa couplings that may produce a realistic fermion mass spectrum. Satisfying all of these phenomenological criteria simultaneously is a highly non-trivial task, and it is indeed a remarkable feat that models which successfully incorporate all of these features have been constructed.

### 3 Calculating Threshold Corrections in Free-Fermionic Models

In this section we first provide a general model-independent summary of how threshold corrections are defined in string theory [19]. We then outline our specific procedure for calculating threshold corrections within the context of free-fermionic string models.

#### *Preliminary Comments Concerning String Unification and Mass Scales*

We begin, however, with some preliminary comments concerning the unification of gauge couplings and mass scales within string theory.

In order to relate string dynamics to low-energy experimental observables, we are interested in the effective field theories of the light (massless) string excitations. In particular, we are interested in the effective gauge couplings of the four-dimensional gauge group, and their beta functions. Unlike the case in field theory, however, in string theory all couplings and mass scales are dynamical variables, and are ultimately set by the values of certain moduli fields. Consequently, determination of the gauge couplings, and especially their “unification scale”, becomes a highly non-trivial issue.

Perhaps the most important factor in this regard is the presence of moduli fields in the string spectrum. Such moduli fields, which are massless gauge-neutral Lorentz scalar fields whose effective potential is classically and perturbatively flat, arise as follows. Recall that the consistency of a heterotic string theory requires 22 internal bosonic degrees of freedom in the non-supersymmetric sector (or more generally, an

internal conformal field theory of total central charge 22). Sixteen of these bosonic degrees of freedom are compactified on a flat torus with fixed radius, and generically give rise to the internal symmetries of the theory which are interpreted as the gauge symmetries of the low-energy field theory. The remaining six bosonic degrees of freedom in the non-supersymmetric sector, combined with six compactified bosonic degrees of freedom in the supersymmetric sector, are compactified on an internal manifold that can be a Calabi-Yau manifold or an orbifold. The moduli fields are then precisely those massless fields which parametrize the size and shape of this six-dimensional internal manifold.

In general, the (left-moving) gauge symmetry that one obtains for generic points in the moduli space of four-dimensional strings is  $U(1)^{22}$ . At special points in the moduli space, however, the gauge symmetries may be enhanced, with additional vector states becoming massless. Indeed, such points with enhanced symmetries can often be realized as the results of compactifications of higher-dimensional string theories, with the enhancement of the gauge symmetry arising for special choices of the compactification moduli (or equivalently, special choices of background fields) [29]. In this paper, we are interested in such points at which the effective gauge symmetry is enlarged to contain at least the MSSM gauge group  $SU(3)_C \times SU(2)_L \times U(1)_Y$ . Similarly, as one moves around in moduli space, there also exist special points at which the internal  $(c_{\text{right}}, c_{\text{left}}) = (9, 22)$  worldsheet conformal field theory effectively decomposes into a product of smaller worldsheet conformal field theories. For example, in the class of models that we study in this paper, all of the internal degrees of freedom can be represented in terms of free fermions propagating on the string worldsheet. Hence, each of the phenomenological models that we study in this paper corresponds to a special set of fixed values for the moduli fields.

The gauge couplings of the four-dimensional gauge group factors are all generally related to the gauge coupling of the string theory in ten dimensions, and are consequently related to each other at tree level. Thus, a natural unification of gauge couplings occurs in string theory regardless of the presence of any grand-unified gauge group. At tree level, the size of these couplings at unification is determined [30] by the VEV of a special moduli field, the dilaton  $\phi$ , via  $g_i \sim e^{-(\phi)}$ . Unfortunately, the presence of a classically flat dilaton potential implies that one does not know, *a priori*, the value of the dilaton VEV. Hence, at the classical level, one does not know the general size of the string coupling constant at unification.

This observation is not just limited to the gauge couplings, but applies to the gravitational coupling as well. Indeed, because string theories naturally incorporate quantum gravity and contain a massless graviton in their spectra, the gauge coupling in the effective four-dimensional gauge group can ultimately be related to the gravitational coupling by calculating the scattering amplitude between two gauge bosons and the graviton [31]. Since the string coupling constant is universal at the classical level (modulo Kac-Moody levels), and since this coupling is determined by the vacuum expectation value of the four-dimensional dilaton field, the scale for the

gravitational coupling is therefore also set by the value of the dilaton VEV. Thus *all* of the string couplings are related at tree level to a single string coupling constant whose value is *a priori* unknown.

Even more importantly, the string “unification scale”  $M_{\text{string}}$  is also not a fixed quantity, for the specific choice of  $M_{\text{string}}$  is ultimately a matter of definition which depends on the chosen renormalization scheme. This will be discussed below. In general, this scale is related to the string tension (or the phenomenological Planck scale) via  $M_{\text{string}} \sim 1/\sqrt{\alpha'} \sim g_{\text{string}} M_{\text{Planck}}$ . It is an important feature that  $M_{\text{string}}$  and  $M_{\text{Planck}}$  be of roughly the same order of magnitude; otherwise, the effective four-dimensional theory will not be weakly coupled [32], and our subsequent perturbative one-loop analysis will not be valid.

The above considerations apply at tree level in string perturbation theory. However, at the one-loop level, this situation becomes even more non-trivial, for in general the *quantum corrections* are sensitive to not only the massless string modes, but also the entire infinite tower of massive string modes, and these in turn generally depend critically on the expectation values of all of the moduli fields. In particular, the quantum corrections to the gauge couplings — *i.e.*, the so-called “threshold corrections” to be discussed below — are complicated functions of the moduli fields, and hence the running of the gauge couplings of the four-dimensional group factors in the effective low-energy theory generally depends on the expectation values of all of these moduli fields. This important dependence has been studied by several groups [33, 34, 35], and is crucial for understanding how an effective potential might be generated which not only selects a preferred string vacuum (thereby lifting the degeneracy of string vacua corresponding to different values of the moduli VEV’s), but which might also provide a means of dynamical supersymmetry breaking (*e.g.*, through the formation of gaugino condensates). Furthermore, understanding the dependence of the threshold corrections on the moduli fields gives great insight into the structure and symmetries of the string effective low-energy supergravity Lagrangian [34].

It should be noted, however, that most of these studies of the moduli dependence of the threshold corrections make some simplifying assumptions that do not hold for the realistic string models that we will be studying here. For example, the moduli dependence in those studies is usually extracted for the case of heterotic string theories with (2, 2) worldsheet supersymmetry,\* and for restricted classes of toroidal compactifications. However, the models that we will be studying here correspond to (2, 0) compactifications in which the moduli fields are not simple to identify. Similarly, this class of models contains twisted moduli and sectors that correspond to Wilson lines in an orbifold formulation. Therefore, the previous results on the moduli dependence of the gauge couplings are in general not applicable to the realistic string models we will be studying, and we will need to develop a different strategy. Of course, as discussed above, in our setting the moduli fields are fixed at particular values in the

---

\* Recent results concerning the moduli-dependence of threshold corrections in (2, 0) compactifications can be found in Ref. [36].

moduli space. Thus our results apply only at (or sufficiently near) those points in the moduli space.

### *Heavy String Threshold Corrections*

We now discuss the heavy string threshold corrections in further detail.

As we have discussed above, a natural unification of couplings occurs in string theory through which (at tree level in string perturbation theory) the gravitational (Newton) coupling constant  $G_N$  and all of the gauge couplings  $g_i$  are related to one fundamental string coupling  $g_{\text{string}}$ . The precise relation is [31]

$$g_{\text{string}}^2 = 8\pi \frac{G_N}{\alpha'} = g_i^2 k_i \quad \text{for all } i, \quad (3.1)$$

where  $\alpha'$  is the Regge slope, and  $g_i$  and  $k_i$  are respectively the gauge coupling and Kač-Moody level of the gauge-group factor  $G_i$ . However, at the one-loop level, the above tree-level relations are modified to

$$\frac{16\pi^2}{g_i^2(\mu)} = k_i \frac{16\pi^2}{g_{\text{string}}^2} + b_i \ln \frac{M_{\text{string}}^2}{\mu^2} + \tilde{\Delta}_i \quad (3.2)$$

where  $b_i$  are the one-loop beta-function coefficients, and  $\tilde{\Delta}_i$  are the quantum corrections which reflect the contributions from the infinite tower of massive string states. These heavy string states are usually neglected in an analysis of the purely massless (*i.e.*, observable) string spectrum, but they nevertheless contribute to the running of the gauge couplings. The threshold correction terms  $\tilde{\Delta}_i$  therefore represent these contributions. Because these terms  $\tilde{\Delta}_i$  enter these equations in the way that threshold corrections do in field theory, they are typically referred to as heavy string threshold corrections.

There are several things to note about these threshold corrections. First, as we have already indicated, these threshold correction terms  $\tilde{\Delta}_i$  are complicated functions of the moduli fields, and hence their values vary as one moves around in moduli space and considers different string vacua. However, our goal is to examine the role of these threshold corrections within a particular set of realistic free-fermionic models, and thus we are essentially evaluating these corrections at particular fixed points in moduli space. Consequently, for our purposes, these threshold corrections are merely numbers, and our conclusions concerning these numbers will apply only at (or sufficiently near) those points in moduli space. For our examination of gauge coupling unification within these string models, however, this will be sufficient.

A second point concerns the renormalization scheme-dependence of these threshold corrections. Clearly the gauge couplings themselves are physical quantities, and thus their values completely scheme-independent. Consequently their unification is indeed a general property. By contrast, the values for the unification scale  $M_{\text{string}}$

and the threshold corrections  $\Delta_i$  are scheme-dependent, and consequently their values can only be specified within a particular scheme. For example, it is possible to choose a definition for  $M_{\text{string}}$  which entirely absorbs the threshold dependence, leading to a definition of  $M_{\text{string}}$  which depends on the VEV's of the string moduli. However, such a definition proves inconvenient, and for supersymmetric theories it is preferable to work within the supersymmetric  $\overline{DR}$  scheme. Thus, by selecting such a scheme, we have intrinsically selected not only certain definition for  $M_{\text{string}}$ , but also a certain corresponding definition for the  $\tilde{\Delta}_i$  which appear in the renormalization group equations (3.2). We shall discuss these choices for the  $\overline{DR}$  scheme below.

Our final point concerns the dependence of these threshold corrections  $\tilde{\Delta}_i$  on the gauge group (*i.e.*, their dependence on the subscript  $i$ ). In general, there are typically two terms that arise in a complete calculation of  $\tilde{\Delta}_i$ , one of which depends on the gauge group in a complicated fashion (and which will be denoted  $\Delta_i$  without the tilde), and the other of which depends on the gauge group only through the Kač-Moody level  $k_i$  at which it is realized:

$$\tilde{\Delta}_i = \Delta_i + k_i Y . \quad (3.3)$$

Here  $Y$  denotes the contribution which is independent of the gauge group [37]. However, in our subsequent calculations, we shall only be interested in the *relative* running of the coupling constants  $g_i$ , and this means that we shall only need to evaluate the *differences* between the threshold corrections  $\tilde{\Delta}_i$  for different gauge group factors. We shall see this explicitly in Sect. 4. Moreover, since all of the realistic string models we will be examining have non-abelian gauge group factors realized at levels  $k_i = 1$ , the value of the group-independent quantity  $Y$  will be irrelevant for our purposes. We shall therefore need to evaluate only the simpler quantities  $\Delta_i$ .

Towards this end, the most important objects that we need to calculate are the one-loop string partition function  $Z(\tau)$  and the so-called ‘‘modified’’ one-loop string partition functions  $B_G(\tau)$  corresponding to each gauge group factor  $G$ . Let us first focus on the partition function  $Z(\tau)$ . In general, the partition function  $Z(\tau)$  of a given theory takes the form

$$Z(\tau) = \sum_{\alpha} (-1)^F \text{Tr}(\alpha) . \quad (3.4)$$

Here the sum over  $\alpha$  represents the sum over all sectors in the theory, the overall factor of  $(-1)^F$  ensures that spacetime bosonic and fermionic states contribute with opposite signs, and  $\text{Tr}(\alpha)$  indicates a trace over the Fock space of mode excitations of the worldsheet fields:

$$\text{Tr}(\alpha) \equiv \text{Tr} q^{H_{\alpha}} \bar{q}^{\overline{H}_{\alpha}} , \quad q \equiv e^{2\pi i \tau} . \quad (3.5)$$

Here  $H_{\alpha}$  and  $\overline{H}_{\alpha}$  are respectively the right- and left-moving Hamiltonians for the worldsheet degrees of freedom in the  $\alpha$ -sector, and thus this trace simply counts

the number of string states at each worldsheet energy  $(H_\alpha, \overline{H}_\alpha)$ , as expected for a partition function. In string models this trace is generically realized as the result of a GSO projection between subsectors of the theory:

$$\text{Tr}(\alpha) = \frac{1}{g} \sum_{\beta} c(\alpha, \beta) \text{Tr}(\alpha, \beta). \quad (3.6)$$

Here the  $\beta$ -sum implements the GSO projection,  $c(\alpha, \beta)$  are the chosen GSO phases,  $g$  is a normalization factor, and  $\text{Tr}(\alpha, \beta)$  indicates a restricted trace over the appropriate  $(\alpha, \beta)$  subsector.

The “modified” partition functions  $B_G$  which are needed in the calculation of the gauge coupling threshold corrections are then defined in a manner similar to the partition function, since they too must weigh the contributions from infinite towers of states. Indeed, they take the same form as  $Z$  in (3.4) except that they are multiplied by two factors of  $\tau_2 \equiv \text{Im} \tau$ , and their corresponding traces are modified through insertions of the square of the spacetime helicity operator  $\overline{Q}_H$  and the square of the gauge group generator  $Q_G$ :

$$\text{Tr}(\alpha) \rightarrow \text{Tr}_G(\alpha) \equiv \tau_2^2 \text{Tr} \overline{Q}_H^2 Q_G^2 q^{H_\alpha} \overline{q}^{H_\alpha} \quad (3.7)$$

[with identical corresponding insertions into  $\text{Tr}(\alpha, \beta)$ ]. Thus, these modified partition functions also count the numbers of states at each string energy level, but as expected each such degeneracy is multiplied by the gauge charge carried by the corresponding state.

Finally, just as the one-loop vacuum energy is defined as the integral of the ordinary partition function over the modular-group fundamental domain  $\mathcal{F}$ , the threshold correction contribution from the infinite tower of massive string states is given [19] by an analogous integral:

$$\Delta_G \equiv \int_{\mathcal{F}} \frac{d^2\tau}{\tau_2^2} \left[ B_G(\tau) - \tau_2 b_G \right]. \quad (3.8)$$

Note that since the contributions of the massless string states have already been included in the calculation of the beta-function coefficient  $b_G$  appearing in (3.2), they must be subtracted from the modified partition function  $B_G$  so that  $\Delta_G$  records only the extra contributions from the infinite towers of *massive* string states. This subtraction which excludes the massless states also renders the integral (3.8) finite. Note that while the measure of integration in (3.8) is modular-invariant, the integrand is not. We shall discuss the modular properties of this expression in Sect. 6.

As we have indicated at the beginning of this section, there are various assumptions which enter the derivation of the one-loop result (3.8), and consequently there are various conditions under which (3.8) may be used. We shall merely list them here for completeness; a full discussion can be found in Ref. [19]. First, as mentioned above, this result is scheme-dependent, and has in fact been derived in the so-called

$\overline{DR}$  renormalization scheme; this is the scheme that is typically used for supersymmetric field theories and renormalization-group equations. Therefore, as we shall see in Sect. 5, it will be necessary to include explicit scheme-conversion corrections when comparing with low-energy data obtained through other schemes (such as the usual  $\overline{MS}$  scheme). Second, as we have discussed above, this choice of scheme in turn fixes the choice of string unification scale [19], and amounts to the definition

$$M_{\text{string}} \equiv \frac{e^{(1-\gamma)/2} 3^{-3/4}}{4\pi} g_{\text{string}} M_{\text{Planck}} \quad (3.9)$$

where  $\gamma \approx 0.577$  is the Euler constant, and where  $g_{\text{string}} \equiv \sqrt{32\pi/(\alpha' M_{\text{Planck}}^2)}$  is the string coupling. Numerically, this yields

$$M_{\text{string}} \approx g_{\text{string}} \times 5 \times 10^{17} \text{ GeV} . \quad (3.10)$$

Third, we reiterate that the result (3.8) is only a partial result which neglects the additional contributions such as the term  $Y$  in (3.3) that are the same for all gauge group factors in a given model. Consequently, by using (3.8) we cannot consider absolute values of the threshold corrections for a given gauge group factor, but rather only the *relative differences* of the threshold corrections  $\tilde{\Delta}_{G_1} - \tilde{\Delta}_{G_2} = \Delta_{G_1} - \Delta_{G_2}$  between two gauge group factors  $G_1$  and  $G_2$  realized at equal Kač-Moody levels  $k_i$ .<sup>†</sup> However, beyond these restrictions, the one-loop expression in (3.8) is completely general. In particular, it makes no additional assumptions about the structure of a given heterotic string model, or the values of various string moduli. Thus this expression (3.8) will be our starting point when evaluating the threshold corrections in the realistic free-fermionic models. In particular, since these models have (2, 0) [rather than (2, 2)] worldsheet supersymmetry, we cannot use various moduli-dependent expressions [33, 34] which are derived from this.

### *Threshold Corrections in Free-Fermionic Models*

We now concentrate on how this general procedure for calculating threshold corrections applies to the case of string models built through the free-fermionic construction [9, 10]. As briefly discussed in Sect. 2, in the free-fermionic construction of four-dimensional heterotic string models, the light-cone gauge worldsheet field content consists of two transverse spacetime coordinate bosons, their two right-moving fermionic superpartners, and an additional set of 62 purely internal fermions of which 18 are right-moving and 44 are left-moving. Collectively these 64 Majorana-Weyl fermions may be denoted  $\psi_\ell$  ( $\ell = 1, \dots, 64$ ), with an ordering such that  $\ell = 1, 2$  correspond to the right-moving superpartner fermions carrying spacetime Lorentz indices,

---

<sup>†</sup> We point out, however, that there has recently appeared an alternative procedure for calculating threshold corrections [38] which includes these gauge-independent constant terms. We will discuss this briefly at the end of Sect. 6. In any case, these constant terms will not be necessary for our analysis, so it will be sufficient for our purposes to use the definition (3.8).



$3 \leq \ell \leq 20$  correspond to the purely-internal right-moving fermions, and  $\ell \geq 21$  correspond to the purely-internal left-moving fermions. A string model is then realized by specifying, for each sector of the theory, the boundary conditions of these 64 fermions as they traverse the two non-contractible loops of the torus, as well as a set of phases which specify the generalized GSO projections which are to be applied in that sector. These parameters are not all independent, however, and must be chosen in such a way that certain self-consistency conditions (guaranteeing a proper worldsheet supercurrent, proper spacetime spin-statistics assignments, physically sensible projections, and modular invariance) are satisfied. The rules governing the construction of such models are given in Refs. [9, 10, 11]. In particular, it is shown that the parameters describing the 64 fermionic boundary conditions in all sectors can ultimately be described via a simple “basis set” of  $(N + 1)$  different 64-component vectors  $\mathbf{V}_i$  ( $0 \leq i \leq N$ ), and that the GSO phases in all sectors can be similarly described through a single matrix  $k_{ij}$  ( $0 \leq i, j \leq N$ ). The number of basis vectors  $N$  which are necessary is of course model-dependent, increasing with the complexity of the model desired, and the complete constraint equations which relate self-consistent choices for the  $\mathbf{V}_i$  vectors and  $k_{ij}$  matrix are given in Ref. [11].

In the free-fermionic construction, each of the  $\alpha$ -sectors discussed above corresponds to a different set of fermionic worldsheet boundary conditions around the *spacelike* cycle of the torus, whereas the GSO projection is realized through the  $\beta$ -summation over different fermionic boundary conditions around the *timelike* cycle of the torus. The corresponding GSO phases and traces are then unambiguously defined once a particular model (*i.e.*, a set of  $\mathbf{V}_i$  and  $k_{ij}$  parameters) is specified. For completeness we now write these phases and traces explicitly in terms of the  $\mathbf{V}_i$  and  $k_{ij}$ . Note that henceforth we will be following the notation and conventions of Ref. [11], where the definitions of any unexplained symbols below can be found. First, in the free-fermionic models, the traces  $\text{Tr}(\alpha, \beta)$  in (3.6) are given by

$$\begin{aligned} \text{Tr}(\alpha, \beta) &\equiv \text{Tr} \left[ \exp \{ -2\pi i \beta \mathbf{V} \cdot \mathbf{N}'_{\alpha \mathbf{V}} \} q^{H_{\alpha \mathbf{V}}} \bar{q}^{\bar{H}_{\alpha \mathbf{V}}} \right] \\ &= \tau_2^{-1} \frac{1}{\bar{\eta}^{12} \eta^{24}} \left\{ \prod_{\ell=1}^{20} \sqrt{\Theta \left[ \begin{matrix} -a_\ell \\ +b_\ell \end{matrix} \right]^*} \right\} \left\{ \prod_{\ell=21}^{64} \sqrt{\Theta \left[ \begin{matrix} -a_\ell \\ +b_\ell \end{matrix} \right]} \right\} \end{aligned} \quad (3.11)$$

where  $N'_{\alpha \mathbf{V}}$  indicates the worldsheet fermionic number operator in the  $\alpha \mathbf{V}$  sector with the Ramond zero modes excluded, the asterisk indicates complex conjugation, and where

$$\begin{aligned} a_\ell &\equiv (\overline{\alpha \mathbf{V}})^\ell, & b_\ell &\equiv (\overline{\beta \mathbf{V}})^\ell \\ \eta(\tau) &\equiv q^{1/24} \prod_{n=0}^{\infty} (1 - q^n) \\ \Theta \left[ \begin{matrix} a \\ b \end{matrix} \right](\tau) &\equiv \sum_{n=-\infty}^{\infty} e^{2\pi i b n} q^{(n+a)^2/2}. \end{aligned} \quad (3.12)$$

Note that the  $\tau_2^{-1}$  factor in (3.11) represents the contribution to the trace from the zero-modes of the two transverse coordinate bosons  $X^i$ , and that the sign of the square roots in (3.11) is not of practical importance for our calculation because there will always be an even number of  $\sqrt{\Theta}$  factors for each type of  $\Theta$ -function. This latter property is guaranteed by the so-called ‘‘cubic constraint’’ of Ref. [11].

With the definition given in (3.11), the corresponding GSO phases and normalization factor in (3.6) are then given by

$$\begin{aligned} c(\alpha, \beta) &= \Gamma_{\beta\mathbf{V}}^{\overline{\alpha\mathbf{V}}} \exp \left\{ 2\pi i \sum_{i=0}^N \beta_i \left( k_{ij} \alpha_j + s_i - \mathbf{V}_i \cdot \overline{\alpha\mathbf{V}} \right) \right\} \\ g &= \prod_{i=0}^N m_i \end{aligned} \quad (3.13)$$

where  $\Gamma_{\beta\mathbf{V}}^{\overline{\alpha\mathbf{V}}} = \pm 1$  represents the additional phase contribution which can arise due to permutations of the Ramond fermionic zero-mode gamma-matrices. The definition of  $\Gamma_{\beta\mathbf{V}}^{\overline{\alpha\mathbf{V}}}$  is given explicitly<sup>‡</sup> in Eq. (3.6) of Ref. [11]. Note that  $\Gamma_{\beta\mathbf{V}}^{\overline{\alpha\mathbf{V}}} = \pm 1$ , since for a given sector  $(\alpha\mathbf{V}, \beta\mathbf{V})$  it can be shown that  $\Gamma_{\beta\mathbf{V}}^{\overline{\alpha\mathbf{V}}}$  always contains an even number of factors of  $\gamma_\ell$  for each necessarily real fermion  $\ell$ . The quantities  $m_i$  in (3.13) are defined in Ref. [11].

The calculation of the ‘‘modified’’ partition functions  $B_G$  is similar to that described above for  $Z$ ; indeed, the GSO phases remain unchanged, and the only change is that the traces are modified as in (3.7) due to the insertions of the charge operators and two extra factors of  $\tau_2$ . Now, these two extra factors of  $\tau_2$  are simple overall factors which merely increase by two the power of  $\tau_2$  in (3.11). Let us therefore focus first on the gauge group generator  $Q_G^2$ . In general, this object may be defined as

$$Q_G^2 \equiv \frac{1}{R} \sum_{r=1}^R \left\{ Q^{(r)} \right\}^2 \quad (3.14)$$

where  $R$  is the rank of the group  $G$  and where  $Q^{(r)}$  are the normalized charge elements of the Cartan subalgebra. In free-fermionic models, these charges  $Q^{(r)}$  generally appear as linear combinations of the individual charge operators corresponding to individual worldsheet fermions; such linear combinations describe how the gauge group  $G$  is ultimately embedded or realized through free fermions. Note that in the

---

<sup>‡</sup> We point out, however, that when calculating  $\Gamma_{\beta\mathbf{V}}^{\overline{\alpha\mathbf{V}}}$ , one must include  $\gamma$ -matrix factors from only those Majorana-Weyl worldsheet fermions which are *necessarily real*, *i.e.*, those fermions which cannot be globally paired in all sectors with any other Majorana-Weyl fermion in all sectors to form a complex Weyl fermion. This crucial restriction is not stated in the definition given in Ref. [11], but must be incorporated in the cases of models which simultaneously contain not only necessarily real fermions but also complex fermions with twisted ‘‘multi-periodic’’ boundary conditions. Most free-fermionic models of phenomenological interest fall into this class. This restriction was also independently pointed out in Ref. [16].

free-fermionic construction, the gauge group can be realized only through those worldsheet real Majorana-Weyl fermions which can be consistently paired in all sectors to form complex Weyl fermions, and it is indeed only for such pairs of real fermions — or equivalently for such complex Weyl fermions — that these fermionic charge operators can be defined. Let us write the indices of such complex Weyl fermions with capital letters, so that  $L \equiv (\ell_1, \ell_2)$  represents a pair of real-fermion indices with corresponding charge operator  $Q_L$ . We find, then, that one can generically expand  $Q_G^2$  as a polynomial in terms of the underlying fermionic charge operators  $Q_L$ :

$$Q_G^2 = \sum_{L,M} c_{LM}^{(G)} Q_L Q_M \quad (3.15)$$

where  $c_{LM}^{(G)}$  are the model-specific coefficients which describe the gauge group embeddings.

Having related the gauge-group generator  $Q_G^2$  to the charge operators  $Q_L$  of the individual (complex) fermions, it is now straightforward to calculate the effect of the insertion of  $Q_G^2$  into the trace. Let us first consider the effect of a single term  $Q_L$  on the contribution to the trace from the corresponding  $L^{\text{th}}$  complex fermion, where  $L \equiv (\ell_1, \ell_2)$ . Without the insertion, this isolated contribution from the two real fermions  $(\ell_1, \ell_2)$  would have been

$$\begin{aligned} \eta^{-1} \sqrt{\Theta \begin{bmatrix} -a_{\ell_1} \\ +b_{\ell_1} \end{bmatrix} \Theta \begin{bmatrix} -a_{\ell_2} \\ +b_{\ell_2} \end{bmatrix}} &= \eta^{-1} \Theta \begin{bmatrix} -a_{\ell_1} \\ +b_{\ell_1} \end{bmatrix} \\ &= \eta^{-1} \sum_{n=-\infty}^{\infty} \exp \{2\pi i b_{\ell_1} n\} q^{(n-a_{\ell_1})^2/2} . \end{aligned} \quad (3.16)$$

The first equality follows since the  $\ell_1$  and  $\ell_2$  fermions cannot be joined to form a complex fermion  $L$  unless they have the same boundary conditions in all sectors, so that  $a_{\ell_1} = a_{\ell_2}$  and  $b_{\ell_1} = b_{\ell_2}$ . The second line is just the expansion of the single  $\Theta$  function. Let us recall, however, that we may equivalently bosonize this complex fermion, in which case each term in this sum represents the contribution to the single-boson trace from a state in the corresponding bosonic one-dimensional momentum lattice  $\mathbf{P}$  with lattice coordinate  $P = n - a_{\ell_1}$  (so that the power of  $q$  in the expansion is the usual worldsheet energy contribution  $H = P^2/2$ ). But this bosonic momentum lattice  $\mathbf{P}$  is nothing but the corresponding fermionic charge lattice  $\mathbf{Q}$  [9]. Thus we immediately recognize that the charge of each state contributing to the  $n^{\text{th}}$  term in (3.16) is simply  $n - a_{\ell_1}$ , so that the trace with a single  $Q_L$  insertion is simply

$$\eta^{-1} \Theta' \begin{bmatrix} -a_{\ell_1} \\ +b_{\ell_1} \end{bmatrix} \equiv \eta^{-1} \sum_{n=-\infty}^{\infty} (n - a_{\ell_1}) \exp \{2\pi i b_{\ell_1} n\} q^{(n-a_{\ell_1})^2/2} . \quad (3.17)$$

Likewise, an insertion of  $Q_L^2$  yields

$$\eta^{-1} \Theta'' \begin{bmatrix} -a_{\ell_1} \\ +b_{\ell_1} \end{bmatrix} \equiv \eta^{-1} \sum_{n=-\infty}^{\infty} (n - a_{\ell_1})^2 \exp \{2\pi i b_{\ell_1} n\} q^{(n-a_{\ell_1})^2/2} . \quad (3.18)$$

Thus for each term  $Q_L Q_M$  in (3.15), the modified trace is the same as (3.11) except that certain  $\Theta$  functions are replaced<sup>§</sup> by either  $\Theta'$  or  $\Theta''$  as defined above: for  $L = M$  we replace the corresponding single factor of  $\Theta$  with  $\Theta''$ , and for  $L \neq M$  we replace each of the two corresponding factors of  $\Theta$  with  $\Theta'$ .

The helicity operator insertion  $\overline{Q}_H^2$  can be handled in precisely the same way, since the spacetime helicity operator is essentially the same as the gauge charge operator, only applied to the two real *right-moving* fermions  $L = (\ell_1, \ell_2) = (1, 2)$  which carry spacetime Lorentz indices, and with an overall minus sign (to take into account that we are dealing with the corresponding complex conjugate  $\overline{\Theta}$ -functions). Thus, the insertion of  $\overline{Q}_H^2$  into the trace simply amounts to an analogous replacement of the corresponding  $\overline{\Theta}$  functions with  $-\overline{\Theta}''$ , as discussed above.

The final issue we discuss is a practical matter concerning the integration which is then necessary to obtain a value of  $\Delta_G$  as in (3.8). It is of course possible to calculate  $b_G$  independently from explicit knowledge of the massless spectrum of the particular string model in question. However, there is an important self-consistency check which can be performed, since if we expand the corresponding modified partition function  $B_G$  as a power series of the form

$$B_G = \tau_2 \sum_{m,n} b_{mn}^{(G)} \overline{q}^m q^n, \quad (3.19)$$

we see that the coefficient  $b_{00}^{(G)}$ , which tallies the contributions from the massless states with total (left,right) worldsheet energies  $(n, m) = (0, 0)$  respectively, should be equal to  $b_G$ :

$$b_{00}^{(G)} = b_G. \quad (3.20)$$

Thus, the subtraction of  $\tau_2 b_G$  within the integrand of (3.8) can be most easily achieved by expanding  $B_G$  in the form (3.19), and then simply setting the coefficient  $b_{00}^{(G)}$  to zero. In any case, as remarked earlier, a non-zero value of  $b_{00}^{(G)}$  will result in a divergent integral for  $\Delta_G$ , so setting the  $b_{00}^{(G)}$  coefficient to zero is an efficient analytic way of removing what would otherwise be a logarithmic divergence. The resulting integral can then be performed by computing the sum

$$\Delta_G = \sum_{m,n} b_{mn}^{(G)} I_{mn}^{(1)} \quad (3.21)$$

---

<sup>§</sup> In performing this replacement, there is in fact a subtle sign ambiguity: although  $\Theta \begin{bmatrix} -a \\ b \end{bmatrix} = \Theta \begin{bmatrix} a \\ -b \end{bmatrix}$  as an algebraic identity, we find  $\Theta' \begin{bmatrix} -a \\ b \end{bmatrix} = -\Theta' \begin{bmatrix} a \\ -b \end{bmatrix}$ . The question then arises as to whether  $\Theta' \begin{bmatrix} -a \\ b \end{bmatrix}$  or  $\Theta' \begin{bmatrix} a \\ -b \end{bmatrix}$  is to be used in the modified trace, amounting to an ambiguity in the overall sign of the charge  $Q_L$ . However, after the GSO projections are performed, the resulting charge lattice  $\mathbf{Q}$  must be always be invariant under the inversion  $\mathbf{Q} \rightarrow -\mathbf{Q}$  (this is tantamount to CPT invariance). Thus, one must ensure only that consistent *relative* signs are used between GSO-related sectors. This amounts to choosing the same sign for  $a_\ell$  in all sectors with identical  $\alpha$ -boundary conditions but different  $\beta$ -boundary conditions.

where the general integrals

$$I_{mn}^{(s)} \equiv \int_{\mathcal{F}} \frac{d^2\tau}{\tau_2^s} \bar{q}^m q^n . \quad (3.22)$$

can each be numerically evaluated. This procedure has the dual advantages of incorporating the cancellations inherent in the GSO projections at an early stage (by calculating the coefficients  $b_{mn}^{(G)}$  prior to integration), and of analytically removing the divergence from the massless physical states  $b_{00}^{(G)}$ . Furthermore, the integrals (3.22) then need to be evaluated only once, for any change in the particular string model under discussion merely amounts to a change in the corresponding coefficients  $b_{mn}^{(G)}$ . Note that inherent in our procedure is an exchange in the order of the summation over  $(m, n)$  and the integration over  $\tau$ . As discussed in Ref. [33], this procedure is valid provided that the sum in (3.19) is convergent as  $\tau \rightarrow i\infty$ . However, this is not necessarily the case for all string theories lacking charged physical tachyonic states. Indeed, any divergences arising from different sectors in the theory will have already cancelled in the sum over all sectors, so that the total coefficients  $b_{mn}$  which we use necessarily have  $b_{mn} = 0$  for all  $n < 0$ . Hence, once the contributions from all sectors have been added together (as we have done here), the interchange is valid.

Finally, we point out that in removing the logarithmic divergence from the massless states, we have defined  $b_{00}$  through the expansion (3.19). In particular, we have *not* followed Ref. [19] in defining

$$b_{00} \stackrel{?}{=} \lim_{\tau \rightarrow i\infty} \left\{ \tau_2^{-1} B(\tau) \right\} , \quad (3.23)$$

as there can be cases for which such an identification is incorrect. For example, if  $B(\tau)$  has non-zero coefficients  $b_{mn}$  with  $m+n < 0$  and  $m \neq n$  (*i.e.*, contributions from charged “unphysical tachyons”), then the  $\tau \rightarrow i\infty$  limit of  $B(\tau)$  diverges, and (3.23) is in error. We shall see explicit examples of this sort of occurrence in Sect. 4, where we shall be considering certain models which are free of *physical* charged tachyons (*i.e.*, which have  $b_{mn} = 0$  for all  $n < 0$ ), but which nevertheless have non-zero coefficients  $b_{mn}$  for negative unequal values of  $m$  and  $n$ . Although we shall find that  $m+n > 0$  for such coefficients, the appearance of such contributions with negative and unequal values of  $m$  and  $n$  shows that these sorts of unphysical tachyons generically appear, and that unphysical tachyons with  $m+n < 0$  cannot be generically ruled out. In any case, however, such unphysical tachyons do not lead to the sorts of divergences in the threshold corrections  $\Delta$  that would arise from physical tachyons with  $m=n$ , since the contributions from *unphysical* tachyons are projected out of the integral in the  $\tau \rightarrow \infty$  region. We shall discuss the implications of such unphysical tachyons in Sect. 6.

## 4 Threshold Corrections in Particular Models

In the previous section we discussed how threshold corrections  $\Delta_G$  can be calculated in general free-fermionic models. In this section we now apply this procedure to the cases of the realistic free-fermionic models described in Sect. 2. In particular, we shall explicitly calculate the threshold corrections  $\Delta_G$  for each gauge group factor in each realistic free-fermionic model which has appeared in the literature to date. This includes the “revamped” flipped  $SU(5)$  model, several  $SU(3) \times SU(2) \times U(1)$  models, and an  $SO(6) \times SO(4)$  model. Furthermore, to test the dependence of our results on the existence of spacetime supersymmetry in these models, we shall also consider the case of a certain *non*-supersymmetric  $SU(3) \times SU(2) \times U(1)$  model.

As we discussed in the previous section, our procedure for each model is essentially the same, and can be broken down into several distinct steps.

First, for each model, we must determine the embedding of each of its gauge group factors within the free worldsheet fermions — *i.e.*, we must essentially determine the coefficients  $c_{LM}^{(G)}$  which appear in (3.15). We will refer to this procedure as obtaining the appropriate *charge polynomial* for each factor. In general, this requires not only analyzing how each gauge group factor arises within the free-fermionic construction for each model, but also calculating the appropriate overall normalizations. These issues will be discussed for each model below.

Second, for each model, we must then actually perform the threshold calculations, and calculate the sum over *all* of the contributing sectors that appear in the model. For each of the realistic models that we will be analyzing, this typically amounts to summing the separate contributions from several thousand individual sectors for each gauge group factor.

Third, for each model, we then perform a set of important self-consistency checks by verifying that the relation (3.20) holds for each gauge group factor in the model. In order to verify this relation, we therefore have to do two separate calculations: we must calculate the  $b_{00}^{(G)}$  coefficient that arises from an explicit expansion of the modified partition function  $B^{(G)}(\tau)$  for each gauge group factor  $G$ , and we must also independently calculate the beta-function coefficient  $b_G$  using our prior knowledge of the massless spectrum of the model in question. Ensuring that these two quantities agree for all gauge group factors thus guarantees that our calculations of both the massless spectrum of the model and the threshold corrections from its massive states are not in error (or inconsistent with each other). This also provides a non-trivial check of our charge polynomials, which in turn verifies our determinations of both the gauge group embeddings, and their non-trivial normalizations.

Finally, for each model, we then put all of these results together to calculate the resulting threshold corrections  $\Delta_i$ . The effects of these threshold corrections on gauge coupling unification will be analyzed in Sect. 5.

## 4.1 Flipped $SU(5)$ model

We first analyze the threshold correction in the “revamped” flipped  $SU(5)$  model [20]. The defining parameters (worldsheet fermion boundary conditions and GSO projection phases) which yield this model are listed in the Appendix. The analysis of heavy threshold corrections for this model was already performed in Ref. [39], but we shall use this example to set the procedure for the analysis in subsequent models. Furthermore, as we shall see, our results differ substantially from the numerical results of Ref. [39]. However, we believe that this difference is ultimately a reflection of our improved method of calculating the modified partition functions  $B(\tau)$ , and of numerically integrating these functions  $B(\tau)$  over the modular-group fundamental domain. In particular, as discussed in the previous section, our procedure *analytically* removes the logarithmic divergence from the massless states, and in so doing explicitly verifies that  $b_G$  and  $b_{00}^{(G)}$  agree (as required for self-consistency). Furthermore, we will see that the size of our results is more in line with those from the other realistic free-fermionic string models we will be examining, as well as from previous string threshold calculations in various orbifold [19, 40] and Type-II [41] models. We therefore believe that our results are more reliable.

### *Determining the Charge Polynomials*

This model has the observable gauge symmetry  $SU(5) \times U(1)$ , which is realized through the following five complex (left-moving) worldsheet fermions:

$$\begin{aligned}
 L = 1 & \iff \ell_i = (33, 49) \longleftarrow \text{fermion } \overline{\psi}^1 \\
 L = 2 & \iff \ell_i = (34, 50) \longleftarrow \text{fermion } \overline{\psi}^2 \\
 L = 3 & \iff \ell_i = (35, 51) \longleftarrow \text{fermion } \overline{\psi}^3 \\
 L = 4 & \iff \ell_i = (36, 52) \longleftarrow \text{fermion } \overline{\psi}^4 \\
 L = 5 & \iff \ell_i = (37, 53) \longleftarrow \text{fermion } \overline{\psi}^5 .
 \end{aligned} \tag{4.1}$$

Explicitly, this means that we are labelling as  $L = 1, \dots, 5$  the five complex fermions which can be formed, as indicated, from the real fermions 33, ..., 37 and 49, ..., 53. This latter numbering reflects the ordering of the real fermions as listed in the Appendix. These five complex fermions  $L = 1, \dots, 5$  are respectively the complex fermions called  $\overline{\psi}^{1, \dots, 5}$  in Sect. 2.

As discussed in Ref. [39], the four traceless  $SU(5)$  generators for this model can then be written in terms of the charges  $Q_L$  corresponding to these complex fermions,

$$\begin{aligned}
 Q_{SU(5)}^{(1)} &= \frac{1}{\sqrt{2}} (Q_1 - Q_2) \\
 Q_{SU(5)}^{(2)} &= \frac{1}{\sqrt{6}} (Q_1 + Q_2 - 2Q_3)
 \end{aligned}$$

$$\begin{aligned}
Q_{SU(5)}^{(3)} &= \frac{1}{\sqrt{12}} (Q_1 + Q_2 + Q_3 - 3Q_4) \\
Q_{SU(5)}^{(4)} &= \frac{1}{\sqrt{20}} (Q_1 + Q_2 + Q_3 + Q_4 - 4Q_5) ,
\end{aligned} \tag{4.2}$$

while the remaining single orthogonal  $U(1)$  generator (essentially the trace of the original larger  $U(5)$  symmetry) is therefore

$$Q_{U(1)}^{(1)} = \frac{1}{\sqrt{5}} (Q_1 + Q_2 + Q_3 + Q_4 + Q_5) . \tag{4.3}$$

Note that each of these generators is normalized so as to produce conformal dimension one for the massless states.

Given these individual generators  $Q^{(r)}$  for the  $SU(5)$  and  $U(1)$  group factors, we then compute the corresponding squared polynomials  $Q_G^2$  for each factor according to (3.14). Note that since the complex fermions  $L = 1, \dots, 5$  all have identical boundary conditions in all sectors of this model, their charges  $Q_L$  will be identical in all sectors. It is therefore possible to replace any occurrence of products of charges of the form  $Q_L Q_M$  with  $Q_1^2$  if  $L = M$ , and with  $Q_1 Q_2$  if  $L \neq M$ .<sup>\*</sup> The resulting squared polynomials then take the simple form

$$\begin{aligned}
Q_{SU(5)}^2 &= Q_1^2 - Q_1 Q_2 \\
Q_{U(1)}^2 &= Q_1^2 + 4 Q_1 Q_2 .
\end{aligned} \tag{4.4}$$

Thus, the only two ‘‘basis’’ charge insertions that we need to consider are  $Q_1^2$  and  $Q_1 Q_2$ .

Note that since we will ultimately be interested in only the *difference* of the threshold corrections for  $SU(5)$  and  $U(1)$ , we could at this stage proceed to consider only the difference of their corresponding charge polynomials in (4.4). Indeed, this would cancel the  $Q_1^2$  term completely, and leave us with a single ‘‘basis’’ insertion  $Q_1 Q_2$ . However, this simplification would later rob us of an important self-consistency check on the corresponding beta-function coefficients, for we would be able to compare only the difference of these coefficients, rather than each one separately. For this reason we shall retain both charge polynomials in our basis.

#### *Threshold Contributions: Results of Calculation*

Following the procedure outlined in the previous section, we now calculate the separate contributions to the threshold corrections that arise from each of these ‘‘basis’’ insertions. Specifically, for each basis insertion  $Q_L Q_M$  (*i.e.*, either  $Q_1^2$  or  $Q_1 Q_2$ ), we calculate the corresponding trace  $B(\tau)$  over mass levels and all sectors, its massless

---

<sup>\*</sup> Note, however, that we must continue to distinguish between the squared charge for a single fermion, and the product of single charges for two separate fermions. These two charge combinations have different effects within the trace, as discussed below (3.18).



expansion coefficient  $b_{00}$ , and its corresponding integral  $\Delta$  with its massless coefficient  $b_{00}$  set to zero (to analytically remove the divergence from the massless states). Our results are as follows:

	$b_{00}$	$\Delta$	
$Q_1^2$	3.5	12.331	(4.5)
$Q_1 Q_2$	4.5	1.53625	

In evaluating  $\Delta$ , we have followed the procedure indicated in (3.21) and (3.22), analytically  $q$ -expanding each modified partition function  $B(\tau)$  to the fourth excited energy level, and numerically evaluating the convergent integrals  $I_{mn}^{(1)}$  to the precision indicated in the results quoted above. This procedure thus minimizes any numerical error, so that essentially none remains to this level of accuracy.

### *Self-Consistency Checks*

Next we perform our self-consistency checks by comparing these values of  $b_{00}$  for each charge insertion with the one-loop beta-function coefficients expected from the (known) spectrum of this model. In general, the one-loop beta-function coefficients are given by

$$\begin{aligned}
 b_{SU(5)} &= -15 + 2 N_g + N_h \\
 b_{U(1)} &= 2 N_g + N_h + \frac{5}{4} N_4 ,
 \end{aligned}
 \tag{4.6}$$

where  $N_g$  is the number of generations and antigerations [with a generation consisting of a full  $\mathbf{16}$  representation of  $SO(10)$  decomposed under  $SU(5) \times U(1)$ ], where  $N_h$  is the number of  $\mathbf{5} + \bar{\mathbf{5}}$  Higgs pairs, where  $N_4$  is the number of hidden  $SU(4)$  pairs  $\mathbf{4} + \bar{\mathbf{4}}$  that carry  $U(1)$  charge  $\pm 5/4$ . In the revamped flipped  $SU(5)$  model, there are four  $\mathbf{16}$  representations and one  $\bar{\mathbf{16}}$  representation of  $SO(10)$ ,  $N_h = 4$  and  $N_4 = 6$ . Thus, the expected one-loop beta-function coefficients are

$$b_{SU(5)} = -1 , \quad b_{U(1)} = 21.5 .
 \tag{4.7}$$

We now compare these numbers with the values of  $b_{00}$  in (4.5). Using the charge polynomials given in (4.4), we indeed find

$$\begin{aligned}
 b_{SU(5)} &= 3.5 - 4.5 = -1 \\
 b_{U(1)} &= 3.5 + 4(4.5) = 21.5 ,
 \end{aligned}
 \tag{4.8}$$

in perfect agreement with (4.7).

### *Final Threshold Corrections*

Given these results, we now compute the final relative threshold correction  $\Delta_{U(1)} - \Delta_{SU(5)}$ . Since  $Q_{U(1)}^2 - Q_{SU(5)}^2 = 5Q_1 Q_2$ , the difference  $\Delta_{U(1)} - \Delta_{SU(5)}$  will simply be five times the value of  $\Delta$  in (4.5) for  $Q_1 Q_2$ , or

$$\Delta_{U(1)} - \Delta_{SU(5)} = 7.68125 .
 \tag{4.9}$$

Note that this result is smaller by approximately a factor of three from the value that was found in Ref. [39].

Given this relative threshold correction, we can then compute its effect on the string unification scale  $M_{\text{string}}$ . From the renormalization-group equations (3.2) for the  $SU(5)$  and  $U(1)$  couplings, and by taking the difference between the  $SU(5)$  and  $U(1)$  one-loop RGE's, we find that the corrected unification scale is in general given by

$$M_{\text{string}}^{(\text{corrected})} = M_{\text{string}}^{(\text{uncorrected})} \exp \left\{ \frac{\Delta_1 - \Delta_5}{2(b_1 - b_5)} \right\}. \quad (4.10)$$

Since  $b_{U(1)} - b_{SU(5)} = 22.5$ , we find using (4.9) that

$$M_{\text{string}}^{(\text{corrected})} \approx 5.93 \times 10^{17} \text{ GeV} \quad (4.11)$$

for this model.

We remind the reader that in the realistic free-fermionic models, one combination of the  $U(1)$  factors is anomalous. This anomalous  $U(1)$  combination arises due to the fact that these free-fermionic models are  $(2, 0)$  compactifications rather than  $(2, 2)$ . The anomalous  $U(1)$  gives rise to a Fayet-Iliopoulos  $D$ -term that breaks supersymmetry and destabilizes the vacuum. The models must therefore choose non-zero VEV's for some of the scalar fields (twisted moduli) so as to cancel the anomalous  $U(1)$   $D$ -term [42]. This corresponds to a shift in the string vacuum, and one can then ask whether this shift can modify the estimate of  $\delta\Delta$ , and consequently our estimate of  $M_{\text{string}}^{(\text{corrected})}$ . However, the contributions to the threshold corrections come from string states weighing  $\geq g_{\text{string}} M_{\text{Planck}} / \sqrt{8\pi}$ , whereas the (extra) masses acquired from shifting the string vacuum are of higher order in  $g_{\text{string}}$ . Hence, these extra masses only affect the value of  $M_{\text{string}}^{(\text{corrected})}$  at higher order, and can be ignored in our analysis [39]. The same also holds true for the other models we will be examining.

## 4.2 First $SU(3) \times SU(2) \times U(1)$ model

This model [21] is listed in the Appendix. The observable gauge group of this model is  $SU(3) \times SU(2) \times U(1)^2$ , with one of the  $U(1)$  factors associated with the  $SU(3)_{\text{color}}$  group factor (arising as the trace of the original larger  $U(3)$  color symmetry), and the other associated with the  $SU(2)_{\text{left}}$  group factor (and arising as the trace of the original larger  $U(2)$  weak isospin symmetry). We shall denote these two  $U(1)$  factors as  $U(1)_C$  and  $U(1)_L$  respectively. The electroweak hypercharge  $U(1)$  is then a linear combination of these two  $U(1)$  factors.

### *Determining the Charge Polynomials*

All of these group factors are realized through the same five complex fermions as in (4.1) for the flipped  $SU(5)$  model. Unlike the case of the flipped  $SU(5)$  model, however, these five fermions no longer share the same boundary conditions (indeed,

it is for this reason that the gauge group is altered). Rather, only the  $L = \{1, 2, 3\}$  fermions share the same boundary conditions; likewise, the remaining  $L = \{4, 5\}$  fermions share the same set of *different* boundary conditions. Therefore, we expect that our needed charge polynomials must be built from the larger set of *five* elementary “basis” charge bilinears  $\{Q_1^2, Q_1Q_2, Q_1Q_4, Q_4^2, Q_4Q_5\}$ .

Explicitly, the generators of the  $SU(3) \times SU(2) \times U(1)^2$  group are as follows. The traceless  $SU(3)$  generators are given by

$$\begin{aligned} Q_{SU(3)}^{(1)} &= \frac{1}{\sqrt{2}} (Q_1 - Q_2) \\ Q_{SU(3)}^{(2)} &= \frac{1}{\sqrt{6}} (Q_1 + Q_2 - 2Q_3) , \end{aligned} \quad (4.12)$$

and the orthogonal  $U(1)_C$  generator corresponding to this color group factor is the trace of the original  $U(3)_C$  symmetry:

$$Q_{U(1)_C}^{(1)} = \frac{1}{\sqrt{3}} (Q_1 + Q_2 + Q_3) . \quad (4.13)$$

As before, we are properly normalizing all of the linear combinations of charges so that massless states will have conformal dimension one. Since the  $L = 1, 2, 3$  fermions all have identical boundary conditions in every sector, the squared charge polynomials corresponding to these factors are then simply given by

$$\begin{aligned} Q_{SU(3)}^2 &= Q_1^2 - Q_1Q_2 \\ Q_{U(1)_C}^2 &= Q_1^2 + 2Q_1Q_2 . \end{aligned} \quad (4.14)$$

Likewise, the traceless  $SU(2)$  generator is

$$Q_{SU(2)}^{(1)} = \frac{1}{\sqrt{2}} (Q_4 - Q_5) , \quad (4.15)$$

and the corresponding orthogonal  $U(1)_L$  generator is the trace of the original  $U(2)_L$  symmetry:

$$Q_{U(1)_L}^{(1)} = \frac{1}{\sqrt{2}} (Q_4 + Q_5) . \quad (4.16)$$

Because the  $L = 4, 5$  fermions also have identical boundary conditions in all sectors, the polynomial insertions in the modified partition function are simply given by

$$\begin{aligned} Q_{SU(2)}^2 &= Q_4^2 - Q_4Q_5 \\ Q_{U(1)_L}^2 &= Q_4^2 + Q_4Q_5 . \end{aligned} \quad (4.17)$$

In this model, the electroweak hypercharge is a combination of  $U(1)_C$  and  $U(1)_L$ ,

$$U(1)_Y = \frac{1}{3} U(1)_C + \frac{1}{2} U(1)_L , \quad (4.18)$$

where the coefficients in this linear combination are appropriate for the *un*-normalized traces  $U(1)_C$  and  $U(1)_L$ . Thus, the properly normalized charge polynomial corresponding to  $U(1)_Y$  is simply

$$\begin{aligned} Q_{U(1)_Y}^2 &= \frac{6}{5} \left( \frac{Q_1 + Q_2 + Q_3}{3} + \frac{Q_4 + Q_5}{2} \right)^2 \\ &= \frac{6}{5} \left( \frac{1}{3} Q_1^2 + \frac{2}{3} Q_1 Q_2 + 2 Q_1 Q_4 + \frac{1}{2} Q_4^2 + \frac{1}{2} Q_4 Q_5 \right), \end{aligned} \quad (4.19)$$

where in the second line we have again used the fact that the boundary conditions within each of the fermion sets  $L = 1, 2, 3$  and  $L = 4, 5$  are identical.

### *Threshold Contributions: Results of Calculation*

Given the charge polynomials  $Q_{SU(3)}^2$ ,  $Q_{SU(2)}^2$ , and  $Q_{U(1)_Y}^2$  for this model, we see that, as anticipated, we need to calculate the contributions from all five of the ‘‘basis’’ charge insertions  $\{Q_1^2, Q_1 Q_2, Q_1 Q_4, Q_4^2, Q_4 Q_5\}$ . Following the same procedure as outlined in the previous section, we calculate the  $b_{00}$  coefficients and integrals  $\Delta$  corresponding to each insertion, with the results:

	$b_{00}$	$\Delta$	
$Q_1^2$	3.5	9.51642	
$Q_1 Q_2$	4.5	1.53625	
$Q_1 Q_4$	0.5	-0.291404	(4.20)
$Q_4^2$	9.5	12.951	
$Q_4 Q_5$	4.5	1.53625	

As an aside, we note that the modified partition function  $B$  for the insertion of  $Q_1 Q_2$  is the *same* as that with the insertion of  $Q_4 Q_5$ . This explains their identical values of  $b_{00}$  and  $\Delta$ . Moreover, this is also the same function  $B$  which appeared for the  $Q_1 Q_2$  insertion in the flipped  $SU(5)$  model. This is a reflection of the similarity of their underlying free-fermionic structures.

### *Self-Consistency Checks*

Let us now verify the self-consistency of the above values of  $b_{00}$ . Indeed, as we shall see, these checks become increasingly non-trivial as the models become more complex.

For this model, the full massless spectrum was presented in Ref. [21]. Here we list only the states and their non-trivial charges under  $SU(3)_C \times SU(2)_L \times U(1)_C \times U(1)_L$ . The sectors  $\mathbf{b}_1$ ,  $\mathbf{b}_2$ , and  $\mathbf{b}_3$  produce three  $\mathbf{16}$  representations of  $SO(10)$ , decomposed under  $SU(3)_C \times SU(2)_L \times U(1)_C \times U(1)_L$ . The Neveu-Schwarz sector produces three pairs of electroweak doublets with  $(U(1)_C, U(1)_L)$  charges  $(0, \pm 1)$ . The sector  $\mathbf{b}_1 + \mathbf{b}_2 + \alpha + \beta$  produces an additional pair of electroweak doublets and a pair of color triplets with  $(U(1)_C, U(1)_L)$  charges  $(0, \pm 1)$  and  $(\pm 1, 0)$  respectively.

Denoting the sector  $\mathbf{1} + \mathbf{b}_1 + \mathbf{b}_2 + \mathbf{b}_3$  as  $I$ , and introducing the notation  $(+I)$  to indicate the two sectors with and without the vector  $I$  added, we find that the four sectors  $\mathbf{b}_2 + \mathbf{b}_3 + \alpha \pm \gamma(+I)$  produce an additional pair of color triplets with  $U(1)$  charges  $(\pm\frac{1}{4}, \pm\frac{1}{2})$ , and eight  $SU(3)_C \times SU(2)_L \times U(1)_Y$  singlets with  $U(1)$  charges  $(\pm\frac{3}{4}, \mp\frac{1}{2})$ . The sectors  $\mathbf{b}_1 + \mathbf{b}_3 + \alpha \pm \gamma(+I)$  produce an additional pair of electroweak doublets with  $U(1)$  charges  $(\pm\frac{1}{4}, \pm\frac{1}{2})$ , and fourteen  $SU(3)_C \times SU(2)_L$  singlets with  $U(1)$  charges  $(\pm\frac{3}{4}, \mp\frac{1}{2})$ . Finally, the sectors  $\mathbf{b}_1 + \mathbf{b}_{2,3} + \alpha \pm \gamma$ ,  $\mathbf{b}_2 + \mathbf{b}_3 + \alpha \pm \gamma$ , and  $\mathbf{b}_1 + \mathbf{b}_2 + \mathbf{b}_3 + \alpha + \beta \pm \gamma(+I)$  produce a total of 32  $SU(3)_C \times SU(2)_L$  singlets with  $U(1)$  charges  $(\pm\frac{3}{4}, \pm\frac{1}{2})$ .

Given this matter content, the one-loop beta-functions coefficients are determined as follows. In general, we have

$$\begin{aligned} b_{SU(3)} &= -9 + 2N_g + N_3 \\ b_{SU(2)} &= -6 + 2N_g + N_2 \\ b_{U(1)_Y} &= \frac{1}{k_1} \text{Tr} Q_{U(1)_Y}^2 \end{aligned} \quad (4.21)$$

where  $N_g$  is the number of **16** representations of  $SO(10)$  in the massless spectrum,  $N_3$  is the number of color triplets in vector-like representations, and  $N_2$  is the number of electroweak doublet pairs. The trace in the  $U(1)$  beta-function is taken over the entire massless spectrum, and the  $U(1)_Y$  normalization is fixed by the standard  $SO(10)$  embedding. Since  $U(1)_C$  and  $U(1)_L$  have the standard  $SO(10)$  embedding,  $U(1)_Y$  has the standard  $SO(10)$  normalization,  $k_1 = 5/3$ . Using  $N_g = 3$ ,  $N_3 = 2$ ,  $N_2 = 5$ , and the  $U(1)$  charges given above, we then find

$$\begin{aligned} b_{SU(3)} &= -1, & b_{SU(2)} &= 5, \\ b_{U(1)_C} &= 12.5, & b_{U(1)_L} &= 14, & b_{U(1)_Y} &= 14.6. \end{aligned} \quad (4.22)$$

It is now straightforward to compare these five results with the values of  $b_{00}$  listed in (4.20). Indeed, given the expressions for the charge polynomials in (4.14), (4.17), and (4.19), we find that in each case, the appropriate linear combinations of these values of  $b_{00}$  agree with the values obtained from the massless spectrum. This check is extremely non-trivial, essentially verifying not only the known massless spectrum and our evaluation of the modified partition functions  $B(\tau)$  as sums over all of the (thousands of) sectors, but also verifying the  $U(1)$  normalizations which we determined through other means. This is therefore an important consistency check on our analysis.

### *Final Threshold Corrections*

Given the charge polynomials in (4.14), (4.17), and (4.19), we take the appropriate linear combinations of the five values of  $\Delta$  listed in (4.20) in order to obtain the relative string threshold corrections for the  $SU(3)_C$ ,  $SU(2)_L$ , and  $U(1)_{\hat{Y}}$  group factors

(where  $\hat{Y}$  refers to the *normalized* weak hypercharge). In this way we obtain the relative thresholds

$$\Delta_{U(1)_{\hat{Y}}} - \Delta_{SU(3)} = 5.0483, \quad \Delta_{U(1)_{\hat{Y}}} - \Delta_{SU(2)} = 1.6137. \quad (4.23)$$

In Sect. 5 we will examine the effects of these threshold corrections on the experimental parameters.

### 4.3 Second $SU(3) \times SU(2) \times U(1)$ model

We now turn to a different  $SU(3) \times SU(2) \times U(1)$  model [17, 23], one whose analysis is substantially more complex due to the fact that portions of its gauge group are realized as *enhanced* symmetries. In particular, this means that some of the corresponding gauge bosons originate not in the Neveu-Schwarz sector of the theory, but rather in various additional twisted sectors. Therefore, for the sake of clarity, we shall first discuss the origin and structure of the gauge symmetry in this model before proceeding with the analysis. The parameters defining this model are given in the Appendix.

#### *The Gauge Structure of the Model*

Due to the enhanced gauge symmetry of this model, it turns out that the gauge group is ultimately realized not only through the five complex fermions listed in (4.1), but also through the following additional five fermions denoted  $L = 6, \dots, 10$ :

$$\begin{aligned} L = 6 &\iff \ell_i = (25, 31) &\longleftarrow & \text{fermion } \bar{y}^3 + i\bar{y}^6 \\ L = 7 &\iff \ell_i = (21, 30) &\longleftarrow & \text{fermion } \bar{y}^4 + i\bar{\omega}^5 \\ L = 8 &\iff \ell_i = (24, 28) &\longleftarrow & \text{fermion } \bar{\omega}^2 + i\bar{\omega}^4 \\ L = 9 &\iff \ell_i = (41, 57) &\longleftarrow & \text{fermion } \bar{\phi}^1 \\ L = 10 &\iff \ell_i = (48, 64) &\longleftarrow & \text{fermion } \bar{\phi}^8. \end{aligned} \quad (4.24)$$

As before, the indices  $\ell_i$  refer to the ordering of the real fermions presented in the Appendix, and the labels  $\bar{y}^i$ ,  $\bar{\omega}^i$ , and  $\bar{\phi}^i$  refer to the discussion in Sect. 2. Three other complex fermions which we will also need to consider in our discussion (although not in our eventual calculations) are

$$\begin{aligned} L = 11 &\iff \ell_i = (38, 54) &\longleftarrow & \text{fermion } \bar{\eta}^1 \\ L = 12 &\iff \ell_i = (39, 55) &\longleftarrow & \text{fermion } \bar{\eta}^2 \\ L = 13 &\iff \ell_i = (40, 56) &\longleftarrow & \text{fermion } \bar{\eta}^3. \end{aligned} \quad (4.25)$$

We begin by outlining the various  $U(1)$  factors which will appear. First, as before, there are the  $U(1)_C$  and  $U(1)_L$  factors which are respectively the traces of the larger  $U(3)_C$  and  $U(2)_L$  symmetries. These correspond respectively to the  $L = \{1, 2, 3\}$  and

$L = \{4, 5\}$  sets of complex fermions. Next, there are  $U(1)$  factors which correspond to each of these additional complex fermions  $L = 6, \dots, 13$  individually. We shall follow the literature in naming these  $U(1)$ 's as follows:

$$\begin{aligned}
(L = 6) &\implies U(1)_4, & (L = 10) &\implies U(1)_9, \\
(L = 7) &\implies U(1)_5, & (L = 11) &\implies U(1)_1, \\
(L = 8) &\implies U(1)_6, & (L = 12) &\implies U(1)_2, \\
(L = 9) &\implies U(1)_7, & (L = 13) &\implies U(1)_3.
\end{aligned} \tag{4.26}$$

In this model, the observable gauge group formed by the gauge bosons from the Neveu-Schwarz sector alone is

$$SU(3)_C \times SU(2)_L \times U(1)_C \times U(1)_L \times U(1)_{1,2,3,4,5,6}. \tag{4.27}$$

However, in this model a new feature arises due to the appearance of two additional gauge bosons from the twisted sector  $\mathbf{1} + \alpha + 2\gamma$  [23], and two corresponding new generators. These new gauge bosons are singlets of the non-Abelian group, but carry  $U(1)$  charges. However, referring to these new generators as  $T^\pm$ , it turns out that we can define the linear combination

$$T^3 \equiv \frac{1}{4} \left[ U(1)_C + U(1)_4 + U(1)_5 + U(1)_6 + U(1)_7 - U(1)_9 \right] \tag{4.28}$$

in such a way that the three generators  $\{T^3, T^\pm\}$  together form the enhanced symmetry group  $SU(2)$ . Due to the custodial role played by this additional  $SU(2)$  in this model, we shall refer to this new factor as  $SU(2)_{\text{cust}}$ . Thus, we find that the original observable symmetry group (4.27) of this model has been enhanced to

$$SU(3)_C \times SU(2)_L \times SU(2)_{\text{cust}} \times U(1)_{C'} \times U(1)_L \times U(1)_{1,2,3} \times U(1)_{4',5',7''} \tag{4.29}$$

where (again following the nomenclature in the literature) we have chosen to define the following linear combinations of remaining  $U(1)$  factors, each of which is orthogonal to  $T^3$ :

$$\begin{aligned}
U(1)_{C'} &\equiv \frac{1}{3} U(1)_C - \frac{1}{2} U(1)_7 + \frac{1}{2} U(1)_9 \\
U(1)_{4'} &\equiv U(1)_4 - U(1)_5 \\
U(1)_{5'} &\equiv U(1)_4 + U(1)_5 - 2U(1)_6 \\
U(1)_{7''} &= U(1)_C - \frac{5}{3} \left[ U(1)_4 + U(1)_5 + U(1)_6 \right] + U(1)_7 - U(1)_9.
\end{aligned} \tag{4.30}$$

The final issue is the definition of the electroweak hypercharge in this model. In fact, due to the extended symmetry, we now have the freedom to define the weak hypercharge in several ways. One option is to define the weak hypercharge just as in

(4.18) for the previous  $SU(3) \times SU(2) \times U(1)$  model. However, in the present model, the  $U(1)_C$  symmetry is now only *part* of the extended custodial symmetry  $SU(2)_{\text{cust}}$ . Indeed, expressing  $U(1)_C$  in terms of the new linear combinations defined above, we have

$$\frac{1}{3}U(1)_C = \frac{2}{5}\left\{U(1)_{C'} + \frac{5}{16}\left[T^3 + \frac{3}{5}U_{7''}\right]\right\}. \quad (4.31)$$

Thus  $U(1)_Y$ , by depending on the  $T^3$  of the custodial  $SU(2)$ , is no longer orthogonal to  $SU(2)_{\text{cust}}$ . We must therefore instead define the new linear combination with this term removed,

$$\begin{aligned} U(1)_{Y'} &\equiv U(1)_Y - \frac{1}{8}T^3 \\ &= \frac{1}{2}U(1)_L + \frac{5}{24}U(1)_C \\ &\quad - \frac{1}{8}\left[U(1)_4 + U(1)_5 + U(1)_6 + U(1)_7 - U(1)_9\right], \end{aligned} \quad (4.32)$$

so that the weak hypercharge is expressed in terms of  $U(1)_{Y'}$  as

$$U(1)_Y = U(1)_{Y'} + \frac{1}{2}T^3 \quad \Longrightarrow \quad Q_{\text{e.m.}} = T_L^3 + Y = T_L^3 + Y' + \frac{1}{2}T_{\text{cust}}^3. \quad (4.33)$$

The final observable gauge group then takes the form

$$SU(3)_C \times SU(2)_L \times SU(2)_{\text{cust}} \times U(1)_{Y'} \times \left\{ \text{seven other } U(1) \text{ factors} \right\}. \quad (4.34)$$

Of course, these remaining seven  $U(1)$  factors must be chosen as linear combinations of the previous  $U(1)$  factors so as to be orthogonal to the each of the other factors in (4.34).

### *Determining the Charge Polynomials*

Given the gauge structure outlined above, we now determine the corresponding charge polynomials for the physically relevant  $SU(3)_C$ ,  $SU(2)_L$ ,  $SU(2)_{\text{cust}}$ , and  $U(1)_{Y'}$  factors.

The charge polynomials for the color  $SU(3)_C$  and the electroweak  $SU(2)_L$  gauge groups are the same as in the previous  $SU(3) \times SU(2) \times U(1)$  model:

$$\begin{aligned} Q_{SU(3)}^2 &= Q_1^2 - Q_1 Q_2 \\ Q_{SU(2)}^2 &= Q_4^2 - Q_4 Q_5. \end{aligned} \quad (4.35)$$

The charge polynomial for the custodial  $SU(2)_{\text{cust}}$  gauge group is obtained from the expression (4.28) for its diagonal generator, and, with proper normalization, is given



by

$$\begin{aligned}
Q_{SU(2)_{\text{cust}}}^2 &= \frac{1}{8} \left\{ 3Q_1^2 + 6(Q_1Q_2 + Q_1Q_6 + Q_1Q_7 + Q_1Q_8 + Q_1Q_9 - Q_1Q_{10}) \right. \\
&\quad + Q_6^2 + 2(Q_6Q_7 + Q_6Q_8 + Q_6Q_9 - Q_6Q_{10}) \\
&\quad + Q_7^2 + 2(Q_7Q_8 + Q_7Q_9 - Q_7Q_{10}) + Q_8^2 + 2(Q_8Q_9 - Q_8Q_{10}) \\
&\quad \left. + Q_9^2 - 2Q_9Q_{10} + Q_{10} \right\}. \tag{4.36}
\end{aligned}$$

Likewise, the normalized charge polynomial combination for  $U(1)_{Y'}$  is found to be

$$\begin{aligned}
Q_{U(1)_{Y'}}^2 &= \frac{24}{17} \left\{ \frac{25}{192}(Q_1^2 + 2Q_1Q_2) + \frac{5}{4}Q_1Q_4 \right. \\
&\quad - \frac{5}{32}(Q_1Q_6 + Q_1Q_7 + Q_1Q_8 + Q_1Q_9 - Q_1Q_{10}) \\
&\quad + \frac{1}{2}Q_4^2 + \frac{1}{2}Q_4Q_5 - \frac{1}{4}(Q_4Q_6 + Q_4Q_7 + Q_4Q_8 + Q_4Q_9 - Q_4Q_{10}) \\
&\quad + \frac{1}{64} \left[ Q_6^2 + 2(Q_6Q_7 + Q_6Q_8 + Q_6Q_9 - Q_7Q_{10}) + Q_7^2 \right. \\
&\quad \quad + 2(Q_7Q_8 + Q_7Q_9 - Q_7Q_{10}) + Q_8^2 \\
&\quad \quad \left. \left. + 2(Q_8Q_9 - Q_8Q_{10}) + Q_9^2 - 2Q_9Q_{10} + Q_{10} \right] \right\}. \tag{4.37}
\end{aligned}$$

In assembling these charge polynomials we have made use of identical boundary conditions wherever possible in order to simplify these expressions.

#### *Threshold Contributions: Results of Calculation*

Given the above polynomials, we see that we must now calculate the contributions from a basis set of 30 different charge insertions corresponding to the ten complex

worldsheet fermions  $L = 1, \dots, 10$ . Our results are as follows:

	$b_{00}$	$\Delta$		$b_{00}$	$\Delta$
$Q_1^2$	1.75	10.2704	$Q_6^2$	6.*	12.4133
$Q_1Q_2$	1.75	1.57939	$Q_6Q_7$	1.	0.803486
$Q_1Q_4$	-0.25	-0.0275848	$Q_6Q_8$	-0.5*	0.696872
$Q_1Q_6$	-0.5	-0.401743	$Q_6Q_9$	-2.5	-0.622422
$Q_1Q_7$	-0.5	-0.401743	$Q_6Q_{10}$	2.5	0.622422
$Q_1Q_8$	-1.	-0.803486	$Q_7^2$	6.*	12.4133
$Q_1Q_9$	-1.75	-0.193094	$Q_7Q_8$	-0.5*	0.696872
$Q_1Q_{10}$	1.5	0.165509	$Q_7Q_9$	-2.5	-0.622422
$Q_4^2$	11.75	12.7601	$Q_7Q_{10}$	2.5	0.622422
$Q_4Q_5$	3.75	1.80007	$Q_8^2$	6.*	11.3147
$Q_4Q_6$	0.	0.	$Q_8Q_9$	-1.	0.582808
$Q_4Q_7$	0.	0.	$Q_8Q_{10}$	1.	-0.582808
$Q_4Q_8$	0.	0.	$Q_9^2$	1.75	10.2704
$Q_4Q_9$	0.25	0.0275848	$Q_9Q_{10}$	-9.5	-2.43452
$Q_4Q_{10}$	-0.5	-0.0551696	$Q_{10}^2$	1.	10.1876

Note that unlike the simpler previous cases, some of these charge insertions resulted in modified partition functions  $B(\tau)$  containing contributions from charged unphysical tachyons. Specifically, in the  $q$ -expansion of some of these functions  $B(\tau)$ , various coefficients  $b_{mn}$  with  $m < 0$  or  $n < 0$  are non-zero. Those cases are indicated with an asterisk following the corresponding value of  $b_{00}$ . This occurrence is not unexpected, however, since such unphysical tachyons are generically present (and in fact unavoidable) in generic string models, and are required for the consistency of the theory [43]. Indeed, they do not lead to any divergence in the corresponding threshold integrals  $\Delta$ , since the fact that they are unphysical (*i.e.*, with  $m \neq n$ ,  $m - n \in \mathbb{Z}$ ) implies that they have no contributions from the region  $\tau_2 \geq 1$  of the fundamental domain  $\mathcal{F}$  from which infrared divergences might arise. We point out, however, that any unphysical tachyonic contributions with  $m + n < 0$  will render incorrect the expression (3.23) which was proposed in Ref. [19]. We will discuss some further implications of these unphysical tachyons in Sect. 6.

Also note from the above results that the charges  $Q_6$  and  $Q_7$  appear interchangeable insofar as their effects on the modified partition functions  $B(\tau)$  are concerned. Despite this fact, however, it can easily be verified that the corresponding  $L = 6$  and  $L = 7$  worldsheet fermions do *not* share the same boundary conditions.

Finally, we observe that in the cases of the insertions  $Q_4Q_6$ ,  $Q_4Q_7$ , and  $Q_4Q_8$ , the corresponding modified partition functions  $B(\tau)$  actually vanish identically. This occurs because each term in these expressions  $B(\tau)$  contains a factor of  $\Theta' \begin{bmatrix} 0 \\ 0 \end{bmatrix}$ ,  $\Theta' \begin{bmatrix} 0 \\ 1/2 \end{bmatrix}$ , or  $\Theta' \begin{bmatrix} 1/2 \\ 0 \end{bmatrix}$ . As can be seen from their definition in (3.17), these particular singly primed  $\Theta'$ -functions vanish.

### Self-Consistency Checks

Given the complexity of this model, it is crucial now more than ever to verify that our self-consistency checks are satisfied. The complete massless spectrum of the model is given in Ref. [23]. The model contains a total of eighteen color triplets, twelve from the sectors  $\mathbf{b}_1$ ,  $\mathbf{b}_2$ , and  $\mathbf{b}_3$  (which produce the light generations), and an additional three pairs from the sectors  $\mathbf{b}_{1,2} + \mathbf{b}_3 + \beta \pm \gamma$  and  $\mathbf{1} + \alpha + 2\gamma$ . Thus, from (4.21), we see that the one-loop beta-function coefficient  $b_{SU(3)_C}$  for the color  $SU(3)$  gauge group factor vanishes. Comparing this against the above values of  $b_{00}$  (in particular, the difference between those for the  $Q_1^2$  and the  $Q_1Q_2$  insertions), we see that agreement is obtained.

Turning now to the  $SU(2)_L$  electroweak symmetry, we recall [23] that this model contains 28 electroweak doublets. Five doublets are obtained from each of the sectors  $\mathbf{b}_1$ ,  $\mathbf{b}_2$ , and  $\mathbf{b}_3$ . An additional doublet beyond the Minimal Supersymmetric Standard Model arises due to the transformation of the lepton left-handed doublet under the custodial  $SU(2)_{\text{cust}}$  symmetry. The Neveu-Schwarz sector and the sector  $\mathbf{b}_1 + \mathbf{b}_2 + \alpha + \beta$  contribute three and two additional pairs, respectively. Finally, three additional electroweak doublets are obtained from each sector,  $\mathbf{1} + \mathbf{b}_i + \alpha + 2\gamma$  for  $i = 1, 2, 3$ . Thus, from (4.21), we find  $b_{SU(2)_L} = 8$ . Consulting the above charge polynomial expression for  $SU(2)_L$  and the corresponding entries in (4.38), we see that once again the values agree.

Finally, we compare the one-loop beta-function coefficients for the custodial  $SU(2)_{\text{cust}}$  symmetry. It turns out that this model contains twelve massless doublets under the custodial  $SU(2)_{\text{cust}}$  symmetry. Thus, the one-loop beta-function coefficient of the  $SU(2)_{\text{cust}}$  group vanishes. From the polynomial expression (4.36) and the appropriate entries from (4.38), it can be verified that the appropriate linear combination of  $b_{00}$ -values vanishes as well.

### Final Threshold Corrections

First we must discuss the Kač-Moody factors associated with the  $U(1)$  factors in this model. In the class of string models we have been examining, the Kač-Moody level of the non-Abelian group factor is always one. The situation is somewhat more complicated for the  $U(1)$  factors, however. In general, a given  $U(1)$  current  $U$  will be a combination of the simple worldsheet  $U(1)$  currents  $U_f \equiv f^*f$  corresponding to individual worldsheet fermions  $f$ , and will take the form  $U = \sum_f a_f U_f$  where the  $a_f$  are certain model-specific coefficients. The  $U_f$  are each individually normalized to one, so that  $\langle U_f, U_f \rangle = 1$ . To produce the correct conformal dimension for the massless states, each of the  $U(1)$  linear combinations  $U$  must also be normalized to one. The proper normalization coefficient for the linear combination  $U$  is thus given by  $N = (\sum_f a_f^2)^{-1/2}$ , so that the properly normalized  $U(1)$  current  $\hat{U}$  is given by  $\hat{U} = N \cdot U$ .

Now, in general the Kač-Moody level of the  $U(1)_Y$  generator can be deduced from

the OPE's between two of the  $U(1)$  currents, and will be

$$k_1 = 2 N^{-2} = 2 \sum_f a_f^2 . \quad (4.39)$$

For a weak hypercharge that is a combination of several  $U(1)$ 's with *different* normalizations, the result (4.39) generalizes to

$$k_1 = \sum_i a_i^2 k_i \quad (4.40)$$

where the  $k_i$  are the individual normalizations for each of the  $U(1)$ 's.

Now, in the model analyzed in Sect. 4.2, the  $U(1)_Y$  generator is given as a combination of simple worldsheet currents that produces the correct weak hypercharges for the Standard Model particles. Thus, in that case,  $k_1$  is simply given by (4.39). For the weak hypercharges (4.32) and (4.33) that appear in this model, however, we instead use (4.40). Thus, for this weak hypercharge, we see from (4.33) and (4.40) that  $k_1 = (1/4)k_{2_C} + k_{Y'} = 1/4 + 17/12 = 5/3$ , which is the same as the standard  $SO(10)$  normalization.

From (4.14) and (4.17), we then obtain the following relative string heavy threshold corrections for  $SU(3)_C$ ,  $SU(2)_L$ ,  $SU(2)_{\text{cust}}$ , and  $U(1)_{\hat{Y}'}$ :

$$\begin{aligned} \Delta_{SU(2)_L} - \Delta_{SU(3)_C} &= 2.2690 , & \Delta_{U(1)_{\hat{Y}'}} - \Delta_{SU(3)_C} &= 5.3767 \\ \Delta_{U(1)_{\hat{Y}'}} - \Delta_{SU(2)_{\text{cust}}} &= 2.8587 , & \Delta_{U(1)_{\hat{Y}'}} - \Delta_{SU(2)_{\text{cust}}} &= 2.4299 . \end{aligned} \quad (4.41)$$

Note that for future convenience [see (5.26)], we have defined

$$\Delta_{U(1)_{\hat{Y}'}} = \frac{3}{5} \left( \frac{1}{4} \Delta_{SU(2)_C} + \frac{17}{12} \Delta_{U(1)_{\hat{Y}'}} \right) , \quad (4.42)$$

whereupon

$$\Delta_{U(1)_{\hat{Y}'}} - \Delta_{SU(2)_{\text{cust}}} = \frac{17}{20} \left( \Delta_{U(1)_{\hat{Y}'}} - \Delta_{SU(2)_{\text{cust}}} \right) . \quad (4.43)$$

Alternatively, we can define the weak hypercharge to be the combination

$$U(1)_Y = \frac{1}{2} U(1)_L + U(1)_{C'} \quad (4.44)$$

where  $U(1)_{C'}$  is given in (4.30). In this case the Kač-Moody levels of  $U(1)_L$  and  $U(1)_{C'}$  are 4 and  $5/3$  respectively, so that  $k_1 = 8/3$ . In this case we find that  $\Delta_{SU(3)_C}$  and  $\Delta_{SU(2)_L}$  are the same as above, and that the relative threshold for the properly normalized  $U(1)_{\hat{Y}'}$  is

$$\Delta_{U(1)_{\hat{Y}'}} - \Delta_{SU(2)_{\text{cust}}} = 2.0939 . \quad (4.45)$$

#### 4.4 $SO(6) \times SO(4)$ model

Next we evaluate the threshold corrections in the  $SO(6) \times SO(4)$  string model of Ref. [24]. The parameters defining this model are also listed in the Appendix.

This string model realizes the Pati-Salam unification scenario, with gauge group

$$SO(6)_C \times SO(4) \simeq SU(4)_C \times SU(2)_L \times SU(2)_R \quad (4.46)$$

and three generations. Here we have only listed that portion of the observable gauge group which is of relevance to our analysis, neglecting both the hidden symmetries [such as an  $SU(8)$ ], and various  $U(1)$ 's. In the construction of this string model, a basis of nine boundary-condition vectors with only periodic and anti-periodic boundary conditions is used. In order to achieve the reduction to three massless generations, five of these vectors are taken to be the basis vectors of the NAHE set, two others are identical to the vectors  $\mathbf{b}_4$  and  $\mathbf{b}_5$  which appear in the flipped  $SU(5)$  model, another is similar to the vector  $2\gamma$  of the flipped  $SU(5)$  model, and a final vector performs the required symmetry breaking from the larger  $SO(10)$ . Thus, within this construction, the  $SO(6)_C$  gauge symmetry is realized through the  $L = 1, 2, 3$  fermions listed in (4.1), while the  $SO(4)$  gauge symmetry is realized through the  $L = 4, 5$  fermions.

##### *Determining the Charge Polynomials*

Given their similar worldsheet structures, the charge polynomials corresponding to the group factors of the  $SO(6) \times SO(4)$  model are easily obtained from those of the first  $SU(3) \times SU(2) \times U(1)$  model presented above in Sect. 4.2. In particular, the three generators of the  $SO(6)$  group are simply the generators  $Q_{SU(3)}^{(1)}$ ,  $Q_{SU(3)}^{(2)}$ , and  $Q_{U(1)_C}^{(1)}$  which appear in (4.12) and (4.13), from which we find that

$$Q_{SO(6)}^2 = Q_1^2. \quad (4.47)$$

Note that all of the non-diagonal terms  $Q_L Q_M$  with  $L \neq M$  have cancelled in this case. Likewise, the generators of the  $SO(4)$  symmetry (or equivalently, of the  $SU(2)_L$  and  $SU(2)_R$  symmetry) are respectively the generators  $Q_{SU(2)}^{(1)}$  and  $Q_{U(1)_L}^{(1)}$  which appear in (4.15) and (4.16). Their squares are therefore, as before,

$$\begin{aligned} Q_{SU(2)_L}^2 &= Q_4^2 - Q_4 Q_5 \\ Q_{SU(2)_R}^2 &= Q_4^2 + Q_4 Q_5. \end{aligned} \quad (4.48)$$

##### *Threshold Contributions: Results of Calculation*

Given these charge insertion polynomials, we see that we have the basis set  $\{Q_1^2, Q_1 Q_2, Q_4^2, Q_4 Q_5\}$  of charge polynomials. Our results are as follows:

	$b_{00}$	$\Delta$	
$Q_1^2$	3.	11.4457	
$Q_1 Q_2$	0.	0.	(4.49)
$Q_4^2$	13.	16.708	
$Q_4 Q_5$	-4.	-3.21395	

Note that for  $Q_1 Q_2$ , the modified partition function  $B(\tau)$  vanishes identically. As before, this occurs because every term in  $B(\tau)$  contains a factor of either  $\Theta' \begin{bmatrix} 0 \\ 0 \end{bmatrix}$ ,  $\Theta' \begin{bmatrix} 0 \\ 1/2 \end{bmatrix}$ , or  $\Theta' \begin{bmatrix} 1/2 \\ 0 \end{bmatrix}$ . Each of these  $\Theta'$ -functions vanishes.

### *Self-Consistency Checks*

We now consider the massless spectrum of this model, and focus on the representations of the  $SO(6) \times SO(4)$  [or  $SU(4) \times SU(2)_R \times SU(2)_L$ ] observable gauge symmetry. The sectors  $\mathbf{b}_{1,\dots,5}$  produce three generations transforming as  $(4, 2, 1) \oplus (\bar{4}, 1, 2)$  and two pairs transforming as  $(4, 1, 2) \oplus (\bar{4}, 1, 2)$  under  $SU(4) \times SU(2) \times SU(2)$ . The Neveu-Schwarz sector produces a pair of Higgs doublets transforming as  $(1, 2, 2)$  and four sextet fields transforming as  $(6, 1, 1)$ , while the sector  $S + \mathbf{b}_4 + \mathbf{b}_5$  produces an additional pair of Higgs doublets transforming as  $(1, 2, 2)$ . The sectors  $\mathbf{b}_{1,4} + \alpha$ ,  $\mathbf{b}_1 + \mathbf{b}_2 + \mathbf{b}_4 + \alpha$ ,  $\mathbf{b}_2 + \mathbf{b}_3 + \mathbf{b}_5 + \alpha$ , and  $\mathbf{b}_1 + \mathbf{b}_4 + \mathbf{b}_5 + \alpha$  produce a total of ten doublets of  $SU(2)_L$  and ten doublets of  $SU(2)_R$ . Finally, the sector  $S + \mathbf{b}_2 + \mathbf{b}_4 + \alpha$  produces an  $SU(4)$  multiplet transforming as  $(4, 1, 1) \oplus (\bar{4}, 1, 1)$ .

The one-loop beta-function coefficients of  $SU(4) \times SU(2) \times SU(2)$  are given by

$$\begin{aligned}
 b_{SU(4)} &= -12 + \frac{1}{2}(n_4 + n_{\bar{4}}) + n_6 \\
 b_{SU(2)_{L,R}} &= -6 + \frac{1}{2}n_{2_{L,R}}
 \end{aligned}
 \tag{4.50}$$

where  $n_4$  and  $n_{\bar{4}}$  are the total number of massless  $\mathbf{4}$  and  $\bar{\mathbf{4}}$  representations, where  $n_6$  is the number of sextet representations, and where  $n_{2_{L,R}}$  are the total number of doublets of  $SU(2)_{L,R}$  respectively. In this model,  $n_4 + n_{\bar{4}} = 22$  (twenty from the sectors  $\mathbf{b}_{1,\dots,5}$  and two from the sector  $S + \mathbf{b}_2 + \mathbf{b}_4 + \alpha$ ), while  $n_6 = 4$  (all sextets from the Neveu-Schwarz sector), and  $n_{2_L} = 46$  and  $n_{2_R} = 30$ . Thus, we find that the one-loop beta-function coefficients are

$$b_{SU(4)} = 3, \quad b_{SU(2)_L} = 17, \quad b_{SU(2)_R} = 9.
 \tag{4.51}$$

With the values of  $b_{00}$  given in (4.49), we see that agreement is again obtained.

### *Final Threshold Corrections*

Given the above results, it is straightforward to calculate the relative threshold corrections for each of the Planck-scale group factors in this model, yielding

$$\Delta_{SU(2)_L} - \Delta_{SU(4)} = 8.4763, \quad \Delta_{SU(2)_R} - \Delta_{SU(4)} = 2.0483. \quad (4.52)$$

We may also consider the threshold correction for the low-energy weak hypercharge. In the Pati-Salam unification scenario [44], there is an intermediate scale at which a further symmetry-breaking occurs, such that

$$\begin{aligned} SU(4) &\longrightarrow SU(3)_C \times U(1)_{B-L} \\ SU(2)_R &\longrightarrow U(1)_R. \end{aligned} \quad (4.53)$$

Here the  $U(1)_{B-L}$  symmetry is generated by the  $(B - L)$  generator of the original  $SU(4)$  symmetry, while the remaining  $U(1)_R$  symmetry is generated by the diagonal generator  $T_R^3$  of the original  $SU(2)_R$  symmetry. The normalized low-energy weak hypercharge is then defined as a linear combination of these two  $U(1)$  factors,

$$U(1)_{\hat{Y}} \equiv \sqrt{\frac{2}{5}} U(1)_{B-L} + \sqrt{\frac{3}{5}} U(1)_R. \quad (4.54)$$

From this relation we deduce that

$$\Delta_{U(1)_{\hat{Y}}} = \frac{2}{5} \Delta_{SU(4)} + \frac{3}{5} \Delta_{SU(2)_R}, \quad (4.55)$$

yielding

$$\Delta_{U(1)_{\hat{Y}}} - \Delta_{SU(4)} = \frac{3}{5} (\Delta_{SU(2)_R} - \Delta_{SU(4)}) = 1.229. \quad (4.56)$$

#### 4.5 Non-supersymmetric version of first $SU(3) \times SU(2) \times U(1)$ model

In order to assess the role that spacetime supersymmetry might play in affecting the overall magnitude of these threshold correction expressions, we have constructed a non-supersymmetric version of the first  $SU(3) \times SU(2) \times U(1)$  model analyzed above. This was achieved by altering the GSO projections of that model in such a way that spacetime supersymmetry is broken at the Planck scale (*e.g.*, the gravitinos are projected out of the spectrum), but no physical tachyons are introduced. Despite the absence of spacetime supersymmetry, the spectra of such tachyon-free models have a number of interesting properties, such as the appearance of a residual so-called “misaligned supersymmetry” [43, 45], and the vanishing of certain mass supertraces [46]. The complete parameters defining this new non-supersymmetric model are listed in the Appendix.

Note that in performing our calculations for this non-supersymmetric model, we have continued to use the threshold-correction expressions (3.8) as originally given by Kaplunovsky [19]. It is claimed in Ref. [19] that these expressions hold for all

(1, 0) string vacua, regardless of whether or not spacetime supersymmetry is present. However, it has recently been shown [38] that for non-supersymmetric vacua, there are also additional terms arising from gravitational interactions such as, *e.g.*, dilaton tadpoles.<sup>†</sup> Such terms are absent in the supersymmetric case, and do not arise in a straightforward “field-theoretic” derivation in which such gravitational interactions are not present, or in Kaplunovsky’s stringy generalization of such a field-theoretic calculation. Nevertheless, they are present in the full string calculation, and are found [38] to contribute to the threshold corrections at the same order in  $\alpha'$ . In this section, however, our goal is merely to construct a toy non-supersymmetric model, and to determine how significantly the original expression of Kaplunovsky changes when the traces are evaluated over its non-supersymmetric spectrum. Consequently we are neglecting those additional terms which would need to be included if we were performing a complete analysis of the gauge coupling unification in such a model. We hope to perform such a calculation in the future.

### *Determining the Charge Polynomials*

Because the boundary conditions of the worldsheet fermions are unaltered relative to those of the supersymmetric version of this model, both the gauge group and its realization in terms of free fermions remain intact. Therefore the charge polynomials for the various group factors are unchanged relative to the supersymmetric case in (4.14), (4.17), and (4.19).

### *Threshold Contributions: Results of Calculation*

We then repeat the calculation with the same five “basis” charge insertions. Since the boundary conditions for all fermions are the same for all sectors as they were in the previous spacetime-supersymmetric case, all changes in the results relative to that case arise due to the changes in the GSO projection phases. In particular, certain particles which had previously been in the spectrum (*e.g.*, various superpartners) have been projected out, while new particles which had previously been projected out now appear. Our results are as follows:

	$b_{00}$	$\Delta$	
$Q_1^2$	6.5*	11.322	
$Q_1Q_2$	5.5*	1.56759	
$Q_1Q_4$	1.5*	−0.260057	(4.57)
$Q_4^2$	8.5*	14.3152	
$Q_4Q_5$	5.5*	1.56759	

As in previous cases, the asterisk indicates contributions from unphysical tachyons. In fact, the existence of such contributions from unphysical tachyons is

---

<sup>†</sup> We thank E. Kiritsis for discussions on this point.



*expected* in non-supersymmetric string models, since the breaking of spacetime supersymmetry in many cases ensures that the contributions from such unphysical bosonic tachyons will not be cancelled by those from any unphysical fermionic tachyonic superpartners. As before, however, the existence of such contributions does not lead to any divergence in the corresponding threshold integrals  $\Delta$ . We will discuss the appearance of these unphysical tachyons in Sect. 6.

### *Self-Consistency Checks*

We now turn to the values of  $b_{00}$ . Although the gauge group and charge polynomials are not altered relative to the supersymmetric version of this model, the breaking of spacetime supersymmetry does modify the spectrum. Nevertheless, calculating the one-loop beta-function coefficients corresponding to the new non-supersymmetric spectrum, we now obtain

$$\begin{aligned} b_{SU(3)} &= 1 , & b_{SU(2)} &= 3 , \\ b_{U(1)_C} &= 17.5 , & b_{U(1)_L} &= 14 , & b_{U(1)_Y} &= 19 . \end{aligned} \quad (4.58)$$

Comparing this to the appropriate linear combinations of the above values of  $b_{00}$ , we see that once again agreement is obtained.

### *Final Threshold Corrections*

Using (4.14), (4.17), and (4.19), we obtain the relative string threshold corrections for the  $SU(3)_C$ ,  $SU(2)_L$ , and normalized  $U(1)_{\hat{Y}}$  group factors,

$$\Delta_{U(1)_{\hat{Y}}} - \Delta_{SU(3)} = 4.934 , \quad \Delta_{U(1)_{\hat{Y}}} - \Delta_{SU(2)} = 1.9408 . \quad (4.59)$$

We emphasize once again that these results are to be interpreted as numerical evaluations of the expression given in (3.8). As discussed above, a complete evaluation of the threshold calculations for such a toy non-supersymmetric model would require the inclusion of additional terms as well [38].

We see from these results, then, that breaking supersymmetry by a GSO projection has no appreciable effect on the magnitude of the expressions (3.8). Thus the assumption of spacetime supersymmetry in these models is not what sets the magnitude of these threshold correction contributions. In Sect. 6 we shall discuss the underlying reasons why these string-theoretic threshold corrections are so small.

## **5 Confrontation with Experiment**

In the previous section we calculated the threshold corrections  $\Delta_G$  within a wide class of realistic free-fermionic string models. In this section we will analyze the effects of these threshold corrections on the experimentally observed parameters which are measured at low energies. In so doing, we shall also consider the other effects

which might affect the running of the couplings, including non-standard hypercharge normalizations, light SUSY thresholds, intermediate gauge structure, and extra non-MSSM matter.

In order to study the effects of the heavy string threshold corrections we have calculated in Sect. 4, one method of approach might be to absorb their contributions  $\Delta_G$  into the logarithms as in (4.10), and thereby obtain a resulting “effective” string unification scale. Indeed, this is the course followed in Ref. [39]. One would then compare this modified string unification scale with the usual value given for  $M_{\text{GUT}}$ , which in turn is obtained by extrapolating the low-energy data under certain field-theoretic assumptions. However, we shall instead choose a more general path which allows us to take into account a number of different factors which might affect the analysis over the whole energy range from the  $Z$  scale to the string scale. In particular, starting from the string scale, we shall solve the one-loop gauge-coupling renormalization group equations (RGE’s) for the measured parameters  $\sin^2 \theta_W(M_Z)$  and  $\alpha_3(M_Z)$  directly at the  $Z$ -scale, and thereby obtain the explicit dependence of these parameters on the string threshold corrections. In these RGE’s, we shall include

- the corrections due to second-loop effects. We shall see, in fact, that the two-loop contributions are quite sizable, and can in some instances alter our results.
- the corrections due to Yukawa couplings.
- the corrections due to scheme conversion. The so-called  $\overline{DR}$ -scheme is used in the definition of the string heavy threshold corrections, and in the supersymmetric RGE’s. However, the  $\overline{MS}$ -scheme is the one used in extracting the low-energy parameters from experiments. One must therefore include explicit scheme-conversion terms in the RGE’s.

Furthermore, by explicitly setting up the RGE’s in this way, we will also be able to include various additional field-theoretic and string-theoretic factors that can affect the analysis. These include:

- the effects due to non-standard values of  $k_1$ , as can occur in string theory. The model-dependent parameter  $k_1$  is the essentially the normalization of the weak hypercharge generator relative to the  $U(1)$  generator in a unified theory. In  $SU(5)$  and  $SO(10)$  unified models, one has  $k_1 = 5/3$ . However, in string models, the normalization of the  $U(1)$  generators is fixed by the requirement that the conformal dimension of the massless states be equal to one. The value  $k_1$  is thus the relative normalization between the properly normalized  $U(1)$  generators, and the  $U(1)$  generator which produces the correct weak hypercharge assignment for the Standard Model quarks and leptons. Therefore, depending on how these  $U(1)$  generators are ultimately realized within a given string model, the value of  $k_1$  may be different from  $5/3$ .

- the effects arising from light SUSY thresholds (*i.e.*, the splittings of the sparticle mass spectrum).
- the effects arising from potential additional non-Abelian gauge structure at intermediate energy scale. Such additional gauge structure occurs, for example, in the Pati-Salam unification scenario, and in the corresponding  $SO(6) \times SO(4)$  string model.
- the effects arising from possible additional matter thresholds at intermediate energy scales.

All of these factors contribute, along with the heavy string thresholds, to the running of the gauge-couplings, and lead to similar correction terms in the corresponding RGE's. Thus, by starting from the string scale and evolving our couplings directly down to the  $Z$ -scale using such corrected RGE's, we can provide a serious test of whether the predictions of string theory are truly in accordance with the experimentally observed low-energy data.

#### *Low-Energy Experimental Inputs*

For our subsequent analysis, the input parameters are the tree-level string prediction [19]

$$M_S \equiv M_{\text{string}} \approx g_{\text{string}} \times 5 \times 10^{17} \text{ GeV} , \quad (5.1)$$

the mass of the  $Z$  [47]

$$M_Z \equiv 91.161 \pm 0.031 \text{ GeV} , \quad (5.2)$$

and the electromagnetic coupling at the  $Z$ -scale [47]

$$a^{-1} \equiv \alpha_{\text{e.m.}}(M_Z)^{-1} = 127.9 \pm 0.1 . \quad (5.3)$$

From the RGE's, we then obtain predictions for  $\sin^2 \theta_W(M_Z)$  and  $\alpha_3(M_Z)$ . The experimental values we wish to obtain are as follows. For the  $\overline{MS}$ -value of  $\sin^2 \theta_W$ , extracted from low-energy data [48], we take

$$\sin^2 \theta_W(M_Z)|_{\overline{MS}} = 0.2315 \pm 0.001 , \quad (5.4)$$

while for the  $\overline{MS}$ -value of  $\alpha_3(M_Z)$  we take [49]

$$\alpha_3(M_Z)|_{\overline{MS}} = 0.120 \pm 0.010 . \quad (5.5)$$

#### *Renormalization Group Equations*

We seek to compare the above experimentally observed values with the predictions from string theory. To do this, we set up our calculation as follows. Recall that in

general, string unification implies that each gauge coupling individually has a one-loop RGE of the form

$$\frac{16\pi^2}{g_i^2(\mu)} = k_i \frac{16\pi^2}{g_{\text{string}}^2} + b_i \ln \frac{M_{\text{string}}^2}{\mu^2} + \Delta_i^{(\text{total})} \quad (5.6)$$

where  $b_i$  are the one-loop beta-function coefficients, and where the  $\Delta_i^{(\text{total})}$  represent the combined corrections from each of the effects outlined above. From (5.6) we wish to obtain expressions for  $\sin^2 \theta_W(M_Z)$  and  $\alpha_3(M_Z)$ . To this end, we solve (5.6) for  $i = 1, 2, 3$  simultaneously in order to eliminate the direct dependence on  $g_{\text{string}}$  from the first term on the right sides of (5.6). A small dependence on  $g_{\text{string}}$  remains through  $M_{\text{string}}$ , and in all subsequent numerical calculations we will allow  $M_{\text{string}}$  to vary slightly in order to account for this. In each case we initially assume the MSSM spectrum between the Planck scale and the  $Z$  scale, and treat all perturbations of this scenario through effective correction terms. The expression for  $\alpha_3(M_Z)$  then takes the general form

$$\alpha_3^{-1}(M_Z)|_{\overline{MS}} = \Delta_{\text{MSSM}}^{(\alpha)} + \Delta_{\text{h.s.}}^{(\alpha)} + \Delta_{\text{l.s.}}^{(\alpha)} + \Delta_{\text{i.g.}}^{(\alpha)} + \Delta_{\text{i.m.}}^{(\alpha)} + \Delta_{2\text{-loop}}^{(\alpha)} + \Delta_{\text{Yuk.}}^{(\alpha)} + \Delta_{\text{conv.}}^{(\alpha)}, \quad (5.7)$$

and likewise for  $\sin^2 \theta_W(M_Z)|_{\overline{MS}}$  with corresponding corrections  $\Delta^{(\text{sin})}$ . Here  $\Delta_{\text{MSSM}}$  represents the one-loop contributions from the spectrum of the Minimal Supersymmetric Standard Model (MSSM) between the unification scale and the  $Z$  scale, and the remaining  $\Delta$  terms respectively correspond to the second-loop corrections, the Yukawa-coupling corrections, the corrections from scheme conversion, the heavy string thresholds that were calculated in the previous section, possible light SUSY threshold corrections, corrections from possible additional intermediate-scale gauge structure between the unification and  $Z$  scales, and corrections from possible extra intermediate-scale matter. Each of these  $\Delta$  terms has an algebraic expression in terms of  $\alpha_{\text{e.m.}}$  as well as model-specific parameters such as  $k_1$ , the beta-function coefficients, and the appropriate intermediate mass scales. In particular, for  $\sin^2 \theta_W(M_Z)$  we find:

$$\begin{aligned} \Delta_{\text{MSSM}}^{(\text{sin})} &= \frac{1}{k_1 + 1} \left[ 1 - \frac{a}{2\pi} (11 - k_1) \ln \frac{M_S}{M_Z} \right] \\ \Delta_{\text{l.s.}}^{(\text{sin})} &= \frac{1}{2\pi} \sum_{\text{sp}} \frac{k_1 a}{k_1 + 1} (b_{1_{\text{sp}}} - b_{2_{\text{sp}}}) \ln \frac{M_{\text{sp}}}{M_Z} \\ \Delta_{\text{i.m.}}^{(\text{sin})} &= \frac{1}{2\pi} \sum_i \frac{k_1 a}{k_1 + 1} (b_{2_i} - b_{1_i}) \ln \frac{M_S}{M_i} \\ \Delta_{\text{h.s.}}^{(\text{sin})} &= \frac{1}{2\pi} \frac{k_1 a}{k_1 + 1} \frac{\Delta_2 - \Delta_{\hat{Y}}}{2}. \end{aligned} \quad (5.8)$$

where  $M_S \equiv M_{\text{string}}$  is the string unification scale,  $a \equiv \alpha_{\text{e.m.}}(M_Z)$ ,  $M_{\text{sp}}$  are the sparticle masses,  $M_i$  are the intermediate gauge mass scales, and  $\Delta_{3,2,\hat{Y}}$  are respectively

the heavy string threshold corrections for the strong, electroweak, and properly normalized hypercharge gauge group factors. Likewise, for  $\alpha_3^{-1}(M_Z)$ , we find:

$$\begin{aligned}
\Delta_{\text{MSSM}}^{(\alpha)} &= \frac{1}{1+k_1} \left[ \frac{1}{a} + \frac{1}{2\pi} (-3k_1 - 15) \ln \frac{M_S}{M_Z} \right] \\
\Delta_{\text{l.s.}}^{(\alpha)} &= \frac{1}{2\pi} \sum_{\text{sp}} \left[ \left( \frac{k_1}{1+k_1} \right) b_{1\text{sp}} + \left( \frac{1}{1+k_1} \right) b_{2\text{sp}} - b_{3\text{sp}} \right] \ln \frac{M_{\text{sp}}}{M_Z} \\
\Delta_{\text{i.m.}}^{(\alpha)} &= -\frac{1}{2\pi} \sum_i \left[ \left( \frac{k_1}{1+k_1} \right) b_{1i} + \left( \frac{1}{1+k_1} \right) b_{2i} - b_{3i} \right] \ln \frac{M_S}{M_i} \\
\Delta_{\text{h.s.}}^{(\alpha)} &= -\frac{1}{4\pi} \frac{1}{1+k_1} [k_1(\Delta_{\hat{Y}} - \Delta_3) + (\Delta_2 - \Delta_3)] \tag{5.9}
\end{aligned}$$

Note that in the above solution of the one-loop RGE's for  $\sin^2 \theta_W(M_Z)$  and  $\alpha_3^{-1}(M_Z)$ , only the *differences* of the RGE's (5.6) for the separate gauge couplings are used. Therefore, the expressions for  $\sin^2 \theta_W(M_Z)$  and  $\alpha_3(M_Z)$  depend only on the differences of the heavy string threshold corrections  $\Delta_{3,2,\hat{Y}}$  of the different group factors, and not on their absolute values. Consequently, the group-independent additive factors in the full expression for the one-loop string threshold corrections do not affect the predictions for the experimentally measured parameters  $\sin^2 \theta_W(M_Z)$  and  $\alpha_3(M_Z)$ . This is important, for these extra factors are neglected in the original definition for  $\Delta_G$  in (3.8).

Finally, before we can proceed, we must estimate the second-loop and Yukawa-coupling corrections. As discussed above, these are calculated assuming the MSSM spectrum between the string unification and  $Z$  scales. To estimate the size of the second-loop corrections, we run the one- and two-loop RGE's for the gauge couplings and take the difference. Likewise, to estimate the Yukawa-coupling corrections, we evolve the two-loop RGE's for the gauge couplings coupled with the one-loop RGE's for the heaviest-generation Yukawa couplings, assuming  $\lambda_t \approx 1$  and  $\lambda_b = \lambda_\tau \approx 1/8$  at the string unification scale. We then subtract the two-loop non-coupled result. As indicated above, these differences are then each averaged for different values of  $M_{\text{string}}$  (in order to account for various values of  $g_{\text{string}}$ ). Numerically, this yields the following results for  $\sin^2 \theta_W(M_Z)|_{\overline{MS}}$ :

$$\begin{aligned}
\Delta_{2\text{-loop}}^{(\sin)} &\sim 0.00678 \\
\Delta_{\text{Yuk.}}^{(\sin)} &\sim -0.00091 \\
\Delta_{\text{conv.}}^{(\sin)} &\sim 0.00026 \ , \tag{5.10}
\end{aligned}$$

while for  $\alpha_3^{-1}(M_Z)|_{\overline{MS}}$  we find:

$$\begin{aligned}
\Delta_{2\text{-loop}}^{(\alpha)} &\sim 0.80757 \\
\Delta_{\text{Yuk.}}^{(\alpha)} &\sim -0.16728 \\
\Delta_{\text{conv.}}^{(\alpha)} &\sim 0.0596831 \ . \tag{5.11}
\end{aligned}$$

In the next subsections, we will discuss and evaluate the various remaining contributions to the experimentally measured parameters  $\sin^2 \theta_W(M_Z)$  and  $\alpha_3(M_Z)$ .

### 5.1 MSSM spectrum between $M_Z$ and $M_{\text{string}}$

In this section we discuss the predictions for  $\sin^2 \theta_W(M_Z)$  and  $\alpha_3(M_Z)$  assuming that the particle spectrum between the string unification scale and the  $Z$ -scale is purely that of the Minimal Supersymmetric Standard Model (MSSM). The contributions of such a spectrum are those given in the first lines of (5.8) and (5.9) respectively. We also include the two-loop and Yukawa-coupling corrections to the one-loop RGE's, and the corrections due to the conversion from the  $\overline{DR}$ -scheme to the  $\overline{MS}$ -scheme. These are the corrections which appear in (5.10) and (5.11).

Using the RGE's with these two terms as discussed in Sect. 5.0, we find that the prediction for  $\sin^2 \theta_W(M_Z)$  deviates from the experimentally measured value by approximately 5%, and that the prediction for  $\alpha_3(M_Z)$  deviates from the experimentally measured value by approximately 100%. The discrepancy with  $\alpha_3(M_Z)$  is, of course, expected, since it is this discrepancy which is ultimately the root of the factor of twenty that separates the string scale  $M_{\text{string}}$  from the MSSM unification scale  $M_{\text{MSSM}}$ . Indeed, in this way we can even see why the value of  $\alpha_3(M_Z)$  should be off by 100%. Suppose, for example, that we were to run the RGE's not from  $M_{\text{string}} \approx 20M_{\text{MSSM}}$  to  $M_Z$ , but rather from  $M_{\text{MSSM}}$  to  $M_Z/20$ . As expected from the running of the QCD coupling below the  $Z$  scale, we would then find that  $\alpha_3(M_Z/20)$  deviates from  $\alpha_3(M_Z)$  by approximately 100%. However, due to the additive nature of the logarithms involved, this effect on  $\alpha_3$  should be identical to that achieved by running instead from  $M_{\text{string}}$  to  $M_Z$ . Indeed, in the string unification scenario, we have simply shifted this discrepancy from the low scale near  $M_Z$  to the high scale near  $M_{\text{string}}$ . Thus, we see that the simplest string unification scenario assuming the MSSM spectrum below the string scale should indeed predict a value of  $\alpha_3(M_Z)$  that is off by 100%.

In Figs. 1 and 2, we have plotted  $\sin^2 \theta_W(M_Z)$  and  $\alpha_3(M_Z)$  versus  $M_{\text{string}}$  in the range  $1 \times 10^{16} \text{ GeV} \leq M_{\text{string}} \leq 7 \times 10^{17} \text{ GeV}$ , both with and without the two-loop corrections. In the analysis for these figures, rather than using the averaged second-loop corrections from (5.10) and (5.11), we have run the full two-loop RGE's over the entire range of  $M_{\text{string}}$ . In Fig. 3, we have plotted the two low-energy variables  $\sin^2 \theta_W(M_Z)$  and  $\alpha_3(M_Z)$  versus each other as  $M_{\text{string}}$  is varied. From these figures we see that for  $3 \times 10^{17} \text{ GeV} \leq M_{\text{string}} \leq 7 \times 10^{17} \text{ GeV}$ , both  $\sin^2 \theta_W(M_Z)$  and  $\alpha_3(M_Z)$  are approximately  $\sim 0.22$ . Thus, as expected, assuming the MSSM spectrum between the  $Z$  scale and the string unification scale results in significant disagreement with the low-energy data.

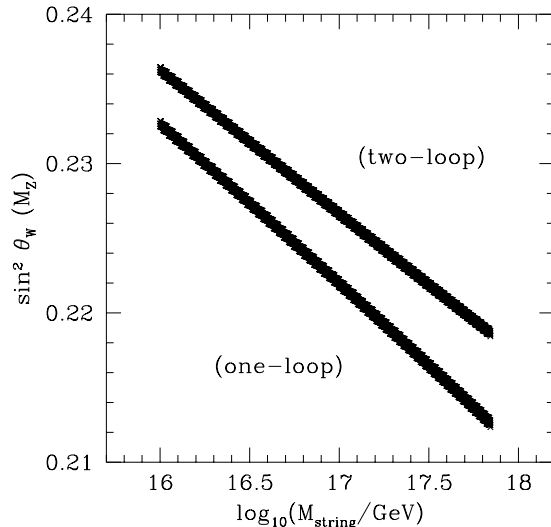


Figure 1: Dependence on the string scale:  $\sin^2 \theta_W(M_Z)$  vs.  $M_{\text{string}}$ . Results for both one-loop and two-loop running are plotted.

## 5.2 Non-standard hypercharge normalizations

We can also examine the extent to which this MSSM string unification scenario depends on the value of the hypercharge normalization  $k_1$ . In the  $SU(5)$  or  $SO(10)$  unification schemes, the value of  $k_1$  is  $5/3$ . However, in string unification, this assumption is not necessary, as other embeddings of the weak hypercharge into the four-dimensional string gauge group are possible. This possibility is also discussed in Ref. [18]. In Figs. 4 and 5, we plot the predictions for  $\sin^2 \theta_W(M_Z)$  and  $\alpha_3(M_Z)$  versus  $k_1$  in the range  $1 < k_1 < 2$ . We take  $3 \times 10^{17} \text{ GeV} \leq M_{\text{string}} \leq 7 \times 10^{17} \text{ GeV}$ . From these figures we find that the one-loop string prediction can be in agreement with the measured values for a value of  $k_1 \approx 1.4$ .

Unfortunately, none of the realistic models we have been analyzing has a value of  $k_1$  of this size, and indeed all of the models have  $k_1 \geq 5/3$ . Similar results have also been found, for example, in the case of semi-realistic orbifold models (see, *e.g.*, Ref. [50]). Moreover, in string theory, there are general reasons to expect that  $k_1 \geq 5/3$  in realistic models. The reason is as follows.\* As discussed at the end of Sect. 4.3, the weak hypercharge is a combination of simple worldsheet currents which are each normalized to one. To produce the correct conformal dimension for the massless states, every  $U(1)$  generator (each of which is ultimately a combination of simple worldsheet currents) must be normalized to one. By contrast, the  $U(1)$  generator that produces the correct weak hypercharges for the Standard Model particles is *not*

\* We thank J. March-Russell for discussions on this point [51].

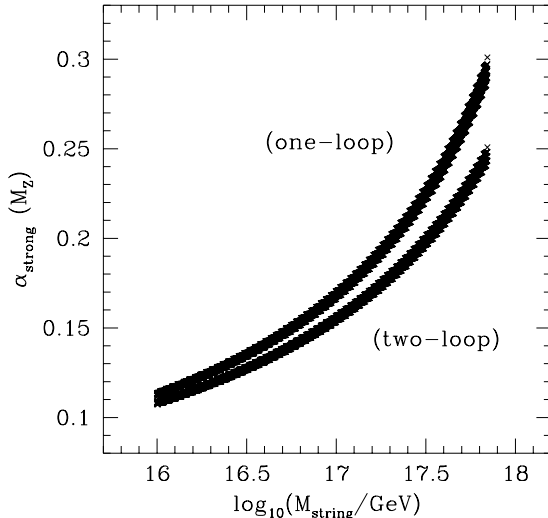


Figure 2: Dependence on the string scale:  $\alpha_3(M_Z)$  vs.  $M_{\text{string}}$ . Results for both one-loop and two-loop running are plotted.

normalized to one, and  $k_1$  is essentially the normalization coefficient of the properly normalized weak hypercharge generator. Since the weak hypercharge generator is a combination of simple worldsheet currents, we can determine the minimal number of simple worldsheet currents that must be used in order to generate the correct hypercharges for all the quark and lepton families and to satisfy the various anomaly cancellation constraints. We then find that the minimal value of  $k_1$  is essentially  $5/3$ . It is not likely, therefore, that this effect can explain the discrepancy between the low-energy data and the suppositions of string unification. Thus, in the analysis below, we shall take  $k_1 = 5/3$  unless otherwise stated.

### 5.3 Light SUSY thresholds

We now study the effect of the light SUSY thresholds on the predictions for  $\sin^2 \theta_W(M_Z)$  and  $\alpha_3(M_Z)$ . These effects correspond to the second lines of (5.8) and (5.9) respectively.

Our purpose here is not a detailed quantitative analysis of the sparticle threshold corrections, but rather a qualitative examination of whether the light SUSY thresholds are capable of removing the discrepancy, found in Sect. 5.1, between the predicted and the experimentally observed values of  $\sin^2 \theta_W(M_Z)$  and  $\alpha_3(M_Z)$ . Consequently, to parametrize the sparticle thresholds, we shall consider the spectrum of the MSSM near the  $Z$  scale, and neglect the contributions from the Yukawa couplings and electroweak VEV's. This implies that all of the supersymmetric scalar mass matrices, including that of the stop quark, will be diagonal, and that the  $D$ -term contributions



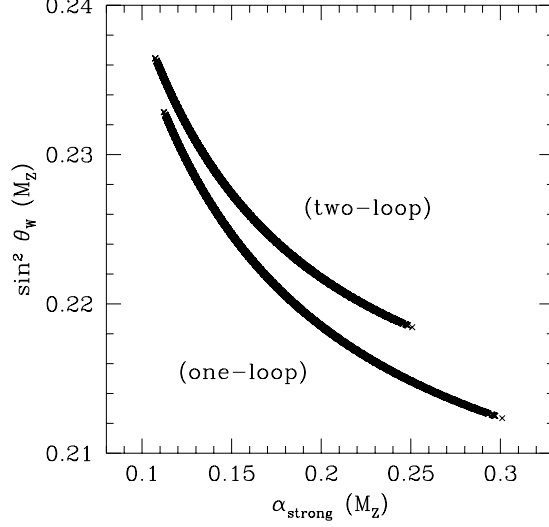


Figure 3: Dependence on the string scale:  $\alpha_3(M_Z)$  vs.  $\sin^2 \theta_W(M_Z)$ , as  $M_{\text{string}}$  is varied. Results for both one-loop and two-loop running are plotted.

to the particle masses are neglected. With these assumptions, the sparticle masses can be obtained from the one-loop RGE's for the soft SUSY-breaking terms. In terms of the usual soft SUSY-breaking parameters  $m_0$ ,  $m_{1/2}$ , and  $\mu$ , the gluino, wino, and higgsino masses are then given by [1]

$$m_{\tilde{g}} = \frac{\alpha_3(m_{\tilde{g}})}{\alpha_3} m_{1/2}, \quad m_{\tilde{w}} = \frac{\alpha_2(m_{\tilde{g}})}{\alpha_3} m_{1/2}, \quad m_{\tilde{h}} = \mu. \quad (5.12)$$

Likewise, the scalar sparticle masses are given by

$$m_{\tilde{p}}^2 = m_0^2 + c_{\tilde{p}} m_{1/2}^2 \quad (5.13)$$

where the coefficients  $c_{\tilde{p}}$  for the different sparticles are given in terms of their hypercharges  $Y_{\tilde{p}}$  by

$$c_{\tilde{p}} = c_3(m_{\tilde{p}}) + c_2(m_{\tilde{p}}) + Y_{\tilde{p}}^2 c_y(m_{\tilde{p}}) \quad (5.14)$$

with

$$\begin{aligned} c_3(m_{\tilde{p}}) &= -\frac{8}{9} [1 - (1 + 3X)^{-2}] \\ c_2(m_{\tilde{p}}) &= \frac{3}{2} [1 - (1 - X)^{-2}] \\ c_y(m_{\tilde{p}}) &= \frac{2k_1}{11} [1 - (1 - 11X/k_1)^{-2}] \end{aligned} \quad (5.15)$$

and

$$X \equiv \frac{1}{2\pi} \alpha_{\text{string}} \ln \frac{M_{\text{string}}}{m_{\tilde{p}}}. \quad (5.16)$$

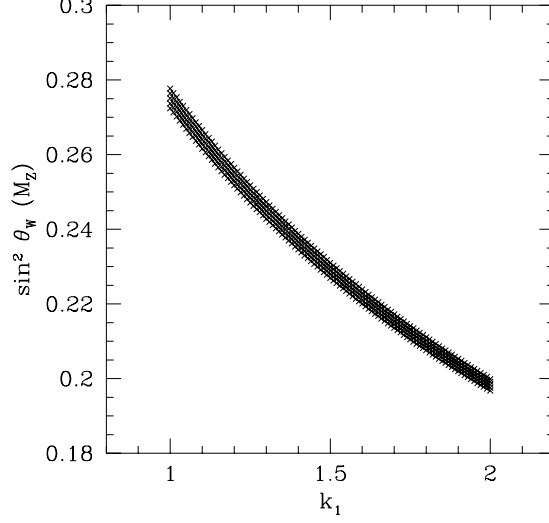


Figure 4: The effects of hypercharge normalization:  $\sin^2 \theta_W(M_Z)$  vs.  $k_1$ . The width of the curve reflects the variations in  $M_{\text{string}}$ .

The corresponding corrections to  $\sin^2 \theta_W(M_Z)$  and  $\alpha_3(M_Z)$  due to these light SUSY thresholds are then given by

$$\Delta_{\text{l.s.}}^{(\sin)} = \frac{1}{2\pi} \frac{k_1 a}{k_1 + 1} \sum_R n_R C_R^{(\sin)} \ln \frac{m_R}{M_Z} \quad (5.17)$$

and

$$\Delta_{\text{l.s.}}^{(\alpha)} = \frac{1}{2\pi} \sum_R n_R C_R^{(\alpha)} \ln \frac{m_R}{M_Z} \quad (5.18)$$

where the summations are over the particle representations  $R$  with masses  $m_R$ . Here  $n_R$  is the number of times a particular generic representation appears in the complete spectrum (*e.g.*, three for three generations), and the  $C_R$ -coefficients are given in terms of the one-loop beta-function coefficients  $b_{3,2,\hat{Y}}(R)$  of the representation  $R$  as

$$\begin{aligned} C_R^{(\sin)} &= b_{\hat{Y}}(R) - b_2(R) \\ C_R^{(\alpha)} &= \frac{k_1}{k_1 + 1} b_{\hat{Y}}(R) + \frac{1}{k_1 + 1} b_2(R) - b_3(R) . \end{aligned} \quad (5.19)$$

Note that  $b_{\hat{Y}}(R) \equiv b_Y(R)/k_1$ . For each representation  $R$ , these beta-function coeffi-

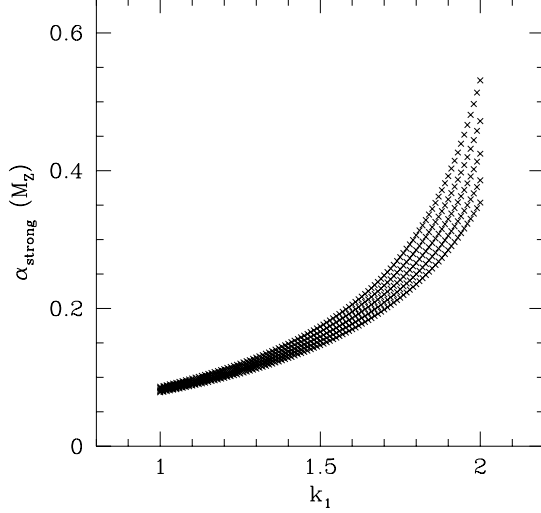


Figure 5: The effects of hypercharge normalization:  $\alpha_3(M_Z)$  vs.  $k_1$ . The higher curves correspond to higher values of  $M_{\text{string}}$ .

cients, degeneracies  $n_R$ , and  $C_R$ -coefficients are as follows:

$R$	$b_Y(R)$	$b_2(R)$	$b_3(R)$	$C_R^{(\text{sin})}$	$C_R^{(\alpha)}$	$n_R$
$\tilde{g}$	0	0	2	0	-2	1
$\tilde{w}$	0	$\frac{4}{3}$	0	$-\frac{4}{3}$	$\frac{4}{3} \frac{1}{k_1+1}$	1
$\tilde{\ell}_\ell$	$\frac{1}{6k_1}$	$\frac{1}{6}$	0	$\frac{1}{6k_1} - \frac{1}{6}$	$\frac{1}{3} \frac{1}{k_1+1}$	3
$\tilde{\ell}_r$	$\frac{1}{3k_1}$	0	0	$\frac{1}{3k_1}$	$\frac{1}{3} \frac{1}{k_1+1}$	3
$\tilde{Q}$	$\frac{1}{18k_1}$	$\frac{1}{2}$	$\frac{1}{3}$	$\frac{1}{18k_1} - \frac{1}{2}$	$\frac{5}{9} \frac{1}{k_1+1} - \frac{1}{3}$	3
$\tilde{d}_r$	$\frac{1}{9k_1}$	0	$\frac{1}{6}$	$\frac{1}{9k_1}$	$\frac{1}{9} \frac{1}{k_1+1} - \frac{1}{6}$	3
$\tilde{u}_r$	$\frac{4}{9k_1}$	0	$\frac{1}{6}$	$\frac{4}{9k_1}$	$\frac{4}{9} \frac{1}{k_1+1} - \frac{1}{6}$	3
$\tilde{h}$	$\frac{1}{3k_1}$	$\frac{1}{3}$	0	$\frac{1}{3k_1} - \frac{1}{3}$	$\frac{2}{3} \frac{1}{k_1+1}$	2
$h$	$\frac{1}{6k_1}$	$\frac{1}{6}$	0	$\frac{1}{6k_1} - \frac{1}{6}$	$\frac{1}{3} \frac{1}{k_1+1}$	1
$t$	$\frac{17}{18k_1}$	1	$\frac{2}{3}$	$\frac{17}{18k_1} - 1$	$\frac{35}{18} \frac{1}{k_1+1} - \frac{2}{3}$	1

Assuming universal boundary conditions for the soft SUSY-breaking terms (*i.e.*, assuming that  $m_{1/2}$  and  $m_0$  are universal), we have analyzed the possible light SUSY threshold contributions for a wide range of points in the parameter space  $\{m_0, m_{1/2}, m_h, m_{\tilde{h}}\}$ . In general we find that the light SUSY thresholds are small, and that the predictions for  $\sin^2 \theta_W(M_Z)$  and  $\alpha_3(M_Z)$  continue to disagree with the measured values. In Fig. 6 we display  $\sin^2 \theta(M_Z)_{\overline{MS}}$  versus  $\alpha_3(M_Z)_{\overline{MS}}$  for a sampling of points in the SUSY-breaking parameter space. Within this parameter space, each free parameter  $X$  is sampled in the interval  $(X_{\min}, X_{\max})$  with spacing  $\Delta X$  between

consecutive points, as follows:

Parameter $X$	$X_{\min}$	$X_{\max}$	$\Delta X$
$m_0$ (GeV)	0	600	200
$m_{1/2}$ (GeV)	50	600	150
$m_h$ (GeV)	100	500	200
$m_{\tilde{h}}$ (GeV)	100	500	200
$M_{\text{string}}$ (GeV)	$3 \times 10^{17}$	$7 \times 10^{17}$	$5 \times 10^{16}$
$\alpha_{\text{string}}^{-1}$	20	32	4

(5.21)

We have taken the top-quark mass  $m_t = 175$  GeV.

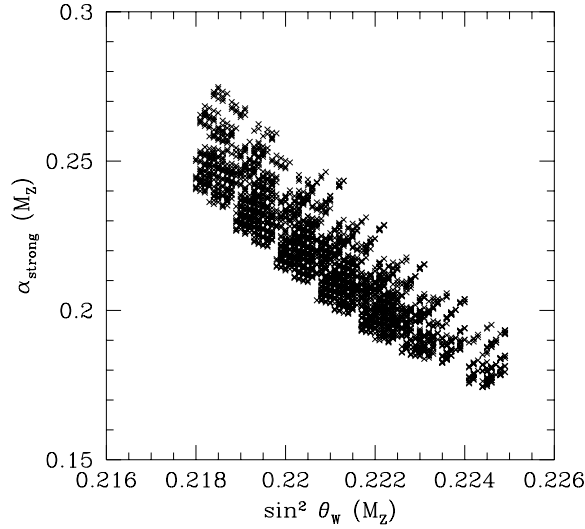


Figure 6: Scatter plot for  $\{\sin^2 \theta_W(M_Z), \alpha_3(M_Z)\}$  for various values of  $\{m_0, m_{1/2}, m_h, m_{\tilde{h}}, M_{\text{string}}\}$ , assuming the MSSM spectrum.

It is important to note that our assumption of universal boundary conditions for the soft SUSY-breaking terms is not necessary. In fact, in string models, such boundary conditions are generally expected to be *non*-universal [52]. We can then ask whether non-universal boundary conditions can bring the string-scale unification into agreement with the experimentally measured couplings at low energy. By examining the different terms in (5.17) and (5.18), we can see that for this purpose, the value of the light SUSY threshold corrections must be positive. Now, the signs of the  $C_R$ -coefficients of the different terms in these two equations are determined by the one-loop beta-function coefficients of the different representations  $R$ . Assuming that all the sparticle masses are larger than  $M_Z$ , we can maximize the light SUSY corrections by setting the masses of the negative contributions equal to the  $Z$  mass. For example, in (5.18), we see from the signs of the coefficients  $C_R^{(\alpha)}$  that the wino, top, sleptons,

higgs and higgsino all give positive contributions. Assuming a common mass  $M$  for all of these but the top, and summing over the resulting coefficients, we obtain  $\Delta_{\text{l.s.}}^{(\alpha)} = 15/(16\pi) \ln(M/M_Z)$ . Thus, with  $\alpha_3^{(\text{predicted})} \sim 0.2$  and  $\alpha_3^{(\text{measured})} \sim 0.14$ , even the best-case scenario requires  $M \approx 100$  TeV. For  $\sin^2 \theta_W$ , on the other hand, only  $\tilde{u}_r$ ,  $\tilde{d}_r$ , and  $\tilde{e}_r$  contribute with positive coefficients. Assuming that all the other thresholds are degenerate at  $M_Z$ , and that  $\tilde{u}_r$ ,  $\tilde{d}_r$ , and  $\tilde{e}_r$  have a common mass  $\tilde{M}$ , we find that agreement with the measured value of  $\sin^2 \theta_W$  requires  $\tilde{M} \sim 10$  TeV. Alternatively, some of the sparticle thresholds may be below  $M_Z$ . Assuming degenerate thresholds  $\tilde{M} = 45$  GeV for the sparticles making negative contributions to  $\sin^2 \theta_W$ , and with  $m_t = 175$  GeV, we find that the contribution for  $\Delta_{\text{l.s.}}^{(\text{sin})}$  from these thresholds is of the order of 0.001, which still requires  $\tilde{M} \sim 10$  TeV. Thus, even with these extreme “best-case” scenarios, light SUSY thresholds cannot by themselves bring the string-unification predictions into agreement with the experimentally observed values.

#### 5.4 Heavy string thresholds

We now analyze the effects of the threshold corrections due to the infinite towers of heavy string states. These corrections were the focus of our calculations in Sect. 4, and contribute to the running of the gauge couplings as indicated in the fourth lines of (5.8) and (5.9).

The calculation of the heavy string threshold corrections in Sect. 4 was performed for normalized gauge group factors  $G_i$  with  $k_i = 1$ . However, as indicated in (3.3), the full string threshold corrections are in general of the form  $\tilde{\Delta}_i = \Delta_i + k_i Y$ , where  $Y$  is independent of the gauge group. In Sect. 4 we calculated the gauge-dependent terms  $\Delta_i$  for the different gauge group factors. Therefore, by taking the *differences* of the threshold corrections for two different gauge groups, the group-independent term cancels. Moreover, as we see from (5.8) and (5.9), it turns out that the solutions of the RGE equations for  $\sin^2 \theta_W(M_Z)$  and  $\alpha_3(M_Z)$  depend only on the differences  $\Delta_i - \Delta_j$  for the different group factors  $G_i$  and  $G_j$  in a given string model. Therefore, the low-energy predictions for  $\sin^2 \theta_W(M_Z)$  and  $\alpha_3(M_Z)$  do not depend on the group-independent factor  $Y$ . One might worry, of course, that the presence of a non-standard normalization for  $k_1$  in certain string models might render this claim incorrect. However, the calculation of the threshold corrections is always done with respect to the properly normalized  $U(1)$  generators. Similarly, only the threshold corrections for the properly normalized  $U(1)$  generators appear in the RGE equations. This is similar to the usual practice in grand unified theories in which the coupling of the properly normalized  $U(1)$  generator evolves below the GUT scale, and the matching with the weak hypercharge coupling is done at the  $Z$  scale. Therefore the value of the gauge-independent term  $Y$  continues to be irrelevant for our analysis.

We now discuss the effects that these string threshold corrections will have on the low-energy parameters. Because the gauge structure and threshold corrections are highly model-dependent, we shall have to consider each realistic free-fermion model

in turn.

Considering first the string model analyzed in Sect. 4.2, we see that the weak hypercharge has the standard  $SO(10)$  embedding. Therefore, we can directly insert the relative values for  $\Delta_{SU(3)}$ ,  $\Delta_{SU(2)}$  and  $\Delta_{U(1)_{\hat{Y}'}}$  that we found in (4.23) into (5.8) and (5.9). For this model, we consequently obtain

$$\Delta_{\text{h.s.}}^{(\text{sin})} = -0.0006 \quad \text{and} \quad \Delta_{\text{h.s.}}^{(\alpha)} = -0.3536 . \quad (5.22)$$

Thus, the effect of the string threshold corrections in this model is to slightly decrease the values of  $\sin^2 \theta_W(M_Z)$  and  $\alpha_3^{-1}(M_Z)$ . Alternatively, of course, this can be regarded as effectively increasing the string unification scale. This can be seen by absorbing the string threshold corrections into  $\ln(M_{\text{string}}/M_Z)$  in (5.8) and (5.9). From (5.9), we see that the corrected string unification scale can be written as

$$M_{\text{string}}^{(\text{corrected})} = M_{\text{string}}^{(\text{uncorrected})} \exp \left[ \frac{k_1(\Delta_1 - \Delta_3) + (\Delta_2 - \Delta_3)}{2(3k_1 + 15)} \right] . \quad (5.23)$$

Numerically, this yields

$$M_{\text{string}}^{(\text{corrected})} \approx 6.72 \times 10^{17} \text{ GeV} \quad (5.24)$$

where we take  $M_{\text{string}}^{(\text{uncorrected})} \approx 5 \times 10^{17} \text{ GeV}$ . Thus, the effect of the string threshold corrections in this model is to enhance the disagreement with the experimentally observed values.

We next analyze the model of Sect. 4.3. As we saw in Sect. 4, in this model the analysis is complicated due to the presence of the enhanced symmetry. The group factors relevant for the analysis are  $SU(3)_C \times SU(2)_L \times SU(2)_{\text{cust}} \times U(1)_{Y'}$ . Above the  $SU(2)_{\text{cust}} \times U(1)_{Y'}$  breaking scale, we have to consider the running of these four group factors. The  $SU(2)_{\text{cust}} \times U(1)_{Y'}$  symmetry can be broken down to  $U(1)_Y$  by, for example, the VEV of the right-handed neutrino, and below this breaking scale we have the standard one-loop RGE's for  $SU(3)_C \times SU(2)_L \times U(1)_{\hat{Y}'}$ . The relation between the weak hypercharge coupling and the  $SU(2)_{\text{cust}} \times U(1)_{Y'}$  couplings is then

$$\frac{1}{\alpha_Y} = \frac{1}{4\alpha_{\text{cust}}} + \frac{17}{12\alpha'_{\hat{Y}'}} \quad (5.25)$$

where  $\alpha_{\hat{Y}'}$  is the coupling of the properly normalized  $U(1)_{\hat{Y}'}$ . The RGE for the  $U(1)_{\hat{Y}'}$  coupling then takes the form

$$\begin{aligned} \frac{1}{\alpha_{\text{string}}} &= \frac{3}{5} \frac{1}{\alpha_1(\mu)} - \frac{3b_Y}{10\pi} \ln \frac{M_I}{\mu} - \frac{1}{2\pi} \frac{3}{5} \left( \frac{1}{4} b_{2c} + \frac{17}{12} b_{\hat{Y}'} \right) \ln \frac{M_S}{M_I} \\ &\quad - \frac{1}{4\pi} \frac{3}{5} \left( \frac{1}{4} \Delta_{2c} + \frac{17}{12} \Delta_{\hat{Y}'} \right) . \end{aligned} \quad (5.26)$$

Let us assume for the moment that the VEV of the right-handed neutrino is of the order of  $M_S$ . This implies that  $M_I = M_S$ . Therefore, below the string scale we have

the three gauge couplings of the Standard Model, and the threshold corrections for the properly normalized weak hypercharge are given by (4.41). Inserting the relative values of  $\Delta_3$ ,  $\Delta_2$ , and  $\Delta_{\hat{Y}}$  from (4.41) into (5.8) and (5.9), we then obtain

$$\Delta_{\text{h.s.}}^{(\sin)} = -0.0012 \quad \text{and} \quad \Delta_{\text{h.s.}}^{(\alpha)} = -0.335 . \quad (5.27)$$

As in the case of the previous model, we see that the effect of the string threshold corrections is to decrease the values of  $\sin^2 \theta_W(M_Z)$  and  $\alpha_3^{-1}(M_Z)$ , or equivalently to increase the effective string unification scale. Using (5.23) with  $M_{\text{string}}^{(\text{uncorrected})} \approx 5 \times 10^{17}$  GeV, we now obtain

$$M_{\text{string}}^{(\text{corrected})} \approx 6.62 \times 10^{17} \text{ GeV} . \quad (5.28)$$

We shall shortly discuss the modifications that arise if  $M_I < M_S$ .

Next, we analyze the effect of the threshold corrections in the  $SO(6) \times SO(4)$  string model which realizes Pati-Salam unification scenario. In this string model, there is an intermediate energy scale at which the  $SU(4) \times SU(2)_L \times SU(2)_R$  symmetry is broken to  $SU(3)_C \times SU(2)_L \times U(1)_Y$ . The low-energy parameters are consequently affected by the presence of this intermediate energy scale. The weak hypercharge  $\hat{Y}$  is a linear combination of  $B - L$  and  $T_{3R}$ :

$$\hat{Y} = \sqrt{\frac{2}{5}} T_{B-L} + \sqrt{\frac{3}{5}} T_{3R} . \quad (5.29)$$

The low-energy parameters are then obtained from the one-loop RGE's via

$$\begin{aligned} \frac{1}{\alpha_3(M_Z)} &= \frac{1}{\alpha_{\text{string}}} + \frac{b_3}{2\pi} \ln \frac{M_I}{M_Z} + \frac{b_4}{2\pi} \ln \frac{M_S}{M_I} + \frac{\Delta_4}{4\pi} \\ \frac{1}{\alpha_2(M_Z)} &= \frac{1}{\alpha_{\text{string}}} + \frac{b_{2L}}{2\pi} \ln \frac{M_I}{M_Z} + \frac{b_{2L}}{2\pi} \ln \frac{M_S}{M_I} + \frac{\Delta_{2L}}{4\pi} \\ \frac{1}{\alpha_1(M_Z)} &= \frac{1}{\alpha_{\text{string}}} + \frac{b_1}{2\pi} \ln \frac{M_I}{M_Z} + \frac{1}{2\pi} \left( \frac{2}{5} b_4 + \frac{3}{5} b_{2R} \right) \ln \frac{M_S}{M_I} \\ &\quad + \frac{1}{4\pi} \left( \frac{2}{5} \Delta_4 + \frac{3}{5} \Delta_{2R} \right) \end{aligned} \quad (5.30)$$

Assuming again that  $M_I \approx M_S$ , the threshold corrections for the three properly normalized group factors are  $\Delta_4$ ,  $\Delta_{2L}$  and  $\Delta_{\hat{Y}} = (2/5)\Delta_4 + (3/5)\Delta_{2R}$ . Inserting the values from (4.52) and (4.56) into (5.8) and (5.9), we find

$$\Delta_{\text{h.s.}}^{(\sin)} = -0.0028 \quad \text{and} \quad \Delta_{\text{h.s.}}^{(\alpha)} = -0.3141 \quad (5.31)$$

Just as in previous models, the effect of the string threshold corrections is therefore to increase the effective string unification scale. Inserting the values of  $\Delta_4$ ,  $\Delta_{2L}$  and  $\Delta_{\hat{Y}}$  into (5.23), we obtain

$$M_{\text{string}}^{(\text{corrected})} \approx 6.5 \times 10^{17} \text{ GeV} . \quad (5.32)$$

Thus, in all of the examples that we have explored, we find that the effect of the string threshold corrections is to *increase* the effective string unification scale. Therefore, the effect of the string threshold corrections in these examples is always to enhance the disagreement with the low-energy observables.

It is an important observation that the sizes of the heavy string threshold corrections are very small in all of these realistic string models, and thus do not greatly affect (either positively or negatively) the magnitude of the string unification scale. Although such threshold corrections receive contributions from infinite towers of massive string states, we have in fact been able to provide a general model-independent argument which explains why these corrections are naturally suppressed in string theory (except of course for large moduli). This will be discussed in Sect. 6. Thus, we conclude that these threshold corrections cannot by themselves resolve the experimental discrepancy.

### 5.5 Intermediate gauge structure

In the last two models that we studied at the end of Sect. 5.4, there exists an intermediate energy scale  $M_I$  at which an extended gauge group is broken to the gauge group of the Standard Model. In each case, we assumed that the extended symmetry is broken at the string scale, and that therefore  $M_I = M_S$ . An obvious issue, then, is to determine the effect of the extended symmetry if it is broken at an intermediate scale  $M_I < M_S$ . In particular, might the breaking at the intermediate scale bring the string-scale predictions into agreement with experiment?

We claim that in the above examples, this cannot happen. Our reasoning is as follows. Since the larger discrepancy with experiment is for  $\alpha_3$ , it is sufficient to focus on this observable. Now, in the first model we considered, the RGE for  $\alpha_3$  does not depend on the intermediate scale breaking at all. Thus the disagreement with the experimentally observed value persists for all  $M_I$ . Of course, this argument is somewhat deficient due to the dependence of the RGE for  $\alpha_3$  on the group-independent contribution  $Y$  to the heavy string threshold corrections. However, unless (and contrary to expectation [53]) this group-independent term  $Y$  is very large, the argument will hold. A more careful argument is provided by solving the RGE's, in the presence of intermediate scale  $M_I$ , for  $\sin^2 \theta_W(M_Z)$  and  $\alpha_3(M_Z)$ . The one-loop RGE for  $\alpha_1$  takes the form

$$\frac{1}{\alpha_1} = \frac{1}{k_1 \alpha_Y} - \frac{1}{2\pi} \frac{b_Y}{k_1} \ln \frac{M_S}{M_Z} - \frac{1}{4\pi} \Delta_{\hat{Y}} + \frac{1}{2\pi} \frac{1}{k_1} (b_Y - (\frac{b_c}{4} + \frac{17}{12} b_{Y'})) \ln \frac{M_S}{M_I} \quad (5.33)$$

where the first three terms in (5.33) are identical to the RGE without an intermediate scale, and the last term incorporates the effect of the intermediate scale. Thus, in the presence of the intermediate scale the solution of the RGE's for  $\sin^2 \theta_W(M_Z)$  in (5.8) has an additional term

$$\dots + \frac{1}{2\pi} \frac{\alpha}{k_1 + 1} \left[ b_Y - (\frac{b_c}{4} + \frac{17}{12} b_{Y'}) \right] \ln \frac{M_S}{M_I} . \quad (5.34)$$



Since  $\sin^2 \theta_W$  appears divided by  $a \equiv \alpha_{\text{e.m.}}$  in the solution of the RGE's for  $\alpha_3^{-1}$ , the effect of the intermediate scale on  $\alpha_3(M_Z)$  is that in (5.34) divided by  $a$ . Now, for a spectrum consisting of three generations and two Higgs doublets, the coefficient of the logarithm in (5.34) is  $-301/48$ . The crucial point here is the *sign* of this coefficient, as it decreases both  $\sin^2 \theta_W(M_Z)$  and  $\alpha_3^{-1}(M_Z)$ . Consequently,  $\alpha_3(M_Z)$  increases, and the disagreement with experiment is enhanced.

Similar considerations also apply to the  $SO(6) \times SO(4)$  model. From (5.30), we see that the effects of the intermediate scale on  $\sin^2 \theta_W(M_Z)$  and  $\alpha_3(M_Z)$  amounts respectively to the additive terms

$$\dots + \frac{4}{10\pi} \frac{k_1 \alpha}{1 + k_1} \ln \frac{M_S}{M_I} \quad (5.35)$$

and

$$\dots + \frac{1}{2\pi} \left( -1 + \frac{4}{5} \frac{k_1}{k_1 + 1} \right) \ln \frac{M_S}{M_I} = \dots - \frac{1}{4\pi} \ln \frac{M_S}{M_I} \quad (5.36)$$

in (5.8) and (5.9). We assume that the spectrum below  $M_I$  is that of the MSSM, and that above  $M_I$  it consists of three  $\mathbf{16}$ 's of  $SO(10)$  that produce the three generations, one  $(1,2,2)$  representation that produces the light Higgs, and  $(4, 1, 2) + (\bar{4}, 1, 2)$  representations that are used to break the  $SU(4) \times SU(2)_R$  symmetry at  $M_I$ . The signs of the coefficients in (5.35) and (5.36) shows that the effect of having  $M_I < M_S$  is to increase  $\sin^2 \theta_W(M_Z)$  and  $\alpha_3(M_Z)$ . Note that in arriving at this conclusion, we have used only the *differences* of heavy string threshold corrections, which are unambiguous. Thus, the effect of having an extended gauge structure broken at an intermediate energy scale is to enhance the disagreement with the experimental results for  $\alpha_3(M_Z)$ .

Likewise, in the case of the flipped  $SU(5)$  model, the effect of the intermediate scale can be incorporated via the following additional term in (5.8):

$$- \frac{1}{2\pi} \frac{32}{5} \frac{k_1 a}{k_1 + 1} \ln \frac{M_S}{M_I}. \quad (5.37)$$

Here we have assumed the spectrum below  $M_I$  to be that of the MSSM, and above  $M_I$  to consist of three  $\mathbf{16}$  representations of  $SO(10)$ , one  $\mathbf{5}$  and  $\bar{\mathbf{5}}$  of  $SU(5)$  that produces the light Higgs doublets, and one  $\mathbf{10}$  and  $\bar{\mathbf{10}}$  of  $SU(5)$  that is used to break the  $SU(5) \times U(1)$  symmetry to  $SU(3) \times SU(2) \times U(1)$ . Thus, the effect of the extended gauge structure in this model is to reduce  $\sin^2 \theta_W(M_Z)$ , and to enhance the disagreement with the experimentally observed value.

It is remarkable that in all of these realistic string models, the availability of an intermediate scale  $M_I$  does not help in removing the discrepancy between string-scale unification and low-energy data. *A priori*, one might have expected that the presence of such an extra degree of freedom would have enabled agreement to be reached. However, we now see that within the context of the realistic string models, this extra degree of freedom only worsens the agreement. Thus, we can effectively rule out intermediate gauge structure as a potential explanation for the discrepancies.

## 5.6 Intermediate matter thresholds

We now turn to the effects induced by additional matter below the string scale [17, 27, 54]. As we shall see, such matter appears naturally in the string models we have examined. It is evident from our analysis up to this point that such intermediate matter now appears to be the *only* way by which the disagreement with experiment can be possibly be resolved. Fortunately, as we shall find, in certain models exactly the required matter appears, in just the right representations and with just the right non-standard hypercharge assignments. Hence, in these models, the disagreement with experiment can be resolved.

In the analysis up to this point, we have assumed that the matter spectrum below the string scale is simply that of the Minimal Supersymmetric Standard Model, *i.e.*, that it consists of exactly three chiral generations with two Higgs doublets. However, in the context of the realistic string models, this assumption is *ad hoc*. In fact, in *all* of the string models constructed to date, additional color triplets and electroweak doublets beyond the MSSM appear in the massless spectrum, in vector-like representations. The number of such additional color triplets and electroweak doublets is of course highly model-dependent, as are their mass scales. However, the assumption that the massless spectrum below the string scale is that of the MSSM is, in general, not justified.

Mass terms for these extra states beyond the MSSM may arise from cubic or higher-order non-renormalizable terms in the superpotential. In the models studied to date, the mass scale of the additional color triplets and electroweak doublets is not the string scale. In general, the masses of the extra states are suppressed relative to the string scale, the reason being that the mass terms arising from non-renormalizable terms are suppressed relative to the cubic-level mass terms. For example, in Ref. [55], the mass scale of an additional pair of color triplets was estimated to be of the order of  $10^{11}$  GeV.

The contributions of such additional color triplets and electroweak doublets to the low-energy parameters are given in the third lines of (5.8) and (5.9). Provided that these additional states exist at the appropriate scales, we shall find that the presence of this additional matter results in agreement between the hypothesis of direct unification at the string scale, and the values of the low-energy parameters  $\sin^2 \theta_W(M_Z)$  and  $\alpha_3(M_Z)$ . Of course, there exist a large number of possible scenarios for the mass scales of the extra states which will allow direct unification at the string scale, and a classification of all these possibilities is beyond the scope of this paper. Indeed, such an analysis would require a detailed investigation of each individual string model, its full spectrum, and its renormalizable and non-renormalizable superpotentials. This is currently being investigated [56]. However, the essential point that cannot be overemphasized is that these string models, in general, produce just the sort of spectrum with additional matter as required to have the possibility of direct string unification.

In the realistic free-fermionic models we have studied, the three generations are obtained from the sectors  $\mathbf{b}_1$ ,  $\mathbf{b}_2$ , and  $\mathbf{b}_3$ . The electroweak doublets that couple to the states from these sectors, and which therefore may correspond to the MSSM Higgs doublets, are obtained from the Neveu-Schwarz sector and a sector which is a combination of the vectors  $\{\mathbf{b}_1, \mathbf{b}_2, \mathbf{b}_3, \alpha, \beta\}$ . For example, in the models of Sects. 4.2 and 4.3, the electroweak doublets are obtained from the Neveu-Schwarz sector and the  $\mathbf{b}_1 + \mathbf{b}_2 + \alpha + \beta$  sector. The Neveu-Schwarz sector and the  $\mathbf{b}_1 + \mathbf{b}_2 + \alpha + \beta$  sector may, in general, also produce color triplets. Color triplets from these sectors couple to the massless fermions from the sectors  $\mathbf{b}_1$ ,  $\mathbf{b}_2$ , and  $\mathbf{b}_3$ . Their mass scale is therefore restricted from proton decay through Higgsino exchange. However, for these two sectors there exist a superstring doublet-triplet splitting mechanism through which the color triplets are removed from the spectrum via GSO projections [8].

In addition to the massless spectrum from the above sectors, the free-fermionic models may contain additional color triplets and electroweak doublets from several other sectors. In the  $SO(6) \times SO(4)$  and the flipped  $SU(5) \times U(1)$  models, additional  $\mathbf{16}$  and  $\overline{\mathbf{16}}$  representations are obtained from the additional vectors beyond the NAHE set that are used to reduce the number of generations to three. Typically, there are one or two of such pairs. These produce the  $(3, 2)_{1/6}$ ,  $(\overline{3}, 1)_{1/3}$ ,  $(\overline{3}, 1)_{-2/3}$ , and  $(1, 2)_{-1/2}$  representations of  $SU(3) \times SU(2) \times U(1)_Y$ . These states have the usual one-loop beta-function coefficients. In the standard-like superstring models, additional color triplets and electroweak doublets may also appear from sectors which arise from combinations of the vectors  $\{\mathbf{b}_1, \mathbf{b}_2, \mathbf{b}_3\} + \{\alpha, \beta, \gamma\}$ . These states, in general, do not have the standard weak hypercharge assignments, and therefore their one-loop beta-function coefficients will be different from those of the MSSM representations. For example, in the model of Ref. [17], there exist color triplets  $\{D_3, \overline{D}_3\}$  and electroweak doublets  $\{\ell, \overline{\ell}\}$  with the following beta-function coefficients:

$$\begin{pmatrix} b_{SU(3)} \\ b_{SU(2)} \\ b_{U(1)} \end{pmatrix}_{D_3, \overline{D}_3} = \begin{pmatrix} 1/2 \\ 0 \\ 1/20 \end{pmatrix}, \quad \begin{pmatrix} b_{SU(3)} \\ b_{SU(2)} \\ b_{U(1)} \end{pmatrix}_{\ell, \overline{\ell}} = \begin{pmatrix} 0 \\ 1/2 \\ 0 \end{pmatrix}. \quad (5.38)$$

To estimate the effect of the intermediate thresholds induced by such additional matter, we shall examine in detail the spectrum of the model of Sect. 4.3. In order to be as general as possible, we will start from (5.8) and (5.9) and from the experimental constraints on the low-energy observables, and derive the corresponding constraints on these intermediate matter thresholds. As our low-energy experimental constraints, we shall impose

$$\begin{aligned} 0.230 &< \sin^2 \theta_W(M_Z) < 0.233 \\ 0.110 &< \alpha_3(M_Z) < 0.135. \end{aligned} \quad (5.39)$$

As before, we set  $M_{\text{string}} = 5 \times 10^{17}$  GeV, and take  $k_1 = 5/3$  and  $\alpha_{\text{e.m.}}(M_Z) = 1/127.9$ . We set all of the sparticle masses to be degenerate at  $M_Z$ . These values, along with the

corrections from two-loop contributions, Yukawa couplings, and scheme-conversion, as well as the values for  $\Delta_i$  given in (4.41), are then inserted into the expressions for  $\sin^2 \theta_W(M_Z)$  and  $\alpha_3(M_Z)$  given in (5.8) and (5.9) respectively. Using our experimental limits (5.39), we then obtain the constraints

$$\begin{aligned} 10.29 &< \sum_i (b_{2_i} - b_{1_i}) \ln \frac{M_S}{M_i} < 14.14 \\ 39.22 &< -\sum_i \left[ k_1 b_{1_i} + b_{2_i} - (1 + k_1) b_{3_i} \right] \ln \frac{M_S}{M_i} < 67.40 . \end{aligned} \quad (5.40)$$

We can also combine these two equations to obtain

$$18.57 < \sum_i (b_{3_i} - b_{1_i}) \ln \frac{M_S}{M_i} < 30.58 . \quad (5.41)$$

We can now use (5.40) and (5.41) to examine the possible general scenarios for intermediate matter states. Our first observation is that in order to accommodate the low-energy parameters, both intermediate color triplets and electroweak doublets are needed. Let us now focus on the representations that are available in the string model of Refs. [17, 23]. In this model, there are three color triplets in vector-like representations, two with the one-loop beta-function coefficients of (5.44), and one with the one-loop beta-function coefficients of (5.38). There are five pairs of electroweak doublets from the Neveu-Schwarz and  $\mathbf{b}_1 + \mathbf{b}_2 + \alpha + \beta$  sectors with the quantum numbers

$$\begin{pmatrix} b_{SU(3)} \\ b_{SU(2)} \\ b_{U(1)} \end{pmatrix}_{h, \bar{h}} = \begin{pmatrix} 0 \\ 1/2 \\ 3/10 \end{pmatrix} , \quad (5.42)$$

and three pairs of electroweak doublets with the quantum numbers of (5.38). Let us suppose that all of the intermediate thresholds are from states that fit into the  $\mathbf{5}$  and  $\bar{\mathbf{5}}$  representations of  $SU(5)$ . For one such pair, we obtain from (5.40) and (5.41) the constraints

$$\begin{aligned} 30.95 &< \ln \frac{M_S}{M_3} - \ln \frac{M_S}{M_2} < \dots \\ 27.725 &< \ln \frac{M_S}{M_2} - \ln \frac{M_S}{M_3} < \dots \end{aligned} \quad (5.43)$$

where the upper limits are not important. It is clear that these two equations cannot be satisfied for any values of  $M_2$  and  $M_3$ , or for any number of doublets and triplets. We therefore conclude that in any string models containing only those states that fit into  $\mathbf{5}$  and  $\bar{\mathbf{5}}$  representations of  $SU(5)$ , intermediate matter thresholds cannot account for the disagreement with the experimentally observed values of  $\sin^2 \theta_W(M_Z)$  and  $\alpha_3(M_Z)$ . It is an important conclusion that some string models can actually be ruled out in this way.

By contrast, in the model of Sect. 4.3, the massless spectrum contains not only states that fit into the  $\mathbf{5}$  and  $\bar{\mathbf{5}}$  representations of  $SU(5)$ , but also color triplets and electroweak doublets with exotic weak hypercharge assignments. These therefore cannot be fit into  $SO(10)$  representations. In this particular model, there are two pairs of color triplets  $\{D_1, \bar{D}_1, D_2, \bar{D}_2\}$  with one-loop beta-function coefficients

$$\begin{pmatrix} b_{SU(3)} \\ b_{SU(2)} \\ b_{U(1)} \end{pmatrix}_{D_1, \bar{D}_1, D_2, \bar{D}_2} = \begin{pmatrix} 1/2 \\ 0 \\ 1/5 \end{pmatrix} \quad (5.44)$$

in addition to one pair of color triplets with the quantum numbers of (5.38), and three pairs of electroweak doublets with the quantum numbers of (5.44). We shall set the masses of these three doublet pairs to be degenerate at one scale,  $M_2$ , and examine possible scenarios for the masses  $M_3$  of the color triplets. With one light color triplet, for example  $\{D_1, \bar{D}_1\}$ , we obtain the limits

$$\text{experimental limit} < M_3 < 18141 \text{ GeV} . \quad (5.45)$$

Setting  $M_3$  at the upper limit of (5.45), we find

$$7.2 \times 10^{13} \text{ GeV} < M_2 < 2.6 \times 10^{14} \text{ GeV} , \quad (5.46)$$

while for a lower limit of  $M_3 \sim 500 \text{ GeV}$  we obtain

$$3.6 \times 10^5 \text{ GeV} < M_2 < 1.7 \times 10^6 \text{ GeV} . \quad (5.47)$$

By contrast, with *two* triplet pairs degenerate at one mass scale  $M_3$ , we instead find

$$4.3 \times 10^6 \text{ GeV} < M_3 < 9.5 \times 10^{10} \text{ GeV} , \quad (5.48)$$

so that taking the upper limit for  $M_3$  yields

$$7.2 \times 10^{13} \text{ GeV} < M_2 < 2.6 \times 10^{14} \text{ GeV} \quad (5.49)$$

while the lower limit on  $M_3$  yields

$$5 \times 10^{12} \text{ GeV} < M_2 < 1.8 \times 10^{13} \text{ GeV} . \quad (5.50)$$

Finally, with all three color triplet pairs degenerate at the scale  $M_3$ , we find

$$2.4 \times 10^{11} \text{ GeV} < M_3 < 7.2 \times 10^{13} \text{ GeV} \quad (5.51)$$

for which the upper and lower limits respectively yield

$$\begin{aligned} 3.7 \times 10^{14} \text{ GeV} &< (M_2)_{\text{upper}} < 1.1 \times 10^{15} \text{ GeV} \\ 5.7 \times 10^{13} \text{ GeV} &< (M_2)_{\text{lower}} < 2 \times 10^{14} \text{ GeV} . \end{aligned} \quad (5.52)$$

Clearly, many viable scenarios exist, and the above examples are not exhaustive. In Fig. 7 we plot  $\sin^2 \theta_W(M_Z)$  versus  $\alpha_3(M_Z)$ , with  $M_3 = 2 \times 10^{12}$  GeV and  $M_2 = 2 \times 10^{14}$  GeV. We have included in this analysis the two-loop, Yukawa, and scheme-conversion corrections given in (5.10) and (5.11), as well as the heavy string threshold corrections and the light-SUSY corrections due to the splitting of the sparticle spectrum. The unification scale is varied between  $3 \times 10^{17}$  GeV  $\leq M_{\text{string}} \leq 7 \times 10^{17}$  GeV, and  $0.03 \leq \alpha_{\text{string}} \leq 0.05$ . It is evident from the figure that in this model, the low-energy experimental parameters can indeed be accommodated, provided that the thresholds from this extra matter exist at appropriate scales.

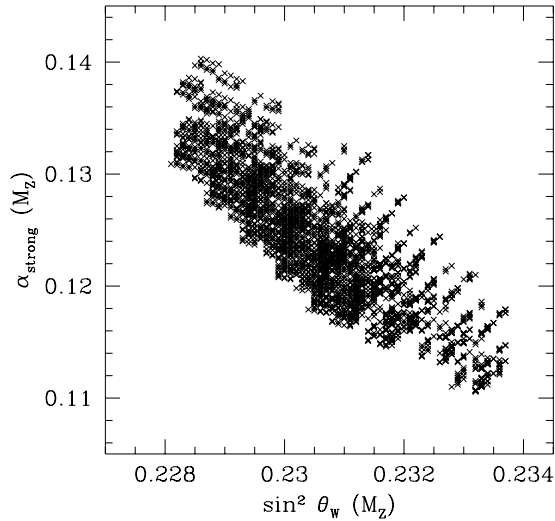


Figure 7: Scatter plot for  $\{\sin^2 \theta_W(M_Z), \alpha_3(M_Z)\}$ , as in Fig. 6, except that the intermediate matter thresholds are now also included in the analysis.

Finally, we examine possible string models that contain additional  $(3, 2)_{1/6}$  representations. These representations are obtained, for example, in the flipped  $SU(5) \times U(1)$  model [57] and in the  $SO(6) \times SO(4)$  models [58], and arise from the additional  $\mathbf{16}$  and  $\overline{\mathbf{16}}$  representations. These may also arise in the standard-like string models. For example, in the model of Ref. [26], a change in the sign of the GSO-projection phase  $C \begin{bmatrix} \mathbf{b}_4 \\ \mathbf{1} \end{bmatrix}$  produces an additional  $(3, 2)_{1/6}$  representation from the sector  $\mathbf{b}_4$ . However, a single  $(3, 2)_{1/6}$  representation (or even several such representations) is not sufficient to accommodate the low-energy data, and indeed at least one  $(3, 1)_{1/3}$  representation is needed. With one pair of each, we find

$$4 \times 10^{13} \text{ GeV} < M_{32} < 1 \times 10^{15} \text{ GeV} , \quad (5.53)$$

with the corresponding constraints

$$3 \times 10^6 \text{ GeV} < (M_{31})_{\text{upper}} < 1.5 \times 10^{15} \text{ GeV}$$

$$5 \times 10^2 \text{ GeV} < (M_{31})_{\text{lower}} < 2.6 \times 10^{11} \text{ GeV} . \quad (5.54)$$

In all of these cases, it is an important observation that such ranges exist in which string-scale gauge coupling unification is consistent with low-energy data. It is of course obvious that the presence of extra matter can in principle resolve the discrepancy between the GUT and string unification scales. What is highly non-trivial, however, is that precisely the required sorts of extra states naturally appear in some of the realistic free-fermion models we have examined, with the necessary non-standard hypercharges to do the job. Indeed, the crucial representations, as we have seen, are those for which the one-loop beta-function coefficients  $b_2$  and  $b_3$  are rather large, while  $b_1$  is small. It is for this reason that this particular string-predicted extra matter is able to modify the running of the strong and electroweak couplings without substantially affecting the  $U(1)$  coupling.

## 5.7 General conclusions

It is apparent from the analysis presented in this section that string gauge coupling unification imposes a strong constraint on the allowed string models. Models that would otherwise provide a very attractive low-energy phenomenology can be ruled out on the basis that gauge coupling unification at the string scale cannot be in agreement with the low-energy data. The model of Ref. [21] is an example of such a model. In this model, the extra color triplets and electroweak doublets that appear all have quantum numbers that fit into  $\mathbf{5}$  and  $\bar{\mathbf{5}}$  representations of  $SU(5)$ . Consequently, as we have shown, the extra states beyond the MSSM in these models cannot bring the string unification prediction into agreement with experiment. We find it very encouraging that some otherwise very appealing string models can be ruled out on this basis.

Perhaps even more importantly, however, there exist realistic string models in which there naturally appears additional matter that does *not* fit into  $\mathbf{5}$  or  $\bar{\mathbf{5}}$  representations of  $SU(5)$ . As we have shown, for such string models the hypothesis of gauge coupling unification at the string scale can be in agreement with the low-energy data. The model of Refs. [17, 23] is one explicit example of such a string model which contains all the needed representations to achieve string gauge coupling unification, in just the right combinations and with just the correct hypercharges.

We have seen, then, that intermediate matter thresholds seem to be the only possible way in which string-scale gauge coupling unification can be achieved in realistic level-one string models. By level-one string models, we mean string models in which the non-Abelian gauge group content of the Standard Model is realized through a level-one Kač-Moody algebra. While our conclusions might be modified for models in which the gauge group is realized by Kač-Moody algebras at higher level, no realistic three-generation models of this sort have been constructed to date. Consequently, the need for (and appearance of) an additional matter spectrum beyond the MSSM seems to be a *prediction* of realistic level-one string models.

It is remarkable that string theory, which predicts an unexpectedly high unification scale  $M_{\text{string}}$ , in many cases also simultaneously predicts precisely the extra exotic particles needed to reconcile this higher scale with low-energy data. As we have shown, all of the other possible effects are not likely to bridge the gap between the MSSM and string unification scales. This is a profound conclusion, and may have important experimental consequences.

## 6 Why are string-induced threshold corrections so small?

In this section we address the general question of the *size* of the string-induced threshold corrections. Our results in Sects. 4 and 5 for the realistic heterotic free-fermionic models, as well as similar previous calculations for orbifold models [19, 40] and Type-II superstring models [41], all consistently indicate that generic string-induced threshold corrections are relatively small. This result is *a priori* surprising, given the infinite towers of massive states which could in principle affect the running of the gauge couplings. Indeed, we have already remarked that the calculation of the heavy string threshold corrections  $\Delta_G$  in (3.8) is similar to that of the one-loop cosmological constant  $\Lambda$ ,

$$\Lambda \equiv \int_{\mathcal{F}} \frac{d^2\tau}{\tau_2^2} Z(\tau) , \quad (6.1)$$

and typical values of this cosmological-constant integral (6.1) for non-supersymmetric string models are found [59] to be in the range  $\Lambda \sim \mathcal{O}(10^2)$ . Taking this as a typical scale for such one-loop string amplitudes, the question then arises as to why a different particular amplitude, namely the one-loop heavy string threshold correction, should be so highly suppressed.

### 6.1 General argument

This suppression of the string-induced threshold correction is independent of any particular class of string model-construction, and is in fact a general property of string theory. We therefore seek a model-independent explanation of the underlying reason for this suppression.

We begin by focusing on the behavior of the modified partition function  $B_G(\tau)$  which serves as the string integrand in the calculation of the threshold correction  $\Delta_G$  in (3.8), and in particular let us compare it with the ordinary partition function  $Z(\tau)$  which plays the same role in the calculation of the cosmological constant  $\Lambda$ . In analogy to (3.19), we can always expand the partition function  $Z$  in the form

$$Z = \tau_2^{-1} \sum_{m,n} a_{mn} \bar{q}^m q^n \quad (6.2)$$

so that, in analogy with (3.21), we have

$$\Lambda = \sum_{m,n} a_{mn} I_{mn}^{(3)} . \quad (6.3)$$



There are therefore two potential sources of difference between the values of  $\Delta$  and  $\Lambda$ : the integrals themselves are different due to the different powers of  $\tau_2$ , *i.e.*,  $I_{mn}^{(1)} \neq I_{mn}^{(3)}$ , and the coefficients may also be different, *i.e.*,  $b_{mn} \neq a_{mn}$ . Now, while it is true that  $|I_{mn}^{(1)}|$  is usually less than  $|I_{mn}^{(3)}|$ , this is not a major source of difference for two reasons: first,  $|I_{mn}^{(1)}|$  is numerically smaller than  $|I_{mn}^{(3)}|$  by only a few percent, and second, the signs of these integrals tend to alternate with different values of  $m$  and  $n$ . Thus, the major difference between the values of  $\Delta$  and  $\Lambda$  must involve the relative behavior of the coefficients  $\{a_{mn}\}$  and  $\{b_{mn}\}$ .

In order to pin down the essential difference in the behavior of these coefficients, let us first recall their physical interpretations. In the ordinary partition function  $Z$ , each coefficient  $a_{mn}$  represents simply the net number of states with spacetime squared masses  $(M_R^2, M_L^2) = (m, n)$ , where “net” refers to the difference between the numbers of spacetime bosonic and fermionic states. By contrast, in the modified partition functions  $B$ , the coefficients  $b_{mn}$  represent the *charges* of these states relative to the gauge group in question. Thus, states only contribute to  $b_{mn}$  if they carry a non-zero gauge charge.

Now, the general behavior of the ordinary state degeneracies  $a_{mn}$  in string theory is well-known (see, for example, Ref. [43]). In particular, there are two generic features which concern us. The first is the appearance of so-called “unphysical tachyons” in non-supersymmetric heterotic string theories — *i.e.*, states which contribute to coefficients  $a_{mn}$  with  $m + n < 0$  (“tachyonic”) but  $m \neq n$  (“unphysical”). More specifically, it can be shown [43] that *any* non-supersymmetric heterotic string theory which contains gravitons will have  $a_{0,-1} \neq 0$ . (Note that this does not imply that the corresponding spacetime spectrum contains physical tachyons; indeed, the absence of *physical* tachyons requires only that  $a_{nn} = 0$  for all  $n < 0$ .) By contrast, physically sensible string models will never have *charged* unphysical tachyons with energy configuration  $(m, n) = (0, -1)$ . This occurs because any state with energy configuration  $(m, n) = (0, -1)$  must arise as the vacuum state in a Neveu-Schwarz sector, and since such a vacuum state is necessarily a gauge singlet, it cannot carry a non-zero gauge charge. We therefore find that although  $a_{0,-1} \neq 0$  for all non-supersymmetric heterotic string models, we must have  $b_{0,-1} = 0$  regardless of whether spacetime supersymmetry is present.

This is a crucial distinction, because the potential contributions from the  $(m, n) = (0, -1)$  unphysical tachyons are typically larger than those from any other state. Indeed, the integral  $I_{0,-1}^{(s)}$  is typically an order of magnitude greater than any other integral  $I_{m,n}^{(s)}$ . This feature alone, therefore, is responsible for a sizable reduction in the total threshold correction.

Of equal importance, however, is the second generic difference between the coefficients  $a_{mn}$  and  $b_{mn}$ : their behavior as  $m, n \rightarrow \infty$ . As is well-known, the number of physical states in string theory grows *exponentially* with energy, so that

$$a_{mn} \sim A n^{-B} e^{C\sqrt{n}} \quad \text{as } n \rightarrow \infty \quad (6.4)$$

where  $A, B, C$  are constants. This exponential growth in the number of states is the famous Hagedorn phenomenon which signals the existence of either a maximum (Hagedorn) temperature, or string phase transition. Indeed, as discussed in [43], the existence of such exponential growth in the number of string states at high energy is directly related, through modular invariance, to the existence of physical and/or unphysical tachyons at the low energy of the string spectrum, and is hence unavoidable. Of course, this rapid growth in the number of physical states does not lead to a divergent cosmological constant  $\Lambda$ , for there is an even stronger corresponding suppression for the integrals  $I_{nn}^{(s)}$ :

$$I_{nn}^{(s)} \sim e^{-C'n} \quad \text{as } n \rightarrow \infty \quad (6.5)$$

where  $C'$  is a positive constant. Nevertheless, the fact that the  $a_{nn}$  grow so quickly opens up a significant range of values of energy  $n$  for which the contributions of massive states of energy  $n$  to the cosmological constant are still sizable. Thus, the cosmological constant receives important contributions not only from the unphysical tachyonic states (and the physical massless states), but also from the first several massive states.

By contrast, for the threshold corrections, this second source of contributions is often removed as well, for in the case of certain threshold corrections it can be shown that the coefficients  $b_{nn}$  will exhibit growth which is at most *polynomial* rather than exponential [43]. This observation, which is ultimately related to the modular properties of the modified partition function  $B(\tau)$ , will be discussed below. In particular, we shall see that this suppressed polynomial rate of growth occurs for those functions  $B(\tau)$  which arise solely from gauge-charge insertions of the form  $Q_L Q_M$  with  $L \neq M$ , and for which there are no contributions from charged unphysical tachyons. Indeed, a quick scan of the intermediate results listed in Sect. 4 for the appropriate tachyon-free models verifies that the values of  $\Delta$  for those cases with  $L \neq M$  are further suppressed by a sizable amount relative to those with  $L = M$ . Thus, in these cases, not only are the contributions from the unphysical tachyonic states absent (as are the contributions from the massless states), but even the contributions from the massive states are extraordinarily suppressed. Therefore, in these cases, there are *two* features which combine to produce the unusual suppression of the  $L \neq M$  string-induced threshold corrections relative to the corresponding cosmological constant. Indeed, for certain free-fermionic embeddings of the gauge group (such as that of the flipped  $SU(5)$  models), these  $L \neq M$  insertions are the only ones which are relevant. This double-suppression mechanism is then directly responsible for the diminished size of total relative threshold corrections such as  $\Delta_{SU(5)} - \Delta_{U(1)}$ .

Let us now briefly discuss the cases in which charged unphysical tachyons do appear. In these cases, although there will be charged unphysical tachyons making contributions to the threshold corrections  $\Delta_G$ , we still must have  $b_{0,-1} = 0$  (for the general reasons indicated above). Thus, the unphysical  $(m, n) = (0, -1)$  tachyons which would have led to the largest contributions to the threshold corrections must

still be absent. For example, the charged unphysical tachyons that end up contributing to the threshold corrections in the non-supersymmetric  $SU(3) \times SU(2) \times SU(1)$  string model discussed in Sect. 4.5 are all of a more harmless variety, with energies  $m$  and  $n$  never more negative than  $-1/4$ :

$$\tau_2^{-1} B(\tau) = (4\bar{q}^{3/4} + 120\bar{q}^{7/4} + \dots)q^{-1/4} + \text{non-tachyonic} . \quad (6.6)$$

Indeed, these charged unphysical tachyonic states do not contribute nearly as much as the  $(0, -1)$  states, since their corresponding integrals are highly suppressed, with  $I_{3/4, -1/4}^{(1)} \approx -1.44 \times 10^{-3}$  as compared to  $I_{0, -1}^{(1)} \approx -11.04$ . Furthermore, even though these milder charged unphysical tachyonic states may lead to exponentially growing values of  $b_{mn}$  even for the  $L \neq M$  basis insertions, modular transformations can be used to show that the resulting *rate* of exponential growth is also highly suppressed; this suppression is ultimately due to the fact that these tachyons are never as tachyonic as the  $(0, -1)$  tachyons which would otherwise control the rate of growth [43]. Thus, even in the cases that charged unphysical tachyons appear, the above arguments remain intact, for its two main features, namely that

$$b_{0, -1} = 0 \quad \text{and} \quad b_{mn} \ll a_{mn} \quad \text{as} \quad m, n \rightarrow \infty , \quad (6.7)$$

remain unaltered. Thus the string-induced threshold corrections continue to be suppressed in spite of the appearance of such unphysical tachyons.

Finally, we remark that this type of analysis can also incorporate the one case in which string-theoretic threshold corrections are *known* to be large [33, 35]: namely, as the values of particular moduli (such as radii of compactification) are taken to infinity. Indeed, we shall see below that taking such a limit changes the modular properties of the modified partition function  $B(\tau)$  in so fundamental a way that the above suppression mechanisms (6.7) no longer apply. Thus, even in this case, the sizes of the threshold corrections can still be understood as a consequence of the modular properties of the modified partition functions  $B(\tau)$  and the behavior of their coefficients  $b_{mn}$ .

## 6.2 The modular properties of the modified partition function

We now turn to the modular properties of the modified partition functions  $B(\tau)$ , and the resulting behavior of their coefficients  $b_{mn}$  as  $m, n \rightarrow \infty$ .

As discussed above, if a given string model is devoid of charged physical or unphysical tachyons, then the corresponding modified partition function  $B(\tau)$  must have coefficients  $b_{mn}$  which always vanish for all  $m + n < 0$ , and which often grow at most *polynomially* as  $m, n \rightarrow \infty$ . However, this is behavior for the coefficients is certainly unusual, given the expectations based on analyzing ordinary partition functions  $Z(\tau)$ . Indeed, it can be shown [43] that any partition function  $Z(\tau)$  with  $a_{mn} = 0$  for all  $m + n < 0$  must in fact have *all* coefficients vanishing, so that  $Z = 0$  identically;

otherwise, if these unphysical tachyonic coefficients are non-zero, then the partition function  $Z$  must have coefficients  $a_{mn}$  which grow *exponentially*. It turns out that this is a general theorem which applies to all partition functions  $Z$  which correspond to string theories in  $D > 2$  uncompactified spacetime dimensions (or equivalently, for all modular functions with modular weights  $k < 0$ ). The question then arises as to how the *modified* partition functions  $B_G(\tau)$  manage to evade these constraints, and survive to exhibit non-zero coefficients  $b_{mn}$  at higher levels despite having no tachyonic contributions in many cases. Moreover, we also wish to determine the underlying reason why this growth is fundamentally different depending on the form of the  $Q_L Q_M$  insertion, polynomial if  $L \neq M$ , and exponential otherwise. We also wish to understand why the limit of large moduli changes these results, and allows the corresponding threshold corrections to grow large.

To answer these questions, we must first recall some facts about modular functions. In general, modular functions  $f_i(\tau)$  (such as conformal-field-theoretic characters  $\chi_i$ ) transform covariantly under modular transformations,

$$f_i\left(\frac{a\tau + b}{c\tau + d}\right) = (c\tau + d)^k \sum_j M_{ij} f_j(\tau), \quad (6.8)$$

where the exponent  $k$  is called the *modular weight* and where the matrix  $M_{ij}$  is a mixing matrix which represents the particular modular transformation in the space of functions  $f_i$ . One then builds a full holomorphic/anti-holomorphic modular invariant function (such as a partition function) by combining two such sets of characters  $f_i$  and  $g_i$ , each with modular weight  $k$ , in the form

$$Z(\tau, \bar{\tau}) = \tau_2^k \sum_{ij} N_{ij} \overline{g_i(\tau)} f_j(\tau) \quad (6.9)$$

where  $\tau_2 \equiv \text{Im } \tau$  and where  $N_{ij}$  is a matrix chosen to satisfy  $\tilde{M}^\dagger N M = N$  (where  $\tilde{M}$  and  $M$  are respectively the modular transformation representation matrices in the spaces of functions  $g_i$  and  $f_i$ ). For example, for the classes of free-fermionic string models we have been examining, our fundamental modular functions are the  $\eta$  and  $\Theta$  functions which appear in (3.11) and (3.12), and from (3.11) we see that the total combined holomorphic and anti-holomorphic functions  $f_i$  and  $g_i$  take the general schematic forms

$$\begin{aligned} f &\sim \eta^{-24} \Theta^{22} \\ g &\sim \eta^{-12} \Theta^{10}. \end{aligned} \quad (6.10)$$

Since the  $\eta$  and  $\Theta$  functions are modular functions with weights  $k = 1/2$ , we see that the total partition functions  $Z$  for these models all have the total modular weight  $k = -1$ . Note that this is consistent with the factor of  $\tau_2^{-1}$  which appears in (3.11). Indeed, the general relation between the total modular weight  $k$  of the partition function  $Z$  and the spacetime dimension of the corresponding string theory is

$$k = 1 - D/2. \quad (6.11)$$

For the *modified* partition functions  $B$ , however, this is no longer the case, for the effect of the charge insertions into the trace is to *increase* the modular weight from  $k$  to  $k + 2$ . We can see this easily as follows. Let us first define the more general  $\Theta$  function of two variables  $z$  and  $\tau$ ,

$$\Theta \left[ \begin{matrix} \alpha \\ \beta \end{matrix} \right] (z|\tau) \equiv \sum_{n=-\infty}^{\infty} e^{2\pi i(z+\beta)(n+\alpha)} q^{(n+\alpha)^2/2}, \quad (6.12)$$

so that our usual  $\Theta$  functions of a single variable  $\tau$  can be obtained from these more general functions by projecting to  $z = 0$ :

$$\Theta \left[ \begin{matrix} \alpha \\ \beta \end{matrix} \right] (\tau) = e^{-2\pi i\alpha\beta} \left\{ \Theta \left[ \begin{matrix} \alpha \\ \beta \end{matrix} \right] (z|\tau) \right\} \Big|_{z=0}. \quad (6.13)$$

Then, in terms of this generalized function, the singly primed function  $\Theta'$  which results from the insertion of a single charge operator  $Q$  into the trace can be written as the result of a single derivative with respect to  $z$ :

$$\Theta' \left[ \begin{matrix} \alpha \\ \beta \end{matrix} \right] (\tau) = e^{-2\pi i\alpha\beta} \left\{ \frac{1}{2\pi i} \frac{d}{dz} \Theta \left[ \begin{matrix} \alpha \\ \beta \end{matrix} \right] (z|\tau) \right\} \Big|_{z=0}. \quad (6.14)$$

Likewise, the doubly primed function  $\Theta''$ , which results from the insertion of *two* charge-operator insertions, can be obtained from  $\Theta(z|\tau)$  via a second derivative with respect to  $z$ :

$$\begin{aligned} \Theta'' \left[ \begin{matrix} \alpha \\ \beta \end{matrix} \right] (\tau) &= e^{-2\pi i\alpha\beta} \left\{ \left( \frac{1}{2\pi i} \right)^2 \frac{d^2}{dz^2} \Theta \left[ \begin{matrix} \alpha \\ \beta \end{matrix} \right] (z|\tau) \right\} \Big|_{z=0} \\ &= \frac{1}{i\pi} \frac{d}{d\tau} \Theta \left[ \begin{matrix} \alpha \\ \beta \end{matrix} \right] (\tau). \end{aligned} \quad (6.15)$$

Now, the general  $\Theta(z|\tau)$  functions have modular transformations of the form

$$\Theta \left( \frac{z}{c\tau + d} \middle| \frac{a\tau + b}{c\tau + d} \right) \sim (c\tau + d)^{1/2} \exp \left( \frac{i\pi cz^2}{c\tau + d} \right) \Theta(z|\tau) \quad (6.16)$$

where we have neglected overall  $\tau$ - and  $z$ -independent phases and mixing matrices. From this result [in particular the exponent of the  $(c\tau + d)$  factor], we easily see that the modular weight of each  $\Theta$ -function is  $k = 1/2$ . However, using (6.16) and taking a derivative with respect to  $z$  before the projection to  $z = 0$ , we find that  $\Theta'$  transforms just like  $\Theta$  except with exponent  $k + 1 = 3/2$ . Likewise, a second derivative with respect to  $z$  further increases the exponent to  $k + 2 = 5/2$ . Now, recall from (3.7) that the modified partition functions  $B$  contain a total of two (helicity) charge insertions for the right-moving anti-holomorphic sector, and two corresponding (gauge) charge insertions for the left-moving holomorphic sector. Thus, the total modular weight of the modified partition function  $B$  is not the negative value  $k = -1$  which we would

have expected for four dimensional theories, but rather  $k' = k + 2 = +1$ . Note that this is also consistent with the two extra factors of  $\tau_2$  which were inserted along with the charge insertions into the trace in (3.7).

It is for this reason that  $B$  can be non-zero even though it may contain no contributions from physical or unphysical tachyons. Indeed, the theorem mentioned above, which would have forced such functions to vanish, holds only for functions with negative modular weights. By contrast, as discussed in Ref. [43], the coefficients for tachyon-free functions with *positive* modular weights are expected to grow polynomially.

Given that the coefficients  $b_{mn}$  are expected to grow polynomially for tachyon-free theories, we still must explain why this growth is in fact exponential for the cases of gauge charge insertions  $Q_L Q_M$  with  $L = M$ , or for the limit of large moduli. Indeed, such exponential growth is more typical for partition functions of negative modular weight.

It turns out that for the cases of insertions  $Q_L Q_M$  with  $L = M$ , this behavior is caused by a modular anomaly which prevents the modified partition functions  $B(\tau)$  from being truly modular-invariant. We can see how this anomaly arises as follows. We have already shown above in (6.14) that a single charge insertion  $Q_L$  is equivalent to differentiation with respect to  $z$  followed by projection to  $z = 0$ , so that if a certain trace  $f_i(\tau)$  without any charge insertion transforms modular-covariantly as in (6.8), then the same trace with a single charge insertion  $f'_i(\tau)$  will transform modular covariantly with increased modular weight:

$$f'_i\left(\frac{a\tau + b}{c\tau + d}\right) = (c\tau + d)^{k+1} \sum_j M_{ij} f'_j(\tau). \quad (6.17)$$

However, this is not the case for the traces  $f''_i(\tau)$  with *two* identical charge insertions. As shown in (6.15), the insertion of two identical charges  $Q_L$  is tantamount to two  $z$ -derivatives or a single  $\tau$ -derivative, yet these derivatives are not covariant with respect to modular transformations. Indeed, it is easy to see that if  $f_i(\tau)$  transforms as in (6.8) under  $\tau \rightarrow \tau' \equiv (a\tau + b)/(c\tau + d)$ , then

$$\frac{d}{d\tau} f_i(\tau) \rightarrow \frac{d}{d\tau'} f_i(\tau') = (c\tau + d)^{k+2} \sum_j M_{ij} \frac{d}{d\tau} f_j(\tau) + ck(c\tau + d)^{k+1} \sum_j M_{ij} f_j(\tau). \quad (6.18)$$

While the first term is of the proper covariant form, the second term is not. Rather, the true ‘‘covariant derivative’’ on the space of modular functions of weight  $k$  is actually

$$D \equiv \frac{d}{d\tau} - \frac{ik}{2\tau_2}; \quad (6.19)$$

here the contribution from the second term cancels the anomaly caused by the first. Thus, double gauge charge insertions of the form  $Q_L Q_M$  with  $L = M$  destroy the modular covariance of the holomorphic or left-moving sector, transforming a modular

function of weight  $k = -1$  into not only a modular function of weight  $k + 2 = +1$ , but also an anomaly term consisting of a modular function of the original weight  $k = -1$  divided by  $\tau_2$ .

It is this feature which ultimately explains why exponential growth of the coefficients  $b_{mn}$  can occur for these double gauge-charge insertions. Recall that regardless of the particular gauge-charge insertion for the left-moving sector, there is always a double charge insertion for the right-moving sector — this is the helicity insertion  $\overline{Q}_H^2$ . Thus, for the  $L = M$  cases, the anomaly term from the right-moving sector can combine with the anomaly term from the left-moving sector to recreate a modular function with equal left- and right-moving modular weights  $k = -1$ . Indeed, such a term will appear divided by two powers of  $\tau_2$ , just as required for reproducing a proper modular function of weight  $k = -1$ . Thus, for the  $L = M$  cases, a remnant of the original  $k = -1$  behavior survives despite the charge insertions. It is this which is ultimately responsible for the exponential growth rate for the coefficients  $b_{mn}$  in these cases.

A similar mechanism occurs in the cases of models for which a modulus (such as a radius of compactification) is taken to infinity. In these cases, we are effectively changing the dimensionality of the theory, so that once again the modular weight  $k$  of the modified partition function is decreased below zero.\* Indeed, the act of taking a radius of compactification to infinity amounts to replacing

$$\frac{\overline{\Theta}\Theta}{\overline{\eta}\eta} \longrightarrow \frac{1}{\sqrt{\tau_2}} \frac{1}{\overline{\eta}\eta} \quad (6.20)$$

in the modified partition functions  $B(\tau)$ . This occurs because the  $\Theta$ -functions, which had previously represented the lattice sums over discrete momentum- and winding-mode vacua, now become continuous integrals which can be evaluated, yielding mere extra inverse factors of  $\tau_2$  in the decompactification limit. Thus, the effective modular weight of the remaining function  $B(\tau)$  is decreased in this limit of large moduli, and the above arguments then lead to larger values of threshold corrections.

Finally, we remark that since the helicity insertion  $\overline{Q}_H^2$  always takes the form of a double-charge insertion (or equivalently a single  $\tau$ -derivative, with its associated modular anomaly), the modified partition functions  $B(\tau)$  are never modular-invariant in any case. However, an improved derivation of the string-theoretic gauge coupling threshold corrections which is manifestly modular-invariant has recently appeared in Ref. [38]. In this analysis, manifestly modular-invariant results are achieved by explicitly introducing an infrared regulator (provided by introducing a curved spacetime), and by taking into account the back-reaction from both gauge and gravitational interactions. Moreover, these modifications result in expressions for threshold corrections which yield their *absolute* sizes, rather than merely their relative differences. These expressions also incorporate the additional contributions (such as those due to dilaton tadpoles) which must be included in the cases of string models without spacetime

---

\* We thank I. Antoniadis for discussions on this point.

supersymmetry. We hope to repeat our threshold analysis using these expressions in a future work.

## 7 Conclusions

In this paper we examined in detail the problem of gauge coupling unification in realistic heterotic string models. The class of models that we studied are all constructed in the free-fermionic formulation, and are among the most realistic string models constructed to date. We believe that this fact is not accidental, but may reflect deeper properties of string compactification that are at present unknown. Indeed, the free-fermionic models are constructed at a highly symmetric point in the string compactification space, and the  $Z_2 \times Z_2$  orbifold structure that is realized in these realistic free-fermionic models may be deeply connected to the existence of only three light generations in nature.

Despite their many attractive properties, however, the realistic free-fermionic models (and string theory in general) predict that the gauge couplings unify at the string scale, which is of approximately  $5 \times 10^{17}$  GeV. This implies that if the string spectrum below the string scale is assumed to be that of the MSSM, then the string-predicted values of the low-energy parameters  $\sin^2 \theta_W(M_Z)$  and  $\alpha_3(M_Z)$  will be in disagreement with the experimentally observed values. We explicitly illustrated this disagreement by evaluating the associated renormalization group equations including two-loop, Yukawa-coupling, and scheme-conversion corrections.

The question then arises as to whether this disagreement with the low-energy observables can be used to rule out this class of realistic string models, or whether other effects may arise to alter this conclusion. To answer this question, therefore, it is necessary to examine all of the possible effects that can modify this result.

One possibility is that the tree-level string predictions may be modified by the one-loop heavy string threshold corrections due to the infinite tower of heavy string modes. We developed a method for evaluating these threshold corrections in the free-fermionic string models, and were able not only to evaluate the string threshold corrections to any desired accuracy, but also to perform various non-trivial consistency checks in our analysis. We evaluated these string threshold corrections within a range of realistic free-fermionic models, and in general we found that the string threshold corrections are small and cannot explain the disagreement with the experimentally observed values. In fact, in all the cases that we studied, we found that the string threshold corrections tend to *elevate* the string unification scale by approximately 20%, and consequently enhance the disagreement with experiment. Moreover, we found that the string threshold corrections are, in general, not significantly affected by the choice of the gauge group, the existence of spacetime supersymmetry, or the presence of charged unphysical tachyons. We were also able to provide a model-independent argument which explains why such threshold corrections are naturally suppressed in string theory, except at points with large moduli. Our argument re-



lied on only the modular properties of the modified partition functions  $B(\tau)$  which enter the calculation of the threshold corrections, and hence should have validity beyond the class of free-fermionic string models studied here. Hence, we conclude that string threshold corrections cannot resolve the disagreement with the experimentally observed values in these models.

Other possible corrections may arise due to stringy modifications of the  $U(1)_{\hat{Y}}$  hypercharge normalizations, light SUSY thresholds, additional gauge structure at intermediate energy scales, or additional matter thresholds at intermediate energy scales. We found that smaller values of the  $U(1)_{\hat{Y}}$  normalization  $k_1$  can result in agreement with experiment, but we argued on general grounds that such smaller values of  $k_1$  are not possible in self-consistent string models. To analyze the possible contributions from light SUSY thresholds, we parametrized the low-energy SUSY spectrum assuming universal soft SUSY-breaking terms, and found that light SUSY thresholds also cannot bring the string predictions into agreement with experiment. This conclusion is unaltered even if the assumption of universality is relaxed. We also examined the possibility of additional gauge structure at intermediate energy scales, and showed that within the context of these realistic free-fermionic string models, this also cannot resolve the discrepancy.

Finally, we examined the effect of intermediate matter thresholds. Because we were able to rule out each of the other effects in the realistic string models, only the presence of additional non-MSSM matter could possibly reconcile string-scale unification with low-energy data. In the realistic free-fermionic string models, additional matter beyond the MSSM generically appears in the massless spectrum. This matter takes the form of color triplets and electroweak doublets, in vector-like representations. While some of these extra matter representations have the weak hypercharge assignments that are common in grand-unified theories, some have weak hypercharge assignments that are unique to the string models and do not arise in regular GUT's. The ultimate mass scales of these extra states will be determined by the renormalizable and non-renormalizable terms in the superpotential, but in general the mass scale of the additional states will not be at the string scale. Therefore, in general it is unjustified to assume that the spectrum below the string scale is that of the MSSM. We showed that in some models, these appearance of these additional states does not resolve the discrepancy between string-scale unification and low-energy data; hence these models can be ruled out. More interestingly, however, we found that certain other realistic string models provide just the right combinations of extra matter representations, with just the right gauge quantum numbers, to allow string-scale unification to be consistent with the low-energy data. Indeed, within these models, we found that a significant window exists for the additional mass scales so that the predicted values of the low-energy parameters  $\alpha_{\text{strong}}(M_Z)$  and  $\sin^2 \theta_W(M_Z)$  will be in agreement with the experimentally observed values. In some of these models (*e.g.*, the model of Refs. [17, 23]), these extra states have a uniquely stringy origin, and may have profound experimental implications. It is then imperative to examine whether

the mass scales of these additional thresholds can be derived from the string models, and take the desired values. Such work is currently in progress, and will be reported in future publications.

## Acknowledgments

We are pleased to thank S. Chaudhuri, S.-W. Chung, L. Dolan, J. Louis, J. March-Russell, J. Pati, M. Peskin, F. Wilczek, E. Witten, and especially I. Antoniadis and E. Kiritsis for discussions. This work was supported in part by DOE Grant No. DE-FG-0290ER40542.

## Appendix A

Here we provide the explicit  $\mathbf{V}_i$  and  $k_{ij}$  defining parameters for each of the models we consider in the text.

As we discussed in Sect. 2, four-dimensional string models in the free-fermionic construction are defined by a set of boundary conditions for the 64 worldsheet Majorana-Weyl fermions, as well as a set of phases which ultimately describe how the generalized GSO projections are to be performed in each sector. In the notation of Ref. [11] which we shall use below, these boundary-condition vectors are denoted  $\mathbf{V}_i$ ,  $i = 0, \dots, N$  (where  $N + 1$  is the model-dependent number of vectors which are necessary); likewise, the phases are defined through an  $(N + 1) \times (N + 1)$  matrix denoted  $k_{ij}$ . However, most of the models we analyze originally appeared in the literature in the different notation of Ref. [10]. In this latter notation, boundary-condition vectors are denoted  $\mathbf{b}_i$  and the generalized GSO phases are denoted  $C \begin{bmatrix} \mathbf{b}_i \\ \mathbf{b}_j \end{bmatrix}$ . For completeness, we now give below the explicit mapping between these two notations:

$$\begin{aligned} \mathbf{b}_i &= -2 \mathbf{V}_i \\ C \begin{bmatrix} \mathbf{b}_i \\ \mathbf{b}_j \end{bmatrix} &= \exp \left[ 2\pi i \left( \mathbf{V}_i^1 + \mathbf{V}_j^1 + k_{ji} - \mathbf{V}_i \cdot \mathbf{V}_j \right) \right] \end{aligned} \quad (\text{A.1})$$

where  $\mathbf{V}_\ell^1$  denotes the first component of the vector  $\mathbf{V}_\ell$  (*i.e.*, the component corresponding to the worldsheet fermion  $\psi^\mu$  carrying spacetime Lorentz indices). Furthermore, inner products such as  $\mathbf{V}_i \cdot \mathbf{V}_j$  are defined with opposite signs in the two notations, so that

$$\mathbf{b}_i \cdot \mathbf{b}_j = -4 \mathbf{V}_i \cdot \mathbf{V}_j. \quad (\text{A.2})$$

Finally, however, we point out that an important issue is the adoption of a self-consistent scheme for handling the zero-modes of real Ramond fermions. In the notation of Ref. [11], an explicit convention is established and we have adopted this convention in our calculations; this is the origin, for example, of the crucial phase contribution  $\Gamma_{\beta\mathbf{V}}^{\alpha\mathbf{V}}$  which appears in (3.13). Without this phase contribution, our

expressions for the partition function  $Z(\tau)$  would not have been modular-invariant. However, in the literature (and, in particular, in the papers in which these models first appeared), other conventions have been implicitly adopted for handling the zero-modes. Thus, it is necessary to take these changes of convention into account when translating between the two notations. Fortunately, for the case of all of the present models, these extra changes of convention can be absorbed through changes in the  $k_{ij}$ -phases [beyond those  $k_{ij}$  values implied by (A.1)]. It is only with these additional effective phase changes that the correct particle spectrum for each model is produced.

Thus, in terms of the exact  $(\mathbf{V}_i, k_{ij})$  notation and zero-mode conventions of Ref. [11], the models which we have analyzed in this paper can be listed as follows. First, as discussed in Sect. 2, they all share the same first boundary-condition vectors which comprise the so-called NAHE set. In the present  $\mathbf{V}$ -notation appropriate for 64 Majorana-Weyl fermions, the NAHE set takes the following form:

	right-movers	left-movers
$\mathbf{V}_0$	11111111111111111111	11
$\mathbf{V}_1$	11100100100100100100	00
$\mathbf{V}_2$	11100100010010010010	0000101010101011111100000000001111110000000000
$\mathbf{V}_3$	11010010100100001001	10100000010111111010000000001111101000000000
$\mathbf{V}_4$	11001001001001100100	01010101000011111001000000001111100100000000

where the entry ‘1’ is shorthand for ‘ $-1/2$ ’. Here the  $\mathbf{V}_0$  through  $\mathbf{V}_4$  vectors correspond to the vectors  $\{\mathbf{1}, S, \mathbf{b}_1, \mathbf{b}_2, \mathbf{b}_3\}$  described previously.

The individual models are then each derived from this underlying NAHE structure through the addition of extra boundary-condition vectors  $V_i$ , and the specific choice of GSO phases  $k_{ij}$ . These are listed below.

### A.1 Flipped SU(5) model

This is the model we considered in Sect. 4.1. This model has the additional boundary-condition vectors

	right-movers	left-movers
$\mathbf{V}_5$	11100100010001001010	00001001011011111100000000001111110000000000
$\mathbf{V}_6$	11001010100100001010	01100000011011111010000000001111101000000000
$\mathbf{V}_7$	00000000000011000011	000101110011-----1100-----1100

where ‘-’ is shorthand for ‘ $-1/4$ ’. Furthermore,  $k_{00}$  and the following phases  $k_{ij}$  with  $i > j$  are equal to  $1/2$ :  $k_{20}, k_{21}, k_{30}, k_{31}, k_{32}, k_{40}, k_{41}, k_{42}, k_{43}, k_{51}, k_{52}, k_{53}, k_{54}, k_{61}, k_{62}, k_{63}, k_{64}, k_{65}, k_{70}, k_{76}$ . The remaining phases with  $i > j$  are vanishing, and those with  $i \leq j$  are determined from those with  $i > j$  using the constraint equations given in Ref. [11].

Note that starting from this model as it was originally published and following the strict mapping given in (A.1), we would have instead found that  $k_{50}$  and  $k_{60}$

should also be non-zero (as well as corresponding changes in those  $i \leq j$  phases which are related to these through the constraint equations of Ref. [11]). However, as discussed above, we must set  $k_{50}$  and  $k_{60}$  to zero in order to account for the difference in the implicit conventions for dealing with the Ramond zero-modes. Only with such modifications is the correct model with the same particle spectrum reproduced.

### A.2 First $SU(3) \times SU(2) \times U(1)$ model

This is the model we considered in Sect. 4.2. This model has the additional boundary-condition vectors

	right-movers	left-movers
$V_5$	00000000011000000011	10010101010111110000011111000011110000011110000
$V_6$	00011000000000011000	01011001101011110000011111000011110000011110000
$V_7$	00000011000011000000	101010100110-----011---0-----011---0

where again ‘-’ is shorthand for ‘ $-1/4$ ’. In this model,  $k_{00}$  and the following phases  $k_{ij}$  with  $i > j$  are equal to  $1/2$ :  $k_{20}, k_{21}, k_{30}, k_{31}, k_{32}, k_{40}, k_{41}, k_{42}, k_{43}, k_{50}, k_{52}, k_{60}, k_{63}, k_{65}, k_{74}, k_{75}$ . All remaining  $i > j$  phases vanish, and those with  $i \leq j$  may be determined from those with  $i > j$  using the constraint equations given in Ref. [11].

In this case, no phase adjustments are necessary in order to account for the difference in Ramond zero-mode conventions.

### A.3 Non-supersymmetric version of first $SU(3) \times SU(2) \times U(1)$ model

This is the model we considered in Sect. 4.5. This model has the same additional boundary-condition vectors and phases as the model above, except that  $k_{51}, k_{61}$ , and  $k_{71}$  are changed from 0 to  $1/2$ . (Of course, given the constraint equations of Ref. [11], this induces corresponding changes in the coefficients  $k_{ij}$  with  $i \leq j$ .) As required, these changes have the effect of breaking spacetime supersymmetry *without* introducing physical tachyons into the spectrum.

### A.4 Second $SU(3) \times SU(2) \times U(1)$ model

This is the model we considered in Sect. 4.3. This model has the additional boundary-condition vectors

	right-movers	left-movers
$V_5$	00011011011011011011	01100110100111110000011111000011110000011110000
$V_6$	00000011000011000000	10101010011011110000011111000011110000011110000
$V_7$	00011000000000011000	010110011010-----011---0-----011---0

In this model,  $k_{00}$  and the following phases  $k_{ij}$  with  $i > j$  are equal to  $1/2$ :  $k_{20}, k_{21}, k_{30}, k_{31}, k_{32}, k_{40}, k_{41}, k_{42}, k_{43}, k_{50}, k_{52}, k_{53}, k_{54}, k_{60}, k_{65}, k_{70}, k_{73}$ . All remaining  $i > j$

phases vanish, and those with  $i \leq j$  may be determined from those with  $i > j$  using the constraint equations given in Ref. [11].

For this model, it is necessary to set  $k_{64}$  to zero in order to be consistent with our Ramond zero-mode conventions.

### A.5 $\text{SO}(6) \times \text{SO}(4)$ model

This is the model we considered in Sect. 4.4. This model has the additional boundary-condition vectors

	right-movers	left-movers
$\mathbf{V}_5$	11100100010001001010	00001001011011111100000000001111110000000000
$\mathbf{V}_6$	11001010100100001010	01100000011011111010000000001111101000000000
$\mathbf{V}_7$	00000000000000000011	000000000011111111111110000111111111110000
$\mathbf{V}_8$	00000000000011000011	00010111001111100110000110001110011000011000

In this model,  $k_{00}$  and the following phases  $k_{ij}$  with  $i > j$  are equal to  $1/2$ :  $k_{20}, k_{21}, k_{30}, k_{31}, k_{32}, k_{40}, k_{41}, k_{42}, k_{43}, k_{50}, k_{51}, k_{52}, k_{53}, k_{60}, k_{61}, k_{65}, k_{70}, k_{72}, k_{73}, k_{74}, k_{80}, k_{84}, k_{86}$ . All remaining  $i > j$  phases vanish, and those with  $i \leq j$  may be determined from those with  $i > j$  using the constraint equations given in Ref. [11].

For this model, in order to be consistent with our Ramond zero-mode conventions, it is necessary to set  $k_{63}$  and  $k_{83}$  to zero, and  $k_{53}$  and  $k_{86}$  to  $1/2$ .

## References

- [1] For reviews, see:  
H.P. Nilles, *Phys. Rep.* **110** (1984) 1;  
R. Arnowitt and P. Nath, *Applied N=1 Supergravity* (World Scientific, Singapore, 1983);  
H.E. Haber and G. L. Kane, *Phys. Rep.* **117** (1985) 75;  
D.V. Nanopoulos and A.B. Lahanas, *Phys. Rep.* **145** (1987) 1.
- [2] F. Abe *et al*, preprint FERMILAB-PUB-95/022-E, hep-ex/9503002;  
S. Abachi *et al*, preprint FERMILAB-PUB-95/028-E, hep-ex/9503003.
- [3] See, *e.g.*, J. Erler and P. Langacker, preprint UPR-0632-T, hep-ph/9411203, and references therein.
- [4] U. Amaldi *et al*, *Phys. Rev.* **D36** (1987) 1385;  
P. Langacker and M. Luo, *Phys. Rev.* **D44** (1991) 817;  
J. Ellis, S. Kelley, and D. V. Nanopoulos, *Phys. Lett.* **B249** (1990) 441; *Phys. Lett.* **B260** (1991) 131; *Nucl. Phys.* **B373** (1992) 55;  
U. Amaldi, W. de Boer, and H. Füstenaу, *Phys. Lett.* **B260** (1991) 447;  
H. Arason *et al*, *Phys. Rev.* **D46** (1992) 3945;  
F. Anselmo, L. Cifarelli, A. Peterman, and A. Zichichi, *Nuovo Cimento* **105A** (1992) 1179;  
P. Langacker and N. Polonsky, *Phys. Rev.* **D47** (1993) 4028, hep-ph/9210235;  
A.E. Faraggi and B. Grinstein, *Nucl. Phys.* **B422** (1994) 3, hep-ph/9308329.
- [5] For a review, see:  
M.B. Green, J.H. Schwarz, and E. Witten, *Superstring Theory, Vols. 1 & 2* (Cambridge University Press, Cambridge, 1987).
- [6] D.J. Gross, J.A. Harvey, J.A. Martinec, and R. Rohm, *Phys. Rev. Lett.* **54** (1985) 502; *Nucl. Phys.* **B256** (1986) 253.
- [7] P. Candelas, G.T. Horowitz, A. Strominger, and E. Witten, *Nucl. Phys.* **B258** (1985) 46.
- [8] E. Witten, *Nucl. Phys.* **B258** (1985) 75;  
J.D. Breit, B.A. Ovrut, and G.C. Segré, *Phys. Lett.* **B158** (1985) 75;  
A. Sen, *Phys. Rev. Lett.* **55** (1985) 33;  
A.E. Faraggi, *Nucl. Phys.* **B428** (1994) 111, hep-ph/9403312.
- [9] H. Kawai, D.C. Lewellen, and S.-H.H. Tye, *Nucl. Phys.* **B288** (1987) 1.
- [10] I. Antoniadis, C.P. Bachas, and C. Kounnas, *Nucl. Phys.* **B289** (1987) 87.

- [11] H. Kawai, D.C. Lewellen, J.A. Schwartz, and S.-H.H. Tye, *Nucl. Phys.* **B299** (1988) 431.
- [12] A.E. Faraggi, *Nucl. Phys.* **B407** (1993) 57, hep-ph/9210256; *Phys. Lett.* **B326** (1994) 62, hep-ph/9311312.
- [13] A.E. Faraggi, *Phys. Lett.* **B274** (1992) 47.
- [14] A.E. Faraggi, *Nucl. Phys.* **B403** (1993) 101, hep-th/9208023;  
A.E. Faraggi and E. Halyo, *Phys. Lett.* **B307** (1993) 305, hep-ph/9301261; *Nucl. Phys.* **B416** (1994) 63, hep-ph/9306235.
- [15] D.C. Lewellen, *Nucl. Phys.* **B337** (1990) 61;  
A. Font, L.E. Ibáñez, and F. Quevedo, *Nucl. Phys.* **B345** (1990) 389.
- [16] S. Chaudhuri, S.-W. Chung, G. Hockney, and J. Lykken, hep-ph/9501361;  
G. Aldazabal, A. Font, L.E. Ibáñez, and A.M. Uranga, hep-th/9410206.
- [17] A.E. Faraggi, *Phys. Lett.* **B302** (1993) 202, hep-ph/9301268.
- [18] L.E. Ibáñez, *Phys. Lett.* **B318** (1993) 73, hep-ph/9408333.
- [19] V.S. Kaplunovsky, *Nucl. Phys.* **B307** (1988) 145; Erratum: *ibid.* **B382** (1992) 436, hep-th/9205070.
- [20] I. Antoniadis, J. Ellis, J. Hagelin, and D.V. Nanopoulos, *Phys. Lett.* **B231** (1989) 65.
- [21] A.E. Faraggi, *Phys. Lett.* **B278** (1992) 131.
- [22] A.E. Faraggi, *Nucl. Phys.* **B387** (1992) 239, hep-th/9208024.
- [23] A.E. Faraggi, *Phys. Lett.* **B339** (1994) 223, hep-ph/9408333.
- [24] I. Antoniadis, G.K. Leontaris, and J. Rizos, *Phys. Lett.* **B245** (1990) 161.
- [25] K.R. Dienes and A.E. Faraggi, *Phys. Rev. Lett.* **75** (1995) 2646, hep-th/9505018.
- [26] A.E. Faraggi, D.V. Nanopoulos, and K. Yuan, *Nucl. Phys.* **B335** (1990) 347.
- [27] J. Lopez, D.V. Nanopoulos, and K. Yuan, *Nucl. Phys.* **B399** (1993) 654, hep-th/9203025.
- [28] S. Kalara, J. Lopez, and D.V. Nanopoulos, *Nucl. Phys.* **B353** (1991) 650.
- [29] K.S. Narain, *Phys. Lett.* **B169** (1986) 41;  
K.S. Narain, M.H. Sarmadi, and E. Witten, *Nucl. Phys.* **B279** (1987) 369.

- [30] E. Witten, *Phys. Lett.* **B155** (1985) 151.
- [31] P. Ginsparg, *Phys. Lett.* **B197** (1987) 139.
- [32] M. Dine and N. Seiberg, *Phys. Rev. Lett.* **55** (1985) 366;  
V.S. Kaplunovsky, *Phys. Rev. Lett.* **55** (1985) 1036.
- [33] L.J. Dixon, V.S. Kaplunovsky, and J. Louis, *Nucl. Phys.* **B355** (1991) 649;  
V.S. Kaplunovsky and J. Louis, *Nucl. Phys.* **B444** (1995) 191, hep-th/9502077.
- [34] See, *e.g.*, the following papers and references therein:  
I. Antoniadis, K.S. Narain, and T.R. Taylor, *Phys. Lett.* **B267** (1991) 37;  
I. Antoniadis, E. Gava, and K.S. Narain, *Phys. Lett.* **B283** (1992) 209, hep-th/9203071;  
J.P. Derendinger, S. Ferrara, C. Kounnas, and F. Zwirner, *Phys. Lett.* **B271** (1991) 307; *Nucl. Phys.* **B372** (1992) 145;  
G. Lopes Cardoso and B.A. Ovrut, *Nucl. Phys.* **B369** (1992) 351;  
P. Mayr and S. Stieberger, *Nucl. Phys.* **B407** (1993) 725, hep-th/9303017; *Nucl. Phys.* **B412** (1994) 502, hep-th/9304055;  
D. Bailin and A. Love, *Phys. Lett.* **B292** (1992) 315;  
D. Bailin, A. Love, W.A. Sabra, and S. Thomas, *Phys. Lett.* **B320** (1994) 21, hep-th/9309133; *Mod. Phys. Lett.* **A10** (1995) 337, hep-th/9407049;  
M. Chemtob, hep-th/9506018.
- [35] L.E. Ibáñez, D. Lüüst, and G.G. Ross, *Phys. Lett.* **B272** (1991) 251.
- [36] P. Mayr and S. Stieberger, hep-th/9412196; hep-th/9504129.
- [37] I. Antoniadis, E. Gava, and K.S. Narain, *Nucl. Phys.* **B383** (1992) 93, hep-th/9204030;  
B. de Wit, V.S. Kaplunovsky, J. Louis, and D. Lüüst, hep-th/9504006;  
I. Antoniadis *et al*, hep-th/9504034.
- [38] E. Kiritsis and C. Kounnas, preprint CERN-TH-7471-94, hep-th/9410212; *Nucl. Phys.* **B442** (1995) 472, hep-th/9501020; preprint CERN-TH-95-172, hep-th/9507051.
- [39] I. Antoniadis, J. Ellis, R. Lacaze, and D.V. Nanopoulos, *Phys. Lett.* **B268** (1991) 188.
- [40] P. Mayr, H.P. Nilles, and S. Stieberger, *Phys. Lett.* **B317** (1993) 53, hep-th/9307171.
- [41] L. Dolan and J.T. Liu, *Nucl. Phys.* **B387** (1992) 86, hep-th/9205094.



- [42] M. Dine, N. Seiberg, and E. Witten, *Nucl. Phys.* **B289** (1987) 589;  
J.J. Atick, L.J. Dixon, and A. Sen, *Nucl. Phys.* **B292** (1987) 109;  
S. Cecotti, S. Ferrara, and M. Villasante, *Int. J. Mod. Phys.* **A2** (1987) 1839.
- [43] K.R. Dienes, *Nucl. Phys.* **B429** (1994) 533, hep-th/9402006.
- [44] J.C. Pati and A. Salam, *Phys. Rev.* **D8** (1973) 1240; *Phys. Rev. Lett.* **31** (1973) 661; *Phys. Rev.* **D10** (1974) 275.
- [45] K.R. Dienes, preprint IASSNS-HEP-94/72, hep-th/9409114 (to appear in the Proceedings of PASCOS '94);  
K.R. Dienes, preprint IASSNS-HEP-95/41, hep-th/9505194 (to appear in the Proceedings of Strings '95).
- [46] K.R. Dienes, M. Moshe, and R.C. Myers, *Phys. Rev. Lett.* **74** (1995) 4767, hep-th/9503055;  
K.R. Dienes, M. Moshe, and R.C. Myers, preprint IASSNS-HEP-95/42, hep-th/9506001 (to appear in the Proceedings of Strings '95).
- [47] Particle Data Group, L. Montanet *et al*, *Phys. Rev.* **D50** (1994) 1173.
- [48] See, *e.g.*, P. Langacker, hep-ph/9412361, and references therein.
- [49] See, *e.g.*, N. Polonsky, preprint UPR-0641-T, hep-ph/9411378, and references therein.
- [50] A. Font, L.E. Ibáñez, F. Quevedo, and A. Sierra, *Nucl. Phys.* **B331** (1990) 421.
- [51] K.R. Dienes, A.E. Faraggi, and J. March-Russell, hep-th/9510223.
- [52] L. Ibáñez and D. Lüst, *Nucl. Phys.* **B382** (1992) 305, hep-th/9202046;  
V.S. Kaplunovsky and J. Louis, *Phys. Lett.* **B306** (1993) 269, hep-th/9303040;  
A. Brignole, L. Ibáñez, and C. Muñoz, *Nucl. Phys.* **B422** (1994) 125, hep-ph/9308271.
- [53] S. Kalara, J. Lopez, and D.V. Nanopoulos, *Phys. Lett.* **B269** (1991) 84.
- [54] M.K. Gaillard and R. Xiu, *Phys. Lett.* **B296** (1992) 71, hep-ph/9206206;  
I. Antoniadis and K. Benakli, *Phys. Lett.* **B295** (1992) 219, hep-th/9209020;  
S.P. Martin and P. Ramond, *Phys. Rev.* **D51** (1995) 6515, hep-ph/9501244.
- [55] A.E. Faraggi, *Phys. Rev.* **D46** (1992) 3204.
- [56] K.R. Dienes and A.E. Faraggi, in preparation.
- [57] I. Antoniadis, J. Ellis, S. Kelley, and D.V. Nanopoulos, *Phys. Lett.* **B272** (1991) 31;  
S. Kelley, J. Lopez, and D.V. Nanopoulos, *Phys. Lett.* **B278** (1992) 140.

- [58] I. Antoniadis, G.K. Leontaris, and N.D. Tracas, *Phys. Lett.* **B279** (1992) 58.
- [59] K.R. Dienes, *Phys. Rev. Lett.* **65** (1990) 1979; Ph.D. dissertation (Cornell University, 1991).